DYNAMICS AND CHATTER STABILITY OF MULTI DELAY MACHINING SYSTEMS

by

Alptunç ÇOMAK

Submitted to the Graduate School of Engineering and Natural Sciences

in partial fulfillment of the requirements for the degree of

Master of Science

Sabancı University

July, 2013

DYNAMICS AND CHATTER STABILITY OF MULTI DELAY MACHINING SYSTEMS

Approved By:

Prof. Dr. Erhan BUDAK (Thesis Advisor)

Assoc. Prof. Bahattin KOÇ

Assoc. Prof. Bülent ÇATAY

Assoc. Prof. Ali KOŞAR

Assoc. Prof. Ayhan BOZKURT

Date of Approval:

to my family,

DYNAMICS AND CHATTER STABILITY OF MULTI DELAY MACHINING SYSTEMS

Alptunç ÇOMAK

Industrial Engineering, MSc. Thesis, 2013

Thesis Supervisor: Prof. Dr. Erhan Budak

Keywords: Chatter Stability, Special Milling Tools, Parallel Milling, Parallel Turning

Abstract

Machining is an industrial process in which parts are shaped by removal of unwanted material in the forms of chips. Manufacturing industry today demands shorter production times and high quality parts at competitive cost. Increased MRR (material removal rate) in milling and turning may provide high productivity but elevated forces and vibrations are still major obstacles to fulfill these requirements. Chatter vibrations may limit the full potential of machining productivity. In this thesis, chatter stability of multi delay systems is investigated. As examples of multi delay systems, variable tooth spacing tools such as variable pitch and helix milling cutters and parallel milling operations are investigated. Although there are few studies about the chatter stability of variable tooth spacing tools, no work has been reported on optimum design for a given cutting condition. Optimization studies are carried out to determine the optimum variable tool geometry and a new design methodology is presented. Moreover, for parallel milling operations, an analytical solution methodology which is based on frequency domain analysis is proposed to solve the chatter stability for the first time in the literature. Optimum cutting conditions are identified and effects of process parameters and workpiece dynamics on the chatter stability of parallel milling are shown. Since the operation contains single time delay, optimization studies are carried out to determine the optimum cutter dynamic properties in parallel turning. Simulated conditions are verified by time domain and experimental tests.

ÇOK FAZLI TALAŞLI İMALAT SİSTEMLERİNİN DİNAMİĞİ VE TIRLAMA KARARLILIĞI

Alptunç ÇOMAK

Endüstri Mühendisliği, Yüksek Lisans Tezi, 2013

Tez Danışmanı: Prof. Dr. Erhan Budak

Anahtar Kelimeler: Tırlama Kararlılığı, Özel Freze Takımları, Eş zamanlı Frezeleme, Eş zamanlı Tornalama

Özet

Talaşlı imalat, üretilecek parçaların talaş kaldırma yoluyla şekil verildiği endüstriyel bir üretim yöntemidir. Günümüzde imalat endüstrisi kısa üretim süreleri, yüksek ürün kalitesi ve rekabetçi fiyatlar talep etmektedir. Frezeleme ve tornalama operasyonlarında yüksek talaş kaldırma oranları üretim verimliliğini artırıcı yönde uygulanabilir olmasına karşın yüksek kesme kuvvetleri ve titreşim değerleri buna engel olmaktadır. Tırlama titreşimleri de talaşlı imalat verimliliğini kısıtlayan sebeplerden birisidir. Bu tezde çok fazlı talaşlı imalat yöntemlerinin tırlama titreşim kararlılığı araştırılmıştır. Çok fazlı talaşlı imalat sistemlerine örnek olarak, değişken adım ve helis aralıklı gibi özel freze takımları ve eş zamanlı frezeleme operasyonları incelenmiştir. Özel freze takımlarının tırlama kararlılığını modelleyen birçok çalışma olmasına karşın, literatürde verilen bir kesme koşulu için bu takımları dizaynına yönelik bir çalışmaya rastlanmamaktadır. Optimum takım geometrisini belirlemek için eniyileme çalışmaları yapılmış ve yeni bir tasarım metodu geliştirilmiştir. Bununla birlikte literatürde ilk kez eş zamanlı frezeleme operasyonlarının tırlama kararlılığının çözümü için frekans kümesinde bir analitik çözüm metodu geliştirilmiştir. En iyi kesme koşulları belirlenmiş, kesme parametreleri ve iş parçası dinamiğinin kararlılık limitine olan etkileri gösterilmiştir. Son olarak, her ne kadar sistem tek fazlı olsa da, eş zamanlı tornalama operasyonlarında en iyi takım dinamik özelliklerinin belirlenmesi yönünde çalışmalar yapılmıştır. Benzetimi yapılan tüm koşullar zaman kümesi modeli ve deneysel çalışmalar yardımı ile doğrulanmıştır.

Acknowledgement

First, I would like to thank Prof. Dr. Erhan Budak who is the supervisor of this Master thesis. I owe my deepest gratitude for his intellectual input, guidance, encouragement and inspiration throughout my graduate studies. He has guided the thesis in such a way that the outcome of thesis is significant for both academy and industry. Other than guiding my academic career, he has also had considerable positive effect on my personal development.

Prof. Dr. Yusuf Altintas, who becomes my life mentor throughout my undergraduate and graduate education, is the paramount factor to apply to Sabancı University and work with Erhan Budak. Without his valuable advices and guidance, it would be too hard to see what is best for me and my future.

I greatly appreciate the support of my family throughout my education life. During my Master study period, I always felt their presence, immeasurable and durable support. I thank my mother Bengi Çomak, my father Zafer Çomak, my sister Muazzez Çomak, my grandmother Muazzez Bahadır and my uncle for being in my life. I dedicate this thesis to them for being my driving force for all my life.

S. Burçe Özler has been the source of joy, motivation and support in my life. Her presence has been essential particularly at the difficult times of my Master study. I thank her for her support and contributions to my life.

It is a pleasure to thank every member of Manufacturing Research Laboratory (MRL) who made this thesis possible both by providing academically and technically supports.

Every former and present members of 1021 Office and my lab mates made my Master study enjoyable and memorable. Their support and friendship was unforgettable during two and a half years.

Lastly, I would like to thank TÜBİTAK (The Scientific and Technological Research Council of Turkey) for supporting me financially by granting a scholarship at the second year of my Master study.

TABLE OF CONTENTS

LIST OF FIGURES

LIST OF TABLES

CHAPTER 1

INTRODUCTION

Machining is the industrial process in which the parts are shaped by removal of unwanted materials in the forms of chips. Machining technology continues to develop in parallel with the improvements in material, machine tool and control technologies. Manufacturing industry today demands shorter production times and high quality parts with competitive costs.

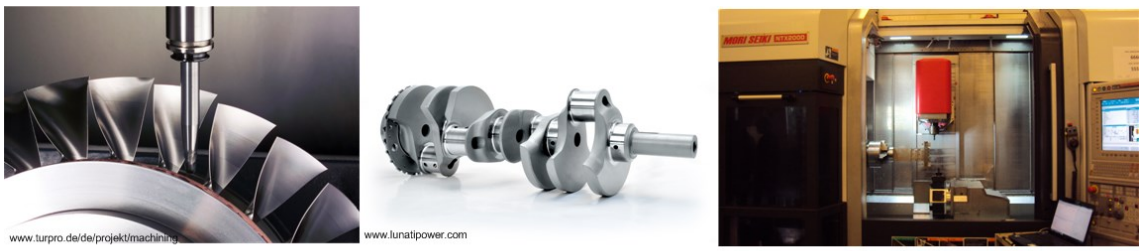

Figure 1.1. Machined parts (a) blisk, (b) camshaft and machine tool (c) NTX2000 Multi-purpose Machine Tool.

Increased MRR (material removal rate) in milling and turning may provide high productivity but elevated forces and vibrations are still being major obstacles to fulfill these requirements. Chatter vibrations may limit the full potential for productivity of the machining operations. The regenerative chatter results from the self-excitement mechanism in chip formation during the machining. Machine tool and workpiece system are excited by cutting forces and wavy surface finish is left on the surface. This wavy surface finish left in the previous revolution in turning or by a previous tooth in milling, is removed in the succeeding revolution or by the tooth which again leaves a wavy surface [1]. The phase difference between these two modulations on the surface may grow exponentially (See Figure 1.2). By virtue of growing vibrations, cutting

forces are increased and damage the machine tool and manufactured part, cause excessive part and tool deflection or tool breakages and reduced the productivity substantially. Hence, dynamics of chatter vibrations should be analyzed and investigated carefully.

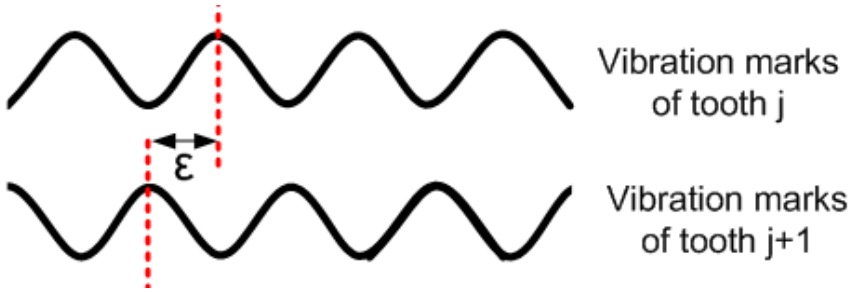

Figure 1.2. Delay between the vibration marks of the tooth j and tooth j+1.

If the milling or turning cutting parameters are selected properly, chatter free material removal rate may be increased. In order to determine optimal cutting parameters, process models and simulations can be used to predict cutting forces and machine tool vibrations. Stability diagrams in milling and turning operations are widely used to predict the stability limits and avoid chatter. Example stability diagram can be seen in Figure 1.3. Any combination of depth of cut and spindle speed above the stability limits results chatter in the process. Stability pockets (lobes) provide the advantage of high depth of cuts without chatter occurrence. Generally, stability pockets are impractical at low speeds and absolute stability limit is preferred as the limiting depth. On the other hand, high MRR is possible only at the high spindle speed values where the stability pockets are extended. Although the high speeds provide high stability limits, it may not be generalized. As shown in Figure 1.3, selection of 2 mm depth of cut at 14500 rpm results chatter in the process whereas the 12800 rpm provides stable cutting conditions. Also, sample surface finish and dynamic cutting force plots are illustrated both for the chatter and stable cutting conditions. Poor surface finish and increased cutting forces are observed in chatter whereas good surface quality can be achieved in stable cutting condition.

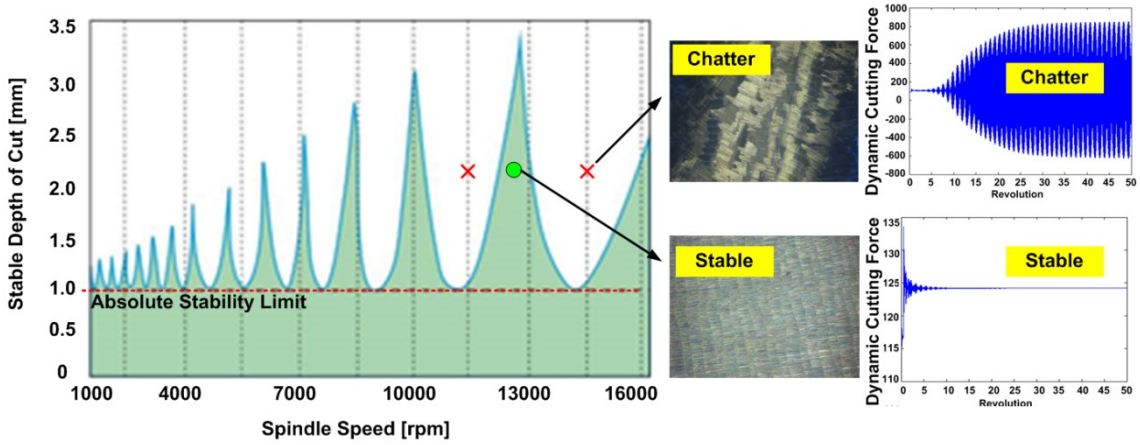

Figure 1.3. Stability diagram and surface photo and variation of cutting forces at stable and unstable conditions.

Special milling tools such as variable pitch and helix geometry tools are employed widely to reduce the cutting forces and increase the chatter stability. Variable tooth spacing between the adjacent teeth of the tool may alter the phase difference between the inner and outer modulations on the surface and suppress the regeneration effect if they are designed or selected properly. Also, variable tool geometry introduces multiple delays into the system. For a regular milling tool, the delay is constant between the adjacent teeth of the tool. However for a variable pitch milling tool, the number of time delays can be at most equal to the number of teeth. For example a variable pitch tool having $88^{\circ} - 92^{\circ} - 88^{\circ} - 92^{\circ}$ pitch angles with constant helix, the number of time delay is two. On the other hand, if both variable pitch and variable helix tool is used, number of time delays increases. Hence, the chatter stability of variable tool geometry tools is a multi-delay system and has complex solution compared to the regular end milling tools.

On the other hand, design of variable tooth spacing milling tools are mainly based on try-and-error method. There have been many works that analyze and model the chatter stability of variable tools but in none of these studies the design of the optimum tool geometry is considered. The existing models can be used to determine the best cutting condition for a given tool. However, in industry, cutting parameters are almost fixed due to various reasons in many applications. For example, the cutting speed may not be changed substantially due to some limitations which are explained in next sections. Hence, the optimum tool geometry should be determined for given cutting conditions in an application.

Simultaneous machining operations have also been continuing to spread in various sectors due to diverse advantages they offer. First of all, processing the part with more than one cutting tool obviously increases the productivity and reduces production time. Furthermore, employing two cutting tools may cancel out the dynamics cutting forces, and thus vibrations increasing stability limits substantially. Parallel turning and parallel milling are two common examples of the simultaneous machining operations. Parallel milling involves more than one milling tool cutting the same or different surface at the same time. In Figure 1.4 geometry of the parallel milling operations are demonstrated.

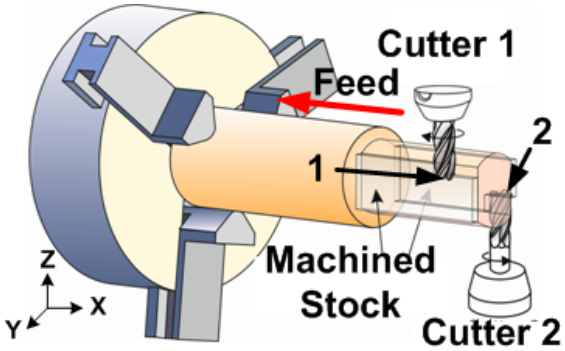

Figure 1.4. Sample demonstration of parallel milling operation.

If the correct process parameters are used, parallel milling has the potential to increase productivity substantially by keeping or further increasing the part quality. On the other hand, as in the conventional milling operations, chatter vibrations may limit the full potential of the operation. Hence, dynamics of parallel milling operations should be investigated to determine proper cutting parameters. Optimum cutting conditions for a given process should be identified to increase productivity. On the other hand, due to existence of two milling tools and different spindle speeds, there may be multiple delays in the system as well. Also, angular offset between the cutting teeth of the tools provides additional delay terms to the chatter stability formulation of parallel milling operations.

Similar to parallel milling, parallel turning operations involve more than one cutting tool removing material from the same surface simultaneously. As in the parallel milling, existence of additional cutting tool may provide higher productivity and suppress the chatter vibrations if the cutting parameters are set properly. Figure 1.5 shows the geometry of the parallel turning operation [2].

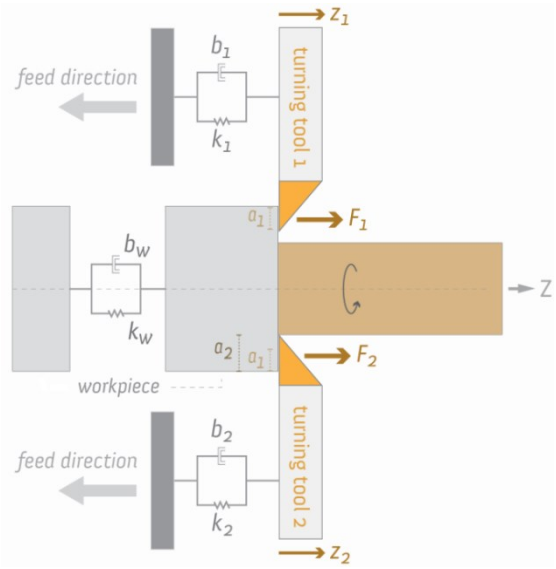

Figure 1.5. Demonstration of parallel turning operation.

In this study, dynamics and chatter stability of multi delay systems are investigated. Chatter stability of the multi delay systems are more complex compared to the standard chatter stability solutions in milling and turning due to existence of additional delay at the system.

As an example of multi delay systems, variable tooth spacing tools and parallel milling operations are examined. Optimum variable tooth geometry is determined by considering the chatter stability of operation. High performance cutting conditions are found for a given cutting condition. Also, dynamics and chatter stability of the parallel milling operations are investigated and an analytical solution methodology in frequency method is proposed. Optimization studies have been concluded to achieve high stability limits. Finally, even there is a single delay in the system, chatter stability of the parallel turning operations are explained briefly and optimum tool geometry and properties are identified to achieve high chatter free stability limits. Optimization studies are conducted by using frequency domain model and verified by time domain model.

For the first time in the literature, a design methodology that provides the optimum variable tool geometry is proposed for the variable tooth spacing milling tools. Without doing many and long optimization simulations, the optimum tool geometry configuration can be found by using the proposed new design method for a given cutting condition.

Also, a new analytical solution methodology for the chatter stability of parallel milling operations in frequency domain is provided. Furthermore, cutting parameters of the parallel milling operation that provides higher stability limits are optimized for the first time in the literature. Similar to the parallel milling operations, optimum cutting conditions for the parallel turning operations are determined.

1.1. Organization of the Thesis

The thesis organized as follows;

- In chapter 2, first chatter stability of the variable tooth spacing milling tools is explained. Then optimization studies are performed by using Single Frequency Averaging Method. Optimum variable tool geometries are found for a given cutting condition and simulation results are verified by experiments. Finally, a design methodology that determines the optimum variable tool geometry is proposed.
- In chapter 3, chatter stability of parallel milling operations is investigated in the frequency domain. Stability diagrams are generated for different cutting conditions and process parameters. Time domain verification of the frequency domain results is provided. Effects of workpiece dynamics on the chatter stability of parallel milling are studied in detail. Moreover, high performance machining conditions are identified by optimization studies and results are verified by experimental tests.
- In chapter 4, dynamics and chatter stability of parallel turning operations are explained briefly and mostly concentrated on the optimization of dynamic properties of cutters. Two different methods are used in the optimization studies. Both methods alter the dynamic properties of the tools. Optimum dynamic cutter properties are identified in frequency domain model and verified with time domain model.
- In chapter 5, conclusions obtained from this study are presented briefly and some possible improvements for future works are proposed.

1.2. Literature Survey

Dynamics and stability of machining have been studied in detail in many works. The theory of chatter in machining was first introduced by Tobias and Fishwick [3] and Tlusty and Polacek [4]. They demonstrated the coupling between the cutting forces and dynamic displacements and estimated the chatter stability limits. Tlusty and İsmail [5] carried out time domain simulations and acquired more accurate results for the stability limits by including the basic nonlinearity in cutting which is the loss of contact between the cutting tool and the material. Altintas and Budak [6] presented an analytical method for the stability of milling which can be used to generate stability diagrams in frequency domain very efficiently. Added lobes in milling due to flip bifurcations have been presented by several authors [7], [8].

Cutting tools with variable helix and variable pitch angles can be used for improving the stability of the milling process. Variation in the tooth spacing alters the delay in the cutting system disturbing regeneration mechanism. The effectiveness of variable pitch cutters in suppressing chatter vibrations in milling was first demonstrated by Slavicek [9]. He assumed a rectilinear tool motion for the cutting teeth, and applied the orthogonal stability theory to irregular tooth pitch. By assuming an alternating pitch variation, he obtained a stability limit expression as a function of the variation in the pitch. Opitz et al. [10] considered milling tool rotation using average directional factors. Their experimental results and predictions showed significant increase in the stability limit using cutters with alternating pitch. Vanherck [11] considered different pitch variation patterns in the analysis by assuming rectilinear tool motion. His computer simulations showed the effect of pitch variation on stability limit. Tlusty et al. [12] analyzed the stability of milling cutters with special geometries such as irregular pitch or serrated edges using numerical simulations. These studies mainly concentrated on the effect of pitch variation on the stability limit; however they do not address the cutting tool design, i.e. determination of the optimal pitch variation. Altintas et al. [13] adapted the analytical milling stability model to the case of variable pitch cutters which can be used more practically to analyze the stability of variable pitch cutters. Later, Budak proposed an optimization methodology [14] for design of variable pitch tools considering the chatter frequency and spindle speeds. He showed that the selection of pitch variation is very critical for increasing chatter stability limits. Olgac and Sipahi

[15] developed an optimization model for similar tools by analyzing the dynamic characteristic equation of the system using cluster treatment method. Later, Ferry [16] developed a mechanical and dynamical model to predict stable cutting regions for serrated variable pitch cutting tools using the Nyquist criteria. Turner et al. [17] obtained coherent results for low radial cutting cases by applying the method [14] developed for variable pitch cutters to variable helix cutters. Zatarain et al. [18] investigated the effect of helix angle on the chatter stability for low radial cutting conditions and concluded that flip bifurcation or period doubling effects should be also considered for low radial cutting conditions where cutting is very interrupted. Also, Sims et al. [19]-[20] investigated the chatter stability of variable helix and variable pitch cutters analytically, and proposed an optimization methodology by comparing three different modeling approaches, i.e. semi-discretization [21],[22], time averaged semi-discretization with similar assumptions to Budak's model [14], and temporal-finite element method (TFEA) [20]. Finally, Dombovari and Stepan investigated the effect of the helix angle variation on the chatter stability by semi-discretization method [23].

Dynamics and stability of parallel milling, on the other hand, has been studied very little. Ozturk and Budak [24] have simulated the dynamics of parallel milling in time domain and generated stability diagrams for various cutting conditions. Brecher and Trofimov [25] also used time domain simulation method and showed the effect of relative angular position offset and spindle speed on the stable depth of cut. Shamoto [26] posed the suppression of chatter in simultaneous milling by speed difference.

Dynamics and chatter stability of conventional single turning is have been investigated by many researches decades. Although there have been many work done on chatter stability of single turning operations, there are few studies about the stability of parallel turning operations. Lazoglu, et. al. [27] formulated the parallel turning operation in time domain where each tool cuts a different surface. They showed that working the cutting tools simultaneously reduce the stability limits of each other. Later, Ozdoganlar and Endres [28] developed a stability model of parallel turning operations but only applicable to symmetric systems only. They verified the developed formulation by means of experiments. After that, Tang, et. al. [29] predicted the cutting forces, spindle power and tool life in parallel turning operations. However, they have not taken into consideration the chatter stability of the parallel turning. In recent years, Ozturk and Budak [2] solved the chatter stability of parallel turning operation in both frequency and

time domains. They modeled the chatter stability of two different cutting conditions in parallel turning. In the first case, the cutting tools located at the same turret and cut the same workpiece simultaneously. The dynamic coupling was between the tools since they were clamped on the same turret. In the second case, turning tools were clamped of different and independent turrets on the parallel turning machine tool. In this case, there was no direct coupling between the tools but they were dynamically coupled through the workpiece. They also have verified the frequency and time domain solutions by experimental studies.

Design of optimum variable tool geometry has never been investigated in the literature so far. All the previous works were aimed to generate stability diagrams for a given variable tooth spacing tool. However, it is significant to design optimum variable tool geometry for a given cutting condition. In this study, design methodology that provides optimum tool geometry for the given cutting conditions is proposed to fill the gap in the literature in this regard.

In parallel milling operations, frequency domain model has never been investigated in the literature before. The previous works obtained a solution methodology which is in time domain which is time consuming and not provide a stability diagram at a time. Hence a new frequency domain model is introduced in this thesis to fill the gap in the literature.

Finally, determining of optimum dynamic properties of cutters in parallel turning has never been worked so far. In this respect, optimum dynamic properties of cutters are identified for parallel turning operations.

CHAPTER 2

CHATTER STABILITY OF VARIABLE PITCH/HELIX TOOLS AND DESIGN OF OPTIMUM VARIABLE TOOL GEOMETRY FOR INCREASED STABILITY

Machining is based on removing material from a bulk or a near net shape part in the form of chips using shearing mechanism involving high strains and strain rates. Manufacturing industry today increasingly demands shorter lead times, competitive prices and higher product quality. In order to fulfill these requirements a milling operation should achieve high productivity with increased MRRs (Material Removal Rate) and tight dimensional, form and surface tolerances under stable cutting conditions. Reduced cutting forces and increased chatter stability can increase productivity and part quality substantially. Special milling tools can be very effective for reduced cutting forces and increased stability when they are designed or selected properly. Cutting tools with variable helix and variable pitch angles can be used for improving the stability of the milling process. Suppressing the delay and chatter vibrations in the dynamic cutting system, make the variable milling tools prior alternative over the regular milling tools.

In some industries, such as aerospace and defense, titanium and nickel alloys that have low machinability, are commonly used. High spindle speeds that provide high stability limits cannot be achieved and stability pockets may not be utilized due to the low machinability of these materials which usually have to be machined at slow speeds. Furthermore, machine tool limitations such as spindle speed as well as power and torque (especially at high speeds) also impose limitations on utilization of deep stability pockets usually available at high cutting speeds. Finally, unbalance in the spindle or

system becomes noxiously high at high spindle speeds. Variable tooth spacing tools (variable pitch/helix) can be used for such cases.

In this chapter, chatter stability models for variable pitch and helix tools are simply explained by concentrating on the optimization of variable tooth spacing to develop a design methodology.

2.1. Description of Variable Geometry Milling Tools

Variable tooth spacing milling tools can be classified in three categories. First one is the variable pitch milling tool which have non uniform pitch angles between adjacent teeth. Second type is the variable helix milling tools and helix angles of each tool are not uniform. Last type is the hybrid version of the variable pitch and variable helix milling tools where the both pitch and helix angles are non-uniform. There are also different types of variations of the variable geometry milling tools. Alternate, linear and sinusoidal variations are commonly used in industry.

In Figure 2.1, illustration of tool geometry of variable pitch tool can be seen. Pitch angles between the teeth are different as $\emptyset_{pi}$ for each tooth.

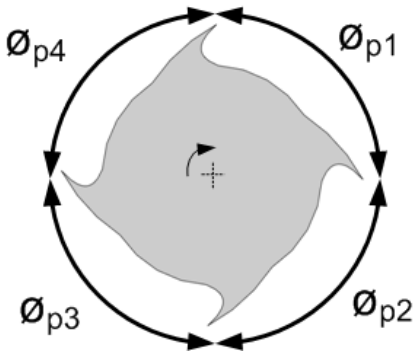

Figure 2.1. Tool geometry of variable pitch tool.

For the variable helix cutters case, helix angles of each tooth are different (Figure 2.2).

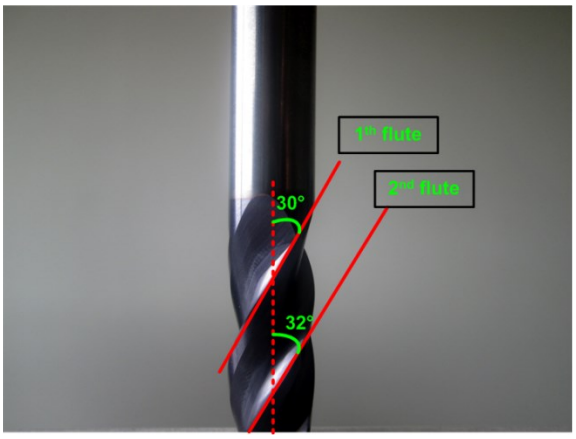

Figure 2.2. Tool geometry of variable helix tool.

In this study, two common variation patterns are considered for both pitch angle and helix angle distribution, which are linear and alternating. For both cases in non-uniform pitch distribution, a pitch angle variation measure, *ΔP,* is introduced and the initial pitch angle is found as follows [14];

$$\left.\begin{aligned} &P_0, P_0 + \Delta P, P_0 + 2\Delta P, \dots, P_0 + (N_t - 1)\Delta P \\ &P_0 = \frac{2\pi}{N_t} - \frac{(N_t - 1)\Delta P}{2} \end{aligned}\right\} \text{Linear} \tag{2.1}$$

$$\left.\begin{aligned} &P_0, P_0 + \Delta P, P_0, \dots, P_0 + \begin{cases} \Delta P & N_t \text{ even} \\ 0 & N_t \text{ odd} \end{cases} \\ &P_0 = \frac{2\pi}{N_t} - \frac{\Delta P}{N_t} \sum_{k=1}^{N_t} ((-1)^k + 1) \end{aligned}\right\} \text{Alternating} \tag{2.2}$$

For example, variable pitch alternate variation tool with 2 degrees of variation (*ΔP*) has the pitch angles as 88°- 92°- 88°- 92°. In the same way, the variable pitch linear variation tool with 2 degrees of variation has the pitch angles as 87°- 89°- 91°- 93°. The same example can be expanded for the variable helix alternate and linear variation tools.

For the helix angle variation for both alternating and linear distributions, the helix variation measure is denoted as *ΔH*. This variation measure has to be tuned to assure no crossing occurs between consecutive teeth due to the lag effect of both helix and pitch variation. This constraint is noted as;

$$\phi_j(z) > \phi_{j-1}(z) \; \forall \; z \tag{2.3}$$

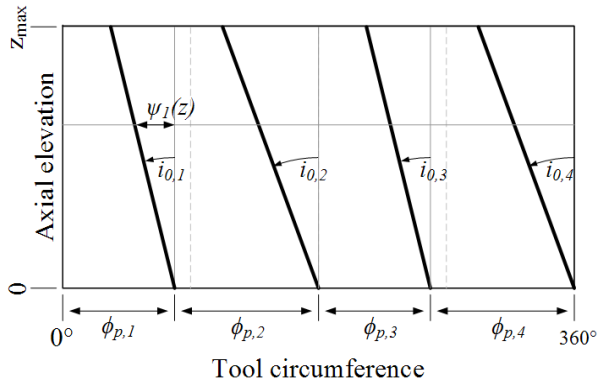

Figure 2.3. Unfolded tool geometry and variable flute parameters.

2.2. Chatter Stability of Variable Helix and Pitch Milling Tools

Due to the geometry of variable pitch and helix milling tools, dynamic cutting system is affected by multiple delays which are originated from the different pitch and helix angle variations of the teeth. Therefore, chatter stability of variable tooth geometry tools is more complex compared to the regular end mills. Stability models for the solution of the variable tool geometry are investigated in a lot of works [30], [31]. Two methods that mentioned in this study are the "Semi-Discretization Method" and "Single Frequency Averaging Method". In this study, stability methods are explained simply and by using one of these methods, optimization and design of variable tool geometries have been concluded.

2.2.1. Semi-Discretization Method

Chatter stability of variable pitch and helix tools can be solved by using semi-discretization method and a lot of works have been concluded. Semi-discretization method is used for the stability analysis of linear – time periodic delay differential equations [21].

First step to solve the stability is the formulation of the governing equation. The stability of milling operations is dependent on the dynamically varying chip thickness which is a function of both current and past vibration marks left on the cut surface. Milling system is modeled with two orthogonal degrees of freedom in x and y process directions. Dynamic chip thickness and orthogonal degrees of freedom are illustrated in Figure 2.4.

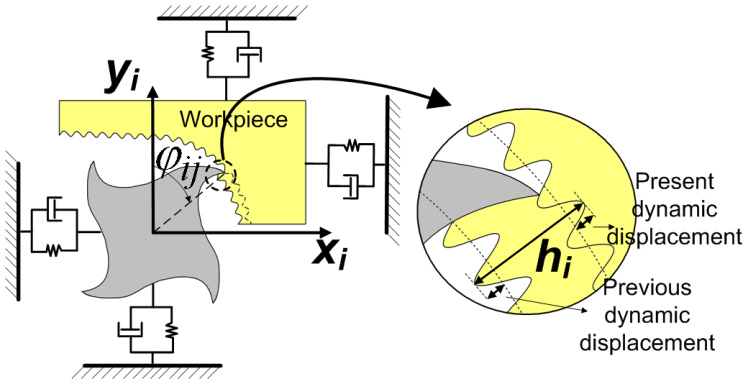

Figure 2.4. Dynamic chip thickness and two orthogonal degrees of freedom.

Equations of motion in *x* and *y* process directions are given as follows:

$$\begin{aligned} \ddot{x}(t) + 2\zeta_x \omega_{nx} \dot{x}(t) + \omega_{nx}^2 x(t) &= \frac{F_x(t)}{m_x} \\ \ddot{y}(t) + 2\zeta_y \omega_{ny} \dot{y}(t) + \omega_{ny}^2 y(t) &= \frac{F_y(t)}{m_y} \end{aligned} \tag{2.4}$$

where ω_{nx} , ω_{ny} , ζ_x, ζ_y, m_x, m_y represent the natural frequencies, damping ratios and modal masses of the most dominant vibration modes of the system in *x* and *y* directions.

In order to take the variable pitch and helix angles into account, the cutting tool is divided into axial disc elements along the tool axis. System equations are written as follows before they are transformed into the first order:

$$\begin{Bmatrix} \ddot{x}(t) + 2\zeta_x \omega_{nx} \dot{x}(t) + \omega_{nx}^2 x(t) \\ \ddot{y}(t) + 2\zeta_y \omega_{ny} \dot{y}(t) + \omega_{ny}^2 y(t) \end{Bmatrix} = \sum_{r=1}^{r=N_D} \left[[DC_r(t)] \begin{bmatrix} x(t) - x(t-\tau_r) \\ y(t) - y(t-\tau_r) \end{bmatrix} \right] \tag{2.5}$$

$DC_r\ (t)$ matrix consists of directional coefficients which are grouped according to their delay values. This is because the variable tool geometry introduces multiple delays into the system. The number of different delays in the system is represented with N_D. The stability analysis of the governing delay differential equation with time-periodic coefficient matrices is done with First Order Semi-Discretization Method (SDM) [21]. In order to analyze the stability of Equation 2.5, the eigenvalues of the infinite-dimensional monodromy matrix is required [21]. With the First Order SDM, the infinite dimensional monodromy matrix is approximated with a finite dimensional one. Then, the stability of the system is analyzed with the approximate monodromy matrix according to the Floquet Theory as stated in [21]. One of the main ideas which semi-

discretization method is based on is to divide the principle period *T* of the system into *p* discrete time intervals.

$$\Delta t = \frac{T}{p} \tag{2.6}$$

where p is the principle period resolution, Δt is the length of discrete time intervals.

Stability of the system is analyzed with the eigenvalues of the resulting matrix according to the Floquet theory. If the largest complex eigenvalue of the monodromy matrix has an absolute value bigger than 1 the system is unstable, if it is equal to 1 the system is on the stability boundary or if it is less than 1 than the system is stable.

2.2.2. Single Frequency Averaging Method

The dynamic milling expression can be written for a regular milling tool as [6];

$$\{F(t)\} = \frac{1}{2} a K_t [A(t)]\{\Delta(t)\} \tag{2.7}$$

where a is axial depth of cut, K_t is the tangential cutting force coefficient and A_0 consists of the directional coefficients and is a periodic at tooth passing frequency $\omega = N\Omega$. Hence it can be expanded into Fourier series.

On the other hand, number of harmonics of the tooth passing frequency ($w_T, 2w_T$) is important to solving the stability equation. If the number of harmonics of the tooth passing frequency is considered as zero which is the most simplistic approximation, the average component of the Fourier series expansion is taken into account and the equation (6) becomes;

$$\{F(t)\} = \frac{1}{2} a K_t [A_0]\{\Delta(t)\} \tag{2.8}$$

where A_0 is the time invariant directional cutting coefficient matrix. This solution of the stability equation is known as “Single Frequency Solution” and applicable to the most of the stability problems in milling and turning operations.

However, the single frequency solution may not be satisfied for some cutting conditions where the width of the cut is small and the milling forces are highly intermittent [8]. In such cases, harmonic components of the tooth passing frequencies have strong

influences in addition to the average value. Hence stability results may not satisfy the physical analysis. So that, solution to the stability equation (Equation 2.8), must be considered as the higher harmonics of the tooth passing frequency in addition to the average Fourier series expansion component. This solution is called as "Multi Frequency Solution". In this study, "Single Frequency Method" is applied to the stability problem and the most dominant mode of the tool is considered.

The stability of a regular milling tool depends on the phase difference between the inner and outer modulations on the surface and the time delay between the consecutive teeth is always constant since the pitch angles are uniform. Since the time delay does not vary along the cutting edge, the regeneration term equals to $(1 - e^{-i\omega_c t})$ and constant at every axial elevation. However, for the variable tooth spacing tools such as variable pitch and helix tools, the regeneration term for the jth cutting edge at elevation z can be written considering the separation angle as follows [31]:

$$b_j(\emptyset, z) = 1 - e^{-i\omega_c \tau_j(z,\emptyset)} \tag{2.9}$$

where $\tau_j(z, \emptyset)$ is the time delay and can be written considering the separation angle as follows:

$$\tau_j(\emptyset, z) = \frac{\delta\emptyset_j(z)}{\Omega} \tag{2.10}$$

The chatter stability model is formed as an eigenvalue problem where the closed loop system is described in terms of dynamic chip thickness [31]. Considering the regenerative effect, the dynamic chip thickness and force components are defined in the frequency domain as;

$$\begin{bmatrix} F_x(t,z) \\ F_y(t,z) \\ F_z(t,z) \end{bmatrix} = \Delta a.\, b_j(\phi, z) \left(\sum_{z=1}^{m} \boldsymbol{B_0}(z) \right) G(i\omega_c) \begin{bmatrix} F_x(t,z) \\ F_y(t,z) \\ F_z(t,z) \end{bmatrix} \tag{2.11}$$

where B_0 (directional coefficient matrix) is the first term of the Fourier series expansion and consists of the multiple delays (m number) in the system. Also, Δa is the length of the axial slice and $G(i\omega_c)$ is the transfer function of the tools. Equation 2.11 is an eigenvalue problem and the stability limit can be calculated for the given condition.

In order to obtain the chatter stability diagram, an iterative method is followed. Due to the varying delay function, for a chosen spindle speed the limiting depth of cut is sought

by sweeping a range of frequencies. The flowchart of the iterative method is explained in Figure 2.5.

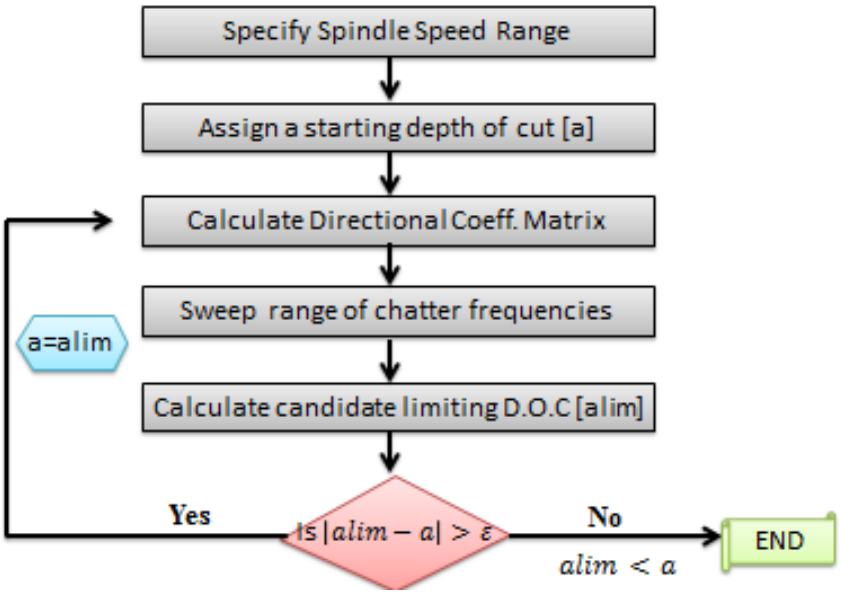

Figure 2.5. Flowchart of the iterative solution methodology.

In the optimization and design of optimum variable tool geometry studies, single frequency averaging method has been used. The paramount factor in this choice is the robustness and flexibility of the solution methodology that can be applied for distinct variable tooth spacing tool geometries.

2.3. Optimization of Variable Helix & Pitch Milling Tools

Selection of pitch and helix angle variation has strong impact on milling process stability. If the variations are not selected properly, the desired improvements may not be achieved. On the other hand, chatter stability limits can be maximized by using optimum pitch and helix variations on special milling tools. This can be done by using stability simulations based on the formulation and the procedure presented in the previous section as it will be demonstrated in this part of the thesis. Up to now, a lot work has been done on the modeling and analysis of chatter stability of for variable pitch and helix tools. These works were aimed to generate stability diagrams for a given variable geometry milling tool. On the other hand, in most industries such as aerospace and die and mold industries, the cutting conditions are mostly fixed due to quality, cost

and productivity requirements. For these cases, the cutting conditions may not be varied substantially. Hence, an optimum variable pitch or helix tool geometry should be identified for given cutting conditions in order to maximize stability in that range. Therefore, the main objective of the optimization study in this thesis is finding the optimum tool geometry that provides maximum chatter free cutting depth for a given condition. For alternating and linear variations of variable pitch and helix milling tools, optimum pitch and helix angles are sought using simulations. It is demonstrated that the stability limits can be increased substantially by simply using the optimal variations on the tools. Chatter tests are conducted to verify predictions by evaluating sound data and surface photos. Experimental results show relatively good agreement with the simulations.

2.3.1. Chatter Stability Simulations

Simulations were carried out for various pitch and helix variations in order to determine the optimal values and Matlab 2008© is used. In all simulations, a milling tool with 12 mm diameter and 4 flutes was considered. Fluted and overhang lengths of the tool are 28 mm and 35 mm, respectively. Radial depth of cut is 3 mm where the feed is 0.05 mm/rev*tooth. The milling cutter performs downmilling operation on an Al7075 test block. Modal parameters of the tools that were used in simulations and experiments are listed in Table 2.1

Table 2.1. Modal parameters of the variable tooth spacing milling tools.

Tool Code	Direction	Natural Frequency [Hz]	Modal Stiffness [N/m]	Modal Damping [%]
Tool 1	Xx	3374	1.37e+7	1.187
	Yy	3360	1.35e+7	1.097
Tool 2	Xx	3994	3.89e+7	1.218
	Yy	3989	2.85e+7	1.140

Also the variations of the helix and pitch variations of the tools are listed in Table 2.2 as follows:

Table 2.2. Cutting flute parameters for custom made variable tools.

Tool Code	Helix Angle [°]	Variation Type	Pitch Angles
Tool 1	30-33-30-33	Alternate	90-90-90-90
Tool 2	30-32-34-36	Linear	90-90-90-90

In the simulations, spindle speed range of 3000 to 4000 rpm was considered. Pitch and helix angle variation amount of 0° and 10° was considered with increments of 0.1°. For each pitch or helix variation amount stable depth of cut at a given spindle speed is calculated, and considering different spindle speeds 3D chatter stability diagrams are constructed. Variation of the chatter frequency with the helix and pitch variations is also considered and shown.

2.3.1.1. Optimization of Variable Helix Alternate Tool

In the case of alternating helix tools, separation angle between consecutive teeth varies alternatingly for instance, 30°-35°-30°-35° for a 4-fluted milling tool where the variation is 5°. Stability diagrams for different values of variation in helix angle are shown in Figure 2.6. In the optimization simulations, dynamics properties of first tool (Tool 1) are used (see Table 2.1). The effect of the helix angle on the stability limit variation can easily be seen by evaluating the 3D stability diagram given in the figure. For this case, the optimum alternating helix variation is found as 1^{o} at 3900 rpm where the maximum stable depth of cut is increased to 3.214 mm compared to the regular end mill which has the highest limit at 3900 rpm and 2.7 mm.

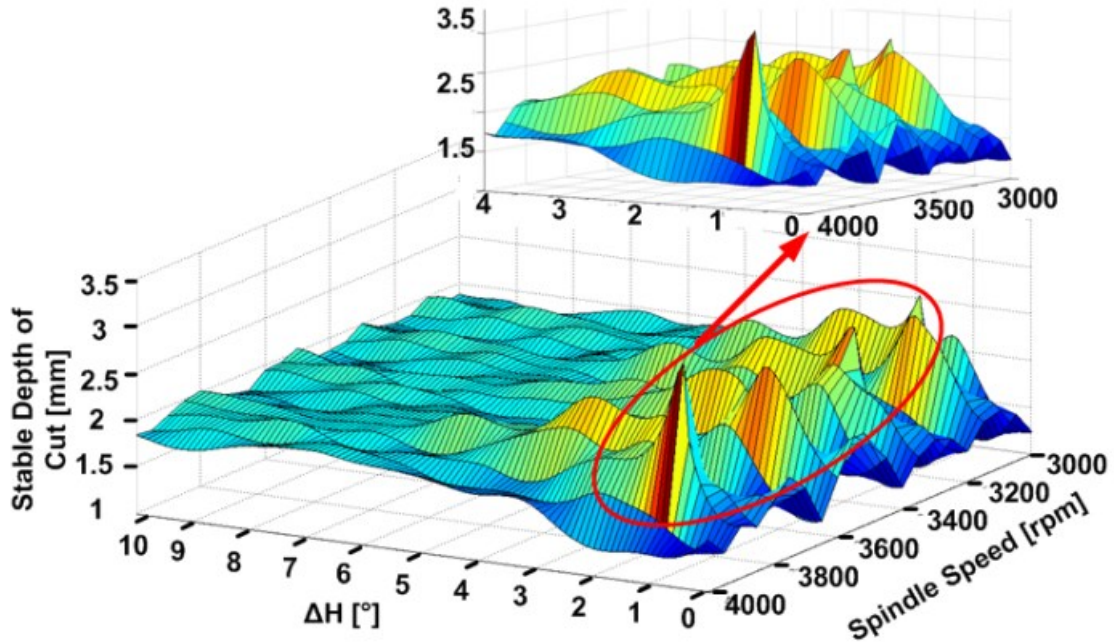

Figure 2.6. Stability diagrams vs. variation in the helix angle for a alternating helix milling tool.

For the optimal tool, the stability diagram is constructed and compared with a non-variable, i.e. regular, tool for the same dynamic and cutting conditions in Figure 2.7. It can be seen from the figure that the absolute stability limit is increased by %60 by using the optimal tool.

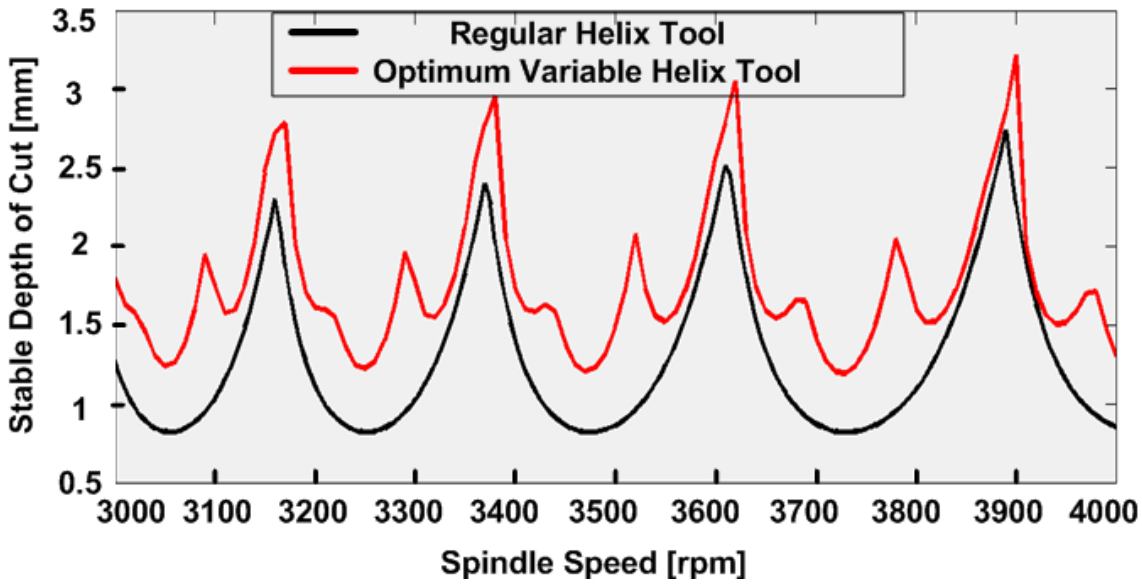

Figure 2.7. Stability diagrams for regular and variable helix tool with optimal variation.

Variable pitch or helix tools change the chatter stability behavior as they affect the phase, or delay, between the outer and inner modulation in a milling process. In general,

the stability limit can be maximized by minimizing or eliminating the delay. This is done by selecting a favorable speed based on stability diagrams for standard milling tools. In case of special geometry milling tools, this can also be done by the variation of the teeth spacing. Since the delay in dynamic cutting depends on cutting speed and chatter frequency, one should expect a strong influence of the teeth spacing helix angles on chatter stability which is also demonstrated in Figure 2.8. The delay or phase can be related to the pitch variation for its cancellation. On the other hand, chatter frequency also varies due to the alterations in the teeth spacing which makes the selection of optimal pitch or helix variations difficult. As an example, variation of the chatter frequency with the helix angle variation at 3900 rpm is shown in Figure 2.8. The natural frequency of the tool is 3370 Hz and the peak value of the chatter frequency occurs at the optimum helix angle.

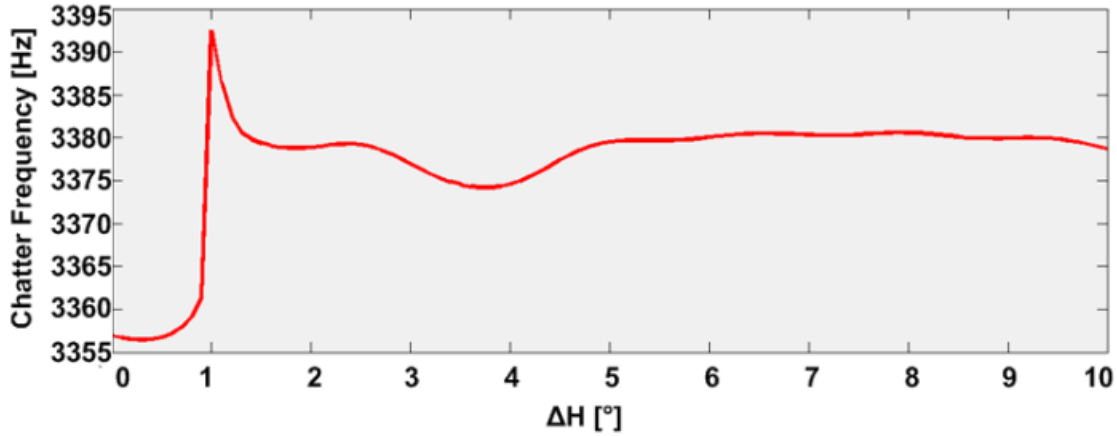

Figure 2.8. Variation of chatter frequency with helix angle alteration.

2.3.1.2. Optimization of Variable Helix Linear Variation Tool

Similar to the case of alternating helix, linear helix angle variation can also be optimized using stability simulations. The same tool geometry and process parameters are used while using the modal parameters of the Tool 2 (Table 2.1). The simulation results are shown in Figure 2.9.

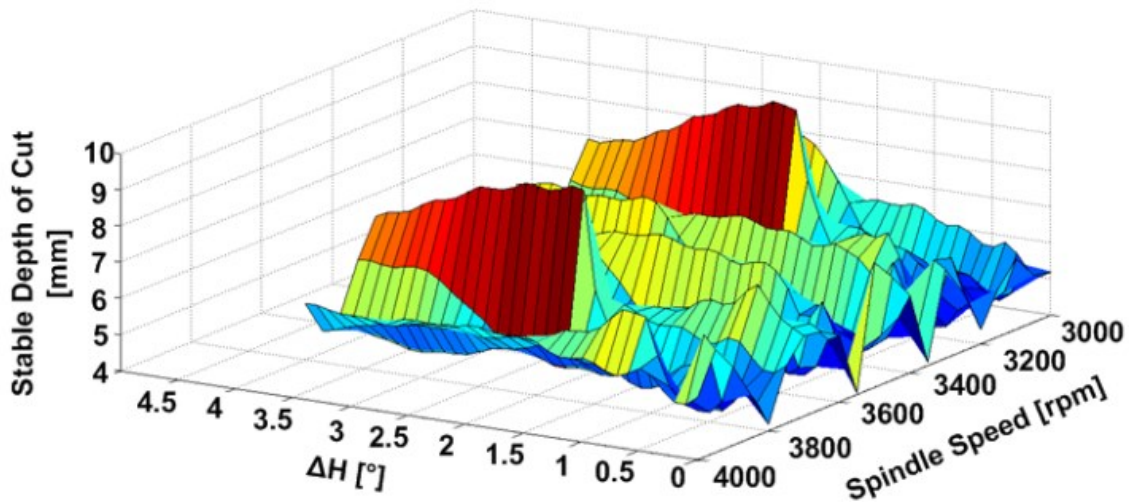

Figure 2.9. Stability diagrams vs. linear variation in the helix angle.

It can be seen that after 3.4° linear helix angle variation measure (ΔH), the flute crossing is occurred in the process.(see Figure 2.10.)

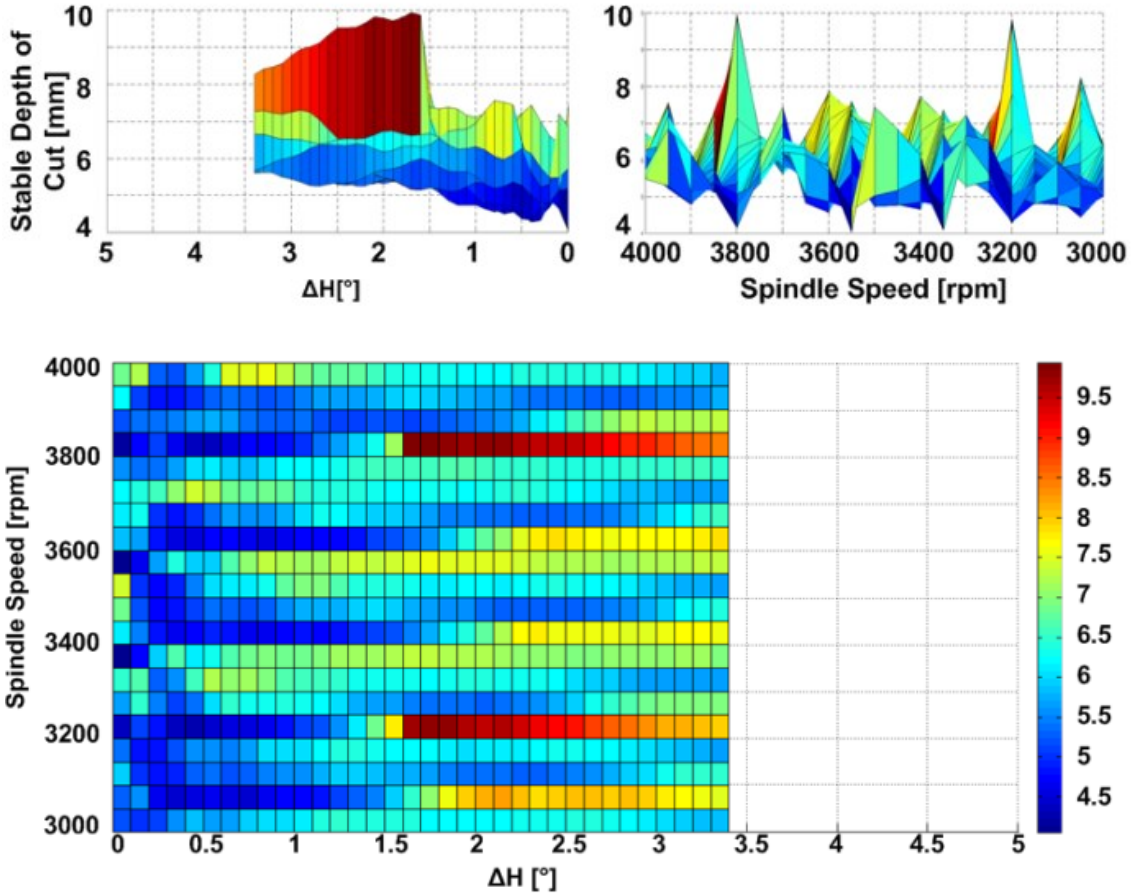

Figure 2.10. Cross-sections of the 3D stability diagram.

The optimum helix angles can be found out as 1.8° for 3800 rpm and 1.7° for 3200 rpm from the simulation results. Figure 2.11, shows the stability diagrams for optimal linearly varying helix angle and standard tools.

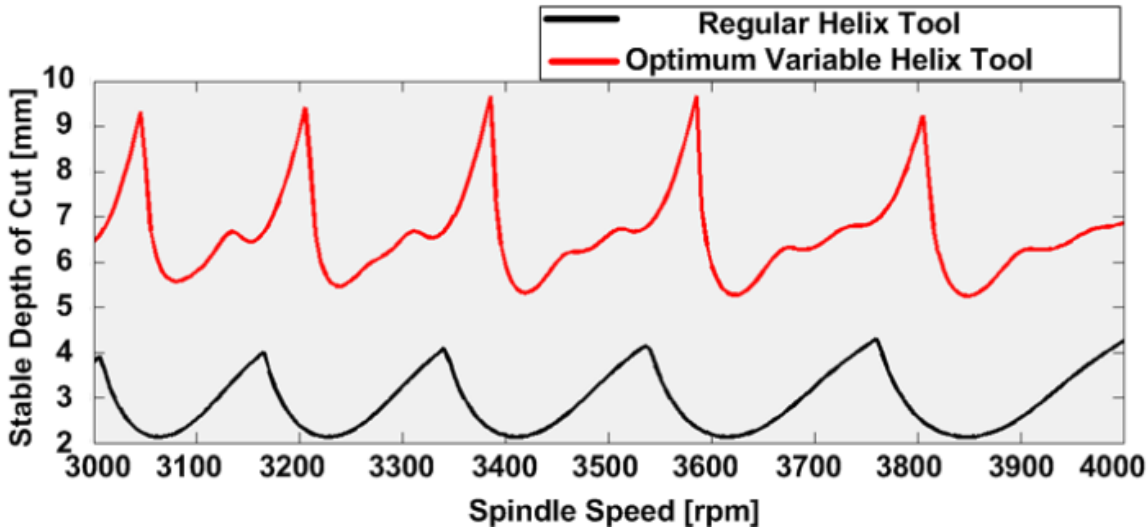

Figure 2.11. Comparison of regular and optimum variable helix with linear variation tool.

It can be seen that, both the absolute and peak stability limits are increased substantially (about three times) using the optimal varition in the helix angle.

Similar to the alternating helix tool, the chatter frequency varies with the helix angle variation in this case as well, as shown in Figure 2.12.

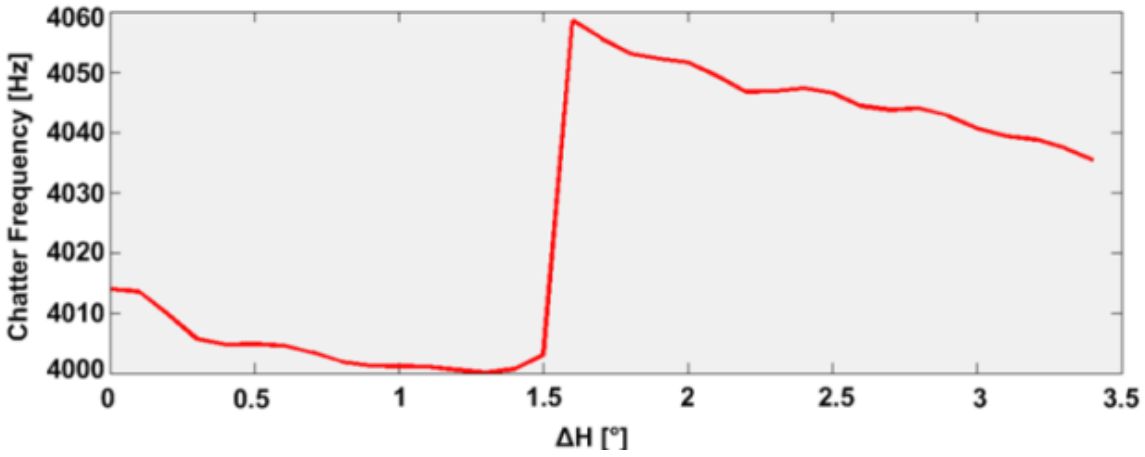

Figure 2.12. Variation of chatter frequency with linear helix angle variation measure.

It is important to note that the natural frequency of the tool is 3994 Hz and the peak value of the chatter frequency corresponds the point of optimum helix angle variation.

This means that the highest stability limit can be achieved by minimizing the delay in the system at that helix variation angle.

2.3.1.3. Optimization of Variable Pitch Alternate Variation Tool

Variable pitch end mills have non-constant spacing between adjacent teeth. Similar to the variable helix optimization, variable pitch milling tools' optimization was also performed. The same cutting parameters, tool geometries and modal parameters are used in the simulations. Then, the optimal pitch angle variations that provide the highest chatter free depth of cuts were determined for a range of spindle speeds. The effect of the pitch angle variation can easily be seen by evaluating the 3D stability diagram given in the Figure 2.13.

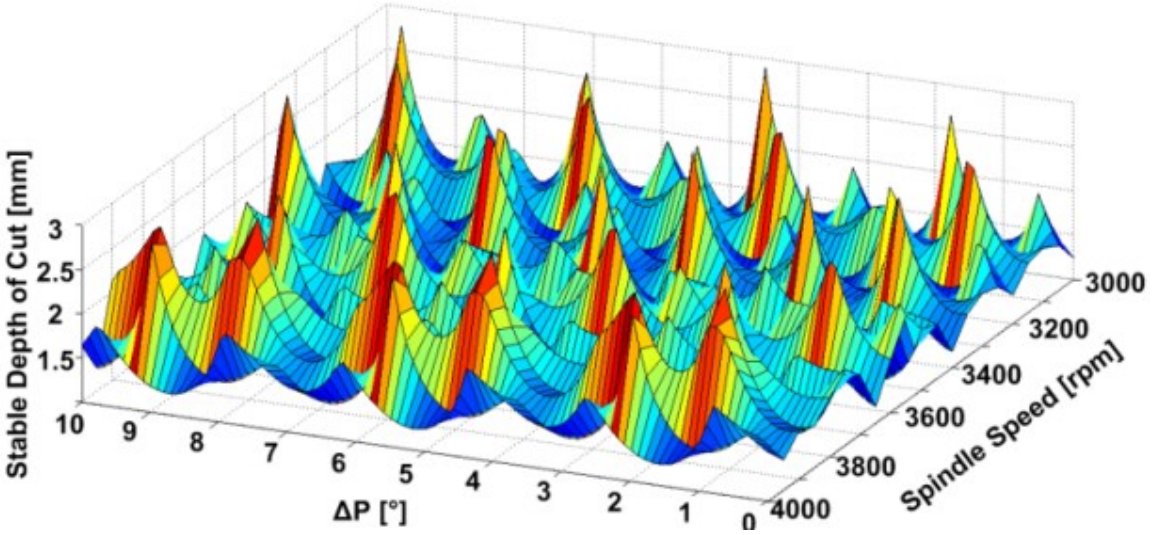

Figure 2.13. Variation of the stable depth of cut with spindle speed and alternating pitch angle.

As seen from the figure, the optimum alternating pitch variations appear at many points for each spindle speed. The maximum stable depth of cut which is about 2.92 mm occurs at 8.1° for 3850 rpm. On the other hand, it is important to note that there are several ΔP and spindle speed pairs that provide closer depths to the optimum (maximum) stable depth of cut possible. In Figure 2.14, comparison of the stability diagrams between the regular and alternating pitch tool can be seen.

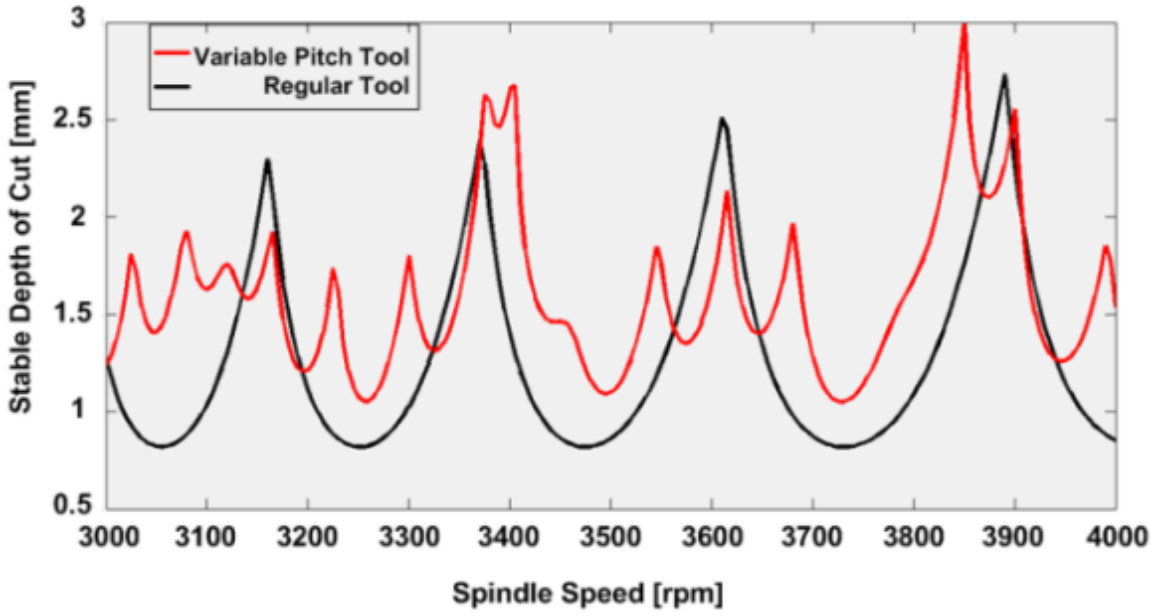

Figure 2.14. Comparison of regular and optimum alternatingly variable pitch tool.

Absolute stability limit is increased by about %25 compared to the regular tool. However, in some certain stability pockets, the stable depth of cut decreases with the introduction of pitch variation. In Figure 2.15, crossection view of the 3D surface (Figure 12) at 3850 rpm can be seen.

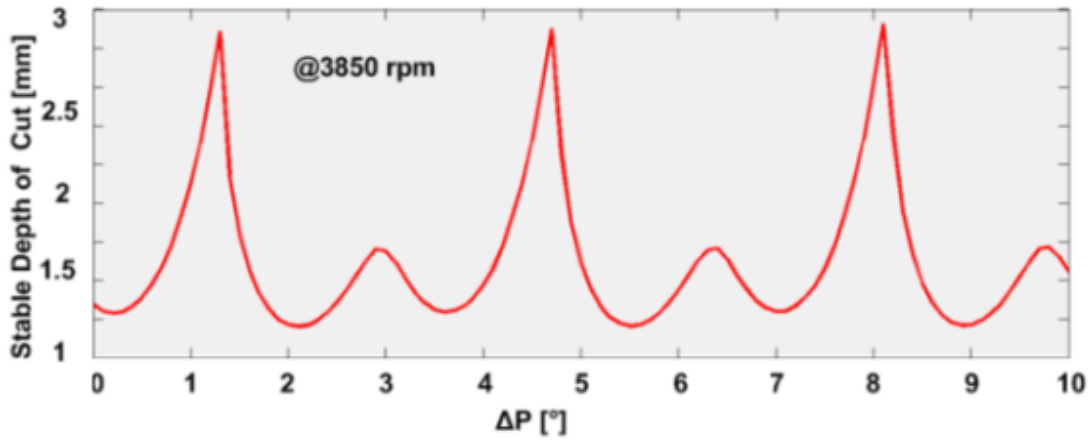

Figure 2.15. Variation of stable depth of cut with pitch variation amount

It is clearly seen from Figure 2.15 that there are multiple optimal pitch variation angles which repeat in a regular manner. Variation of the chatter frequency with the pitch angle variation at 3850 rpm is also shown in Figure 2.16. As in the optimization of variable helix tools, the maximum chatter frequency occurs at the optimum pitch angle variation that provides maximum stable depth of cut. This is again due to the minimized delay in the system at those conditions.

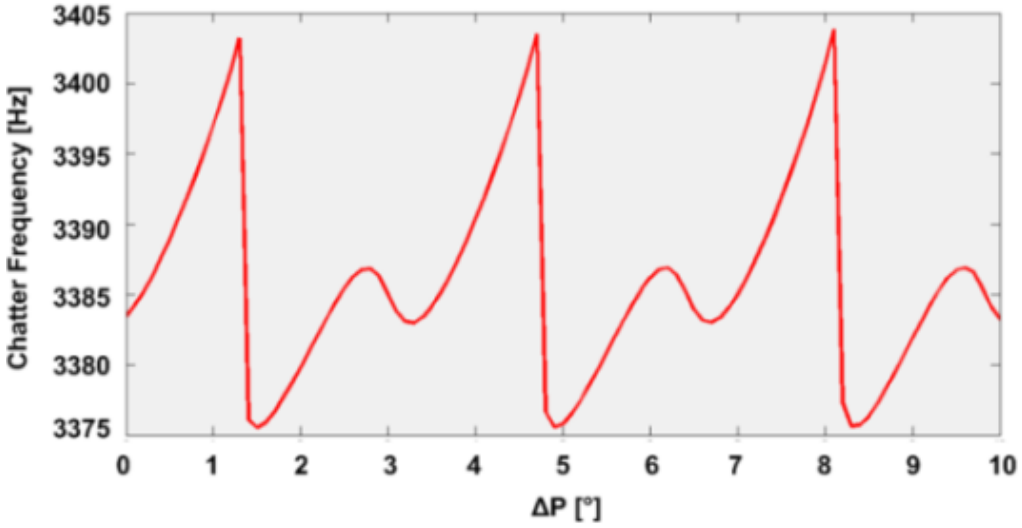

Figure 2.16. Variation of chatter frequency with alternatingly pitch angle variation amount.

2.3.1.4. Optimization of Variable Pitch Linear Variation Tool

Similar to the variable pitch alternate variation tool optimization, optimization of variable pitch linear variation tool was also performed. The same tool geometry and modal parameters are used as previous variable pitch optimization. Then, the optimal pitch angle variations that provide the highest chatter free depth of cuts were determined for a range of spindle speeds. The effect of the pitch angle variation can easily be seen by evaluating the 3D stability diagram given in the Figure 2.17

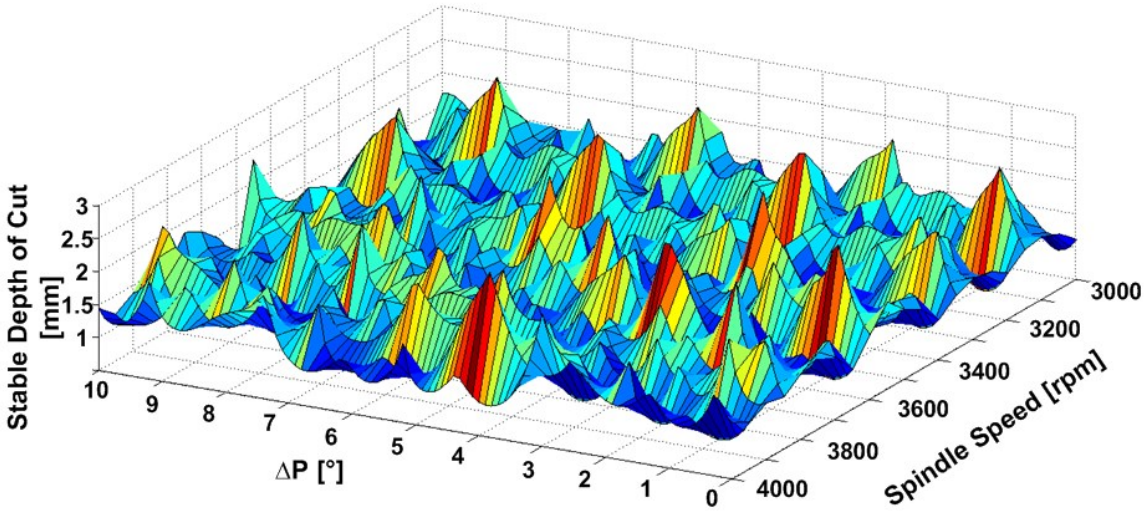

Figure 2.17. Variation of the stable depth of cut with spindle speed and linear pitch angle.

As in the variable pitch alternate variation tool case, there are multiple optimum points that provide maximum stable depth of cut limits. Numerically, optimum point corresponds to the combination of 4.1° of pitch variation and 3950 rpm spindle speed. On the other hand, it is important to note that there are several ΔP and spindle speed pairs that provide closer depths to the optimum (maximum) stable depth of cut possible. Figure 2.18 shows the comparison of the optimum variable pitch tool with the regular tool.

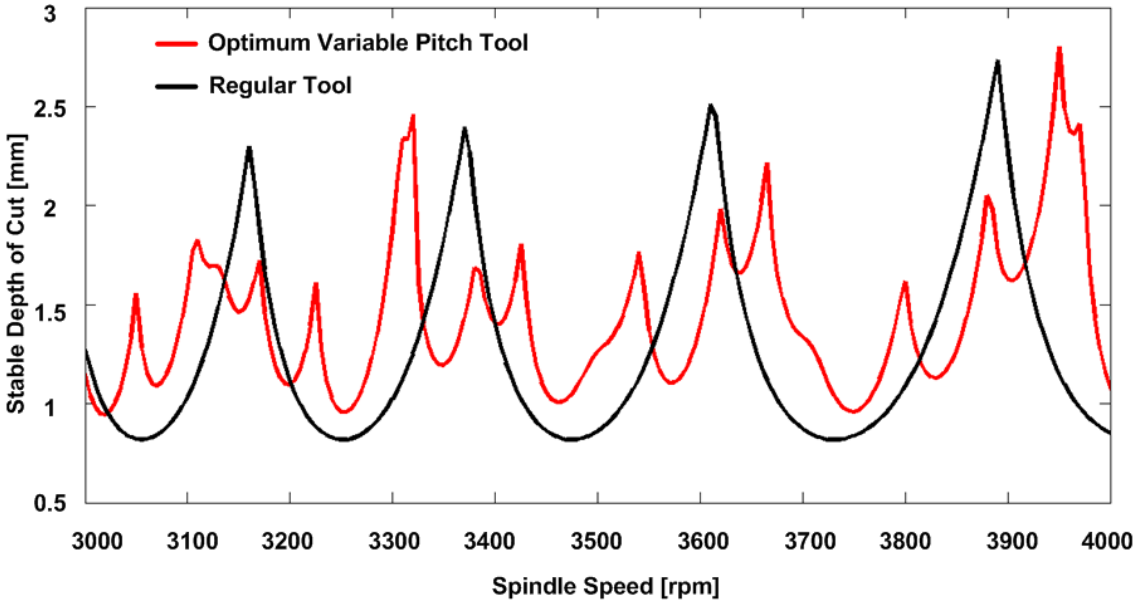

Figure 2.18. Comparison of optimum variable linearly varying pitch tool and regular tool.

Absolute stability limit is increased by % 20 compared to regular tools. On the other hand, in some stability lobes, stable depth of cut value is decreased with the introduction of pitch variation.

Comparing the variable pitch tools as alternate and linear variation for the same cutting geometry and modal data helps us to see the difference between these variations. In Figure 2.19 comparison of the optimum variable pitch alternate variation and variable pitch linear variation tools can be seen.

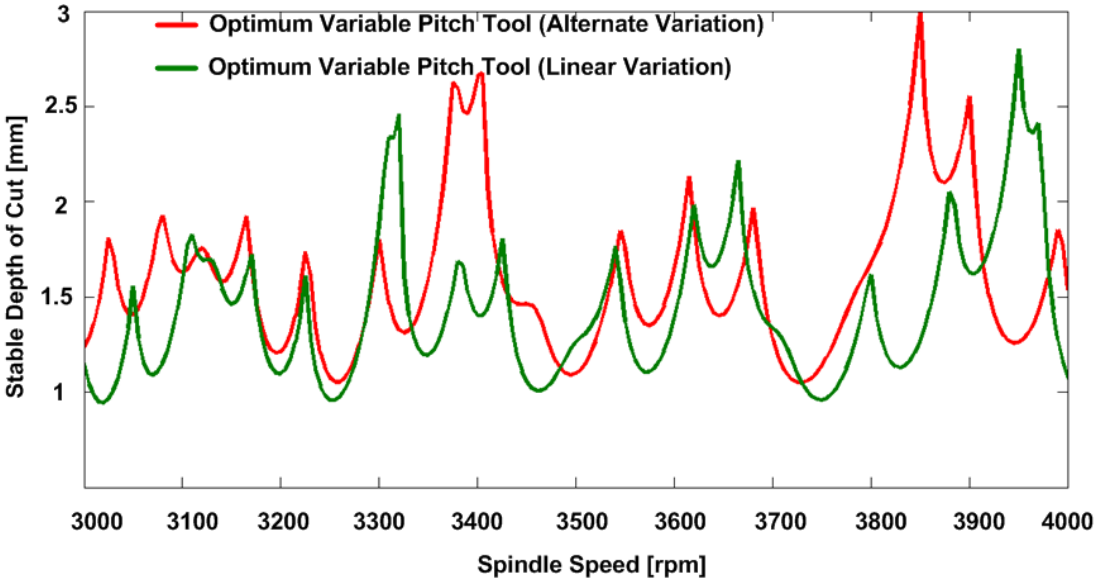

Figure 2.19. Comparison of alternate and linear variations for variable pitch tool.

It is hard to say which tool is the best one. Absolute stability limits of both variations are almost the same and alternate variation variable pitch tool has slightly higher stability limits for some stability pockets.

On the other hand, the significant point is the optimized cutting conditions of each tool. Alternate variation tool was designed at 3850 rpm of spindle speed where linearly varying variable pitch tool was designed at 3950 rpm. It can be easily seen that, alternately varying tool is effective at its optimized condition which is 3850 rpm and linearly varying variable pitch tool is also more effective than the alternately varying tool at 3950 rpm. For alternately varying tool, stability limit is about 3 mm at 3850 rpm where the stability limit of linearly varying tool is only about 1.25 mm. Nevertheless, linearly varying variable pitch tool has 2.8 mm stable depth of cut at 3950 rpm but alternately varying variable pitch tool has the stability limit of 1.26 mm at the same cutting condition.

Finally, for the same tool geometry, modal parameters and the cutting conditions, it can be concluded that variable helix tools are superior to the variable pitch tools for alternating variation. Stable depth of cut for the variable helix tool was calculated as 3.214 mm which is about %10 higher than the limit for the variable pitch tool (2.9 mm). The comparison of both optimum variable helix tool, optimum variable pitch tool and the regular flat end mill are shown in Figure 2.20.

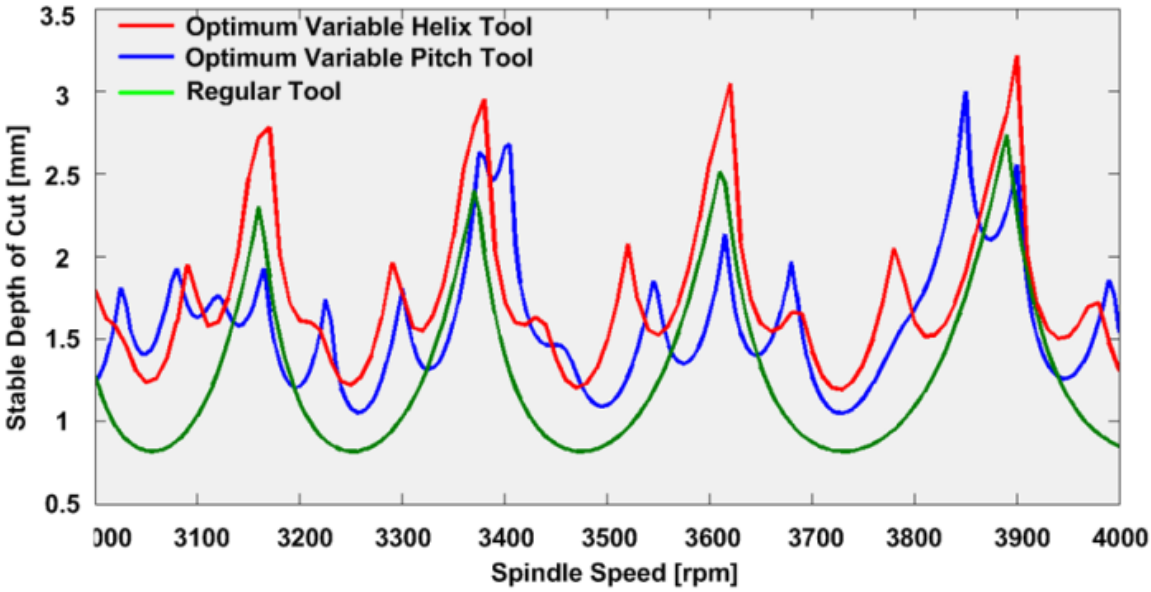

Figure 2.20. Comparison of optimum variable helix, pitch and regular end mill tools.

2.3.2. Experimental Verifications

Experiments were performed in Mazak Nexus 510C-II machine tool for the simulated cases. Different spindle speeds and axial depth of cuts for two milling tools are used and the stability of the process is evaluated. Two different variable helix tools with alternating and linear variations and constant pitch angles at the tip of the tools are used in the chatter tests (see Table 2.2).

Since the helix variations of both tools are known, the stability diagrams can be generated easily by following the procedure given in section 3. In order to be able to see the effect of the helix variation on the stability limits, stability diagrams for the regular, i.e. non-variable tool, are also generated.

In the experiments, several axial depth of cuts at different spindle speeds for both linearly varying and alternating helix tools are used, and the process status is identified as stable, marginal and chatter. Microphone and laser sensor are used to detect chatter. Also, the surface photos of each test are evaluated to confirm the stable and unstable regions. Experimental set up can be seen in Figure 2.21.

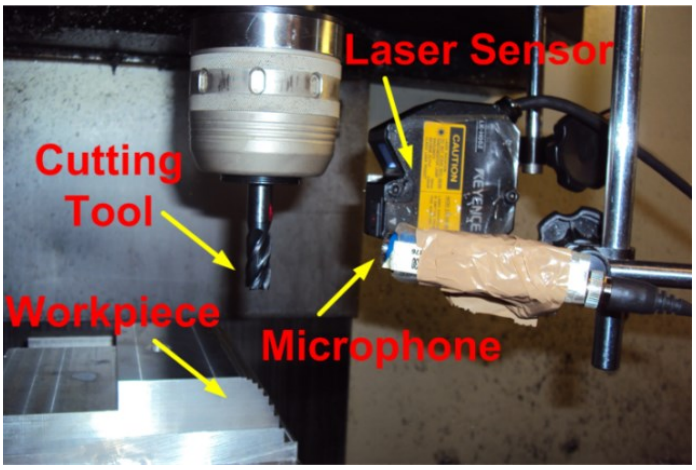

Figure 2.21. Test setup.

Experimental results for the first tool (alternating variation) are shown in Figure 2.22 together with the predictions. The sound spectrum and the machined surface pictures of point A (stable) and point B (unstable) are given in Figure 2.23 and Figure 2.24. Point A is in the stable zone as can be seen from the sound spectrum which shows no dominant frequency. Point B, on the other hand, is in the unstable region, and chatter is observed both in sound spectrum and the machined surface picture. As can be seen from the figure, the chatter frequency is at 3360 Hz and the surface quality is poor.

Based on these comparisons it can be concluded that the experimental results have good agreement with the simulations.

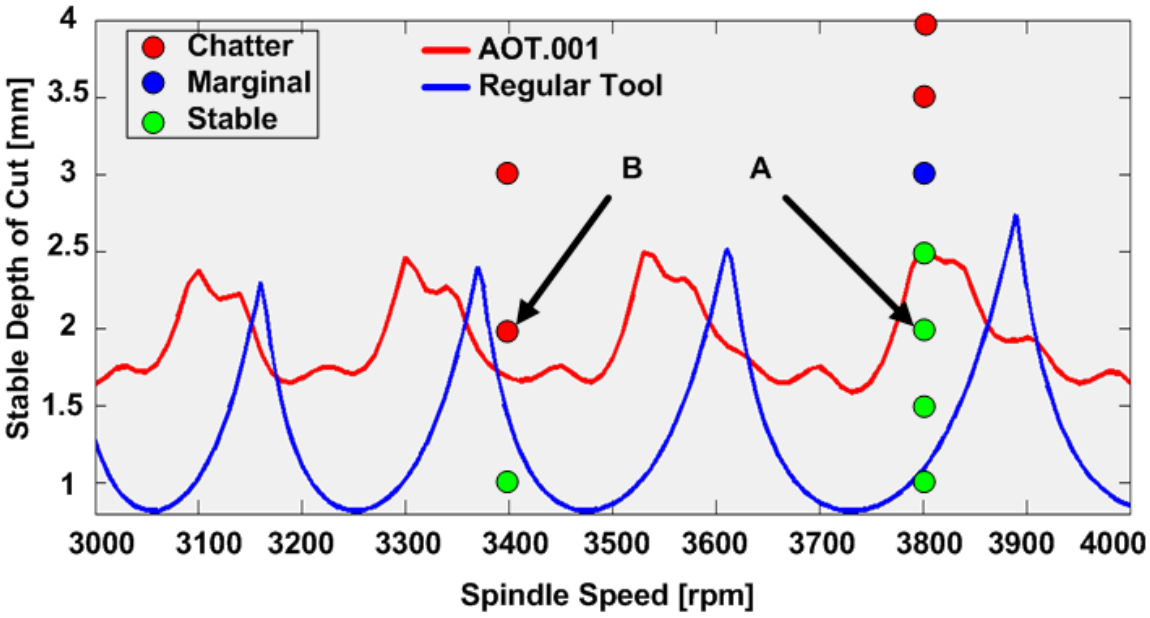

Figure 2.22. Stability diagram and test results for tool 1.

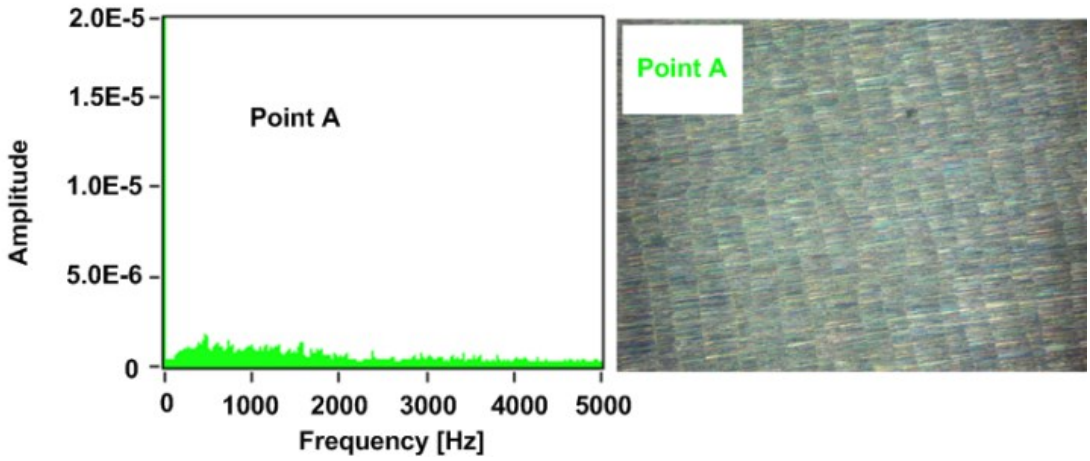

Figure 2.23. Sound FFT and surface photo of point A.

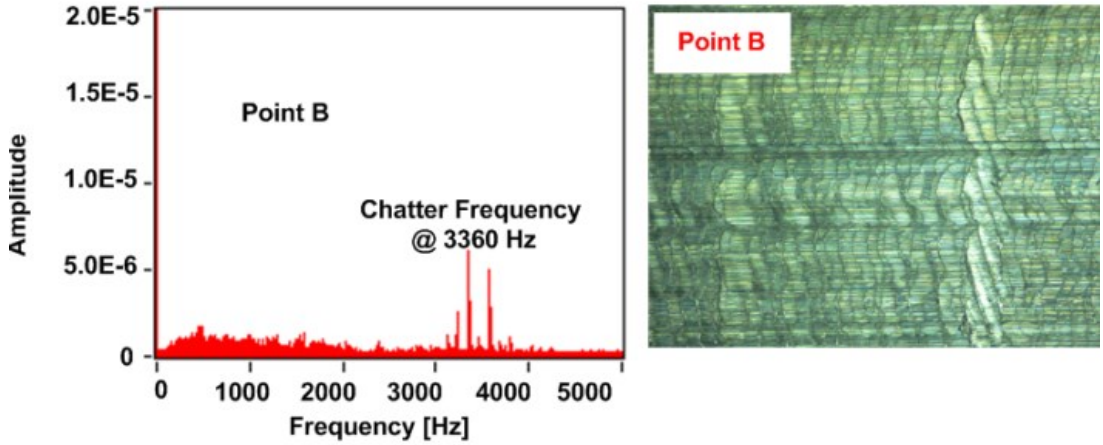

Figure 2.24. Sound FFT and surface photo of point B.

Because of the relatively low spindle speeds and tightness of the stability pockets, it is hard to perform cutting operation in these lobes. Hence, absolute stability limits become more important and decisive. Absolute stability limit for the regular milling tool is about 0.8 mm whereas for the alternating helix tool it is 2 times higher.

For the second (linear helix variation) tool, experimental results are shown in Figure 2.25 together with the predictions. Different axial depth of cuts and spindle speeds were tested where sound and surface photos were also analyzed. Results are identified as stable, marginal stable and chatter and show good agreement with the simulations.

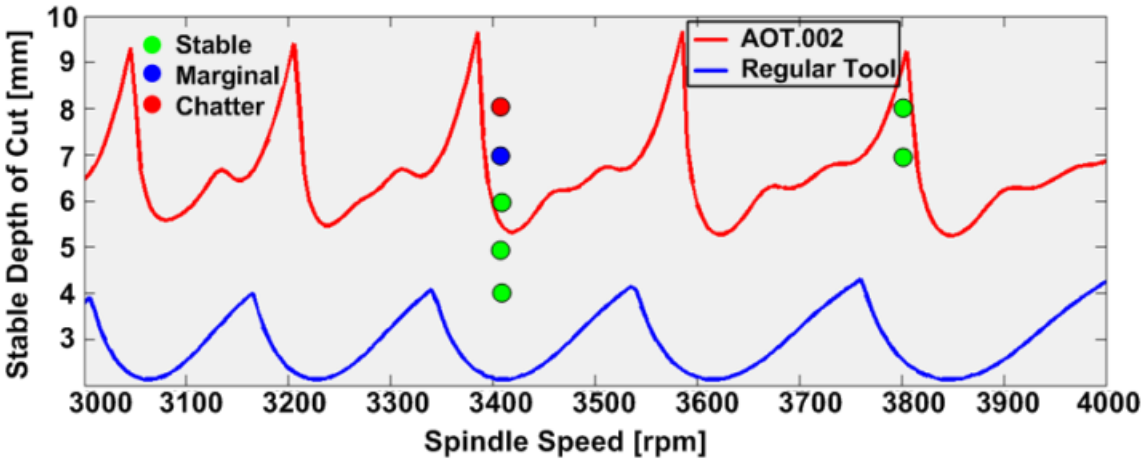

Figure 2.25. Stability diagram and test results for tool 2.

2.3.3. Effect of Radial Depth of Cut on Optimum Solution

Optimization studies have been done for one value of the radial depth of cut which is 3 mm for a 12 mm diameter end mill. At these conditions, comparisons of the variable pitch/helix and alternate/linear variations were also done. In the light of these simulations, one can identify the optimum tool and variation combination for the cutting operation. On the other hand, in order to be able to generalize the results to other conditions, different radial depth of cuts should be tried. In this section, comparisons of variable pitch/helix and alternate/linear variations for different radial immersions are made.

For the previous optimization simulations, 3 mm radial depth of cut value is used for all cases. For the alternate variation case, it has been shown that optimum designed variable helix tool is better than the optimum variable pitch tool. To generalize this rule, for a 12 mm diameter tool, radial depth of cut values are expanded into 1, 6 and 9 mm and it has been observed that the optimum variable helix tools with alternate variation still provides higher stability limits than the optimum variable pitch tool. Hence, it can be generalized that optimum designed variable helix alternate variation tools are always better than the optimum designed variable pitch alternate variation tool regardless of the radial immersion.

Similarly, optimum variable helix alternate variation tool provides higher stability limits than the optimum variable helix linear variation tool for the 3 mm radial depth of cut value. This situation is again generalized for different radial depth of cuts which are 1, 6

and 9 mm, and the optimum variable helix, alternate variation provides higher stability limits than the linear variation. So it can be concluded that alternate variation is better than the linear variation at every radial immersion condition for the optimum variable helix tools.

Finally, for the previous optimization studies, optimum variable pitch tools were compared for the alternate and linear variations and alternate variation was slightly provided higher stability limits for the 3 mm of radial depth of cut value. Moreover, it is expanded for the 1, 6 and 9 mm radial immersion values and it is observed that alternate variation still provides higher limits than the linear variation. Hence, it can be generalized that results of the optimization studies can be expanded for every radial immersion value in a similar way.

2.3.4. Design Methodology of Optimum Variable Tool Geometry

In the previous section, optimum tool geometry was determined for a given cutting condition through simulations. These simulations take long time to find the optimum pitch or helix variations. Determining the optimum pitch or helix variations by optimization simulations is the most reliable way but it can be computationally expensive. A design methodology would be very practical for industrial applications without losing time. Then, the main objective of this section is to develop a design method that gives the best tool geometry for a given cutting condition.

Investigation of the optimum tool geometry in the previous section where optimal pitch and helix variations were found is the first step of the design methodology. The relationship between the optimum variation and the minimization of the delay is the starting point of our design logic. Phase difference between the inner and outer modulations is expected to be equal to the corresponding delay generated by the optimal pitch or helix variations.

By taking this into consideration, optimum variations for the variable pitch tools are analyzed. Variable helix optimization studies are excluded because of the complexity of its delay system, i.e. the delay is variable along the axial depth due to changing pitch between successive cutting teeth. This means that, the phase difference at the bottom of the tool is not equal to the phase difference at any point of the tool along its axial depth of cut. One assumption would be to use an average phases along the axial depth of cut

but it is not guaranteed to provide reliable results. On the other hand, for variable pitch tools, there is only one phase difference between the successive teeth and it is the same all along the tool length. This allows us to analyze the optimum pitch variations and the phase difference in the system.

As stated before, analyzing of the optimum pitch variations is the starting point of the design methodology. The main aim of this analysis is to verify the relationship between the phase difference and optimum pitch variations.

Firstly, all optimum points at different spindle speeds and corresponding chatter frequencies are gathered from the optimization simulations by evaluating the 3D stability diagrams (Figure 2.13 and Figure 2.17). Also, optimum points at different radial depth of cut values are considered.

Secondly, for each of the optimum points gathered before, the length of a vibration wave is calculated by considering the spindle speed and chatter frequency at those points. Then, the equivalent wave length that corresponds the optimum pitch variation is calculated and denoted by the symbol of "β and shown in Figure 2.26.

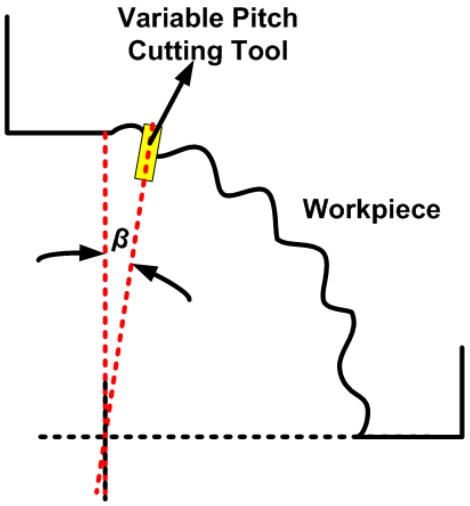

Figure 2.26. Equivalent wave length corresponds optimum pitch variation.

Then, the phase difference between the inner and outer modulations of vibration waves is calculated and denoted by the symbol of "ε" and shown in Figure 2.27.

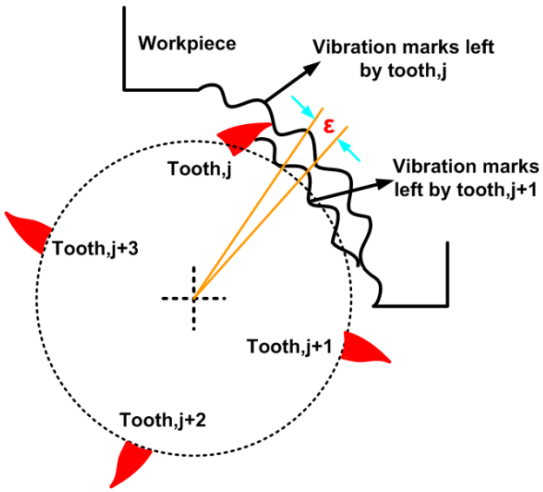

Figure 2.27. Phase difference between present and previous waves.

Finally, our decision criteria is tested for the values of β and ε, i.e. β and ε are checked whether they are equal to each other or not. One should expect that the equivalent wave length of optimum pitch variation should be equal or close to the phase difference between the inner and outer modulations of the vibration waves so that the delay is eliminated or minimized. The flowchart of the analysis of the optimum pitch variations and phase difference in the dynamic system is illustrated in Figure 2.28.

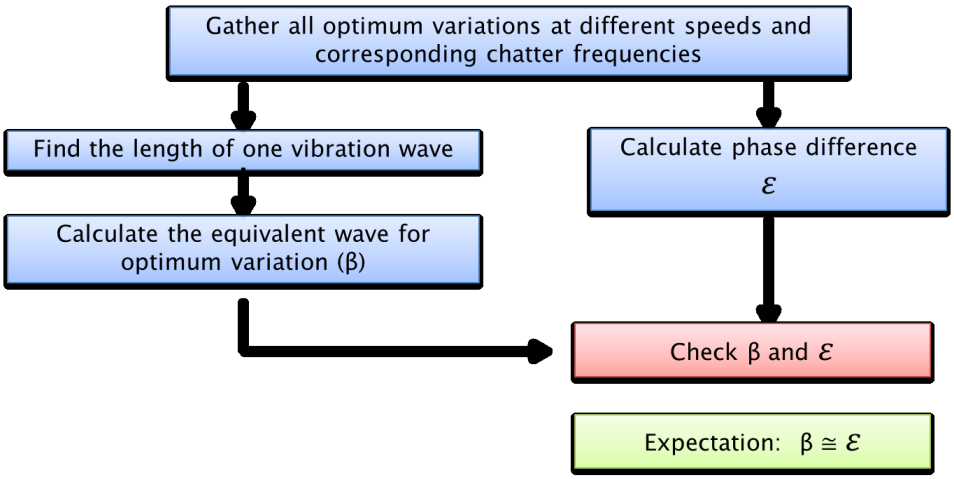

Figure 2.28. Flowchart of the optimum pitch variations analysis.

There are some formulations that are used while analyzing the optimum points. Length of one full vibration wave in terms of degree (θ) (See Figure 2.29) can be found as:

$$\left(\frac{\omega_c}{n_{rps}}\right)/2 = \theta \tag{2.12}$$

where ω_c and n_{rps} stands for chatter frequency and spindle speed (revolution per second) respectively. Equivalent vibration length for the corresponding optimum pitch variation (β) can be calculated in the same way by taking the ratio of one vibration wave and optimum pitch angle. Then, phase difference between the inner and outer modulations of the vibration waves can be calculated as follows:

$$\omega_c T = \varepsilon + 2k\pi \tag{2.13}$$

where T is the tooth passing period, ε is the phase difference and k is the number of full waves left in the surface.

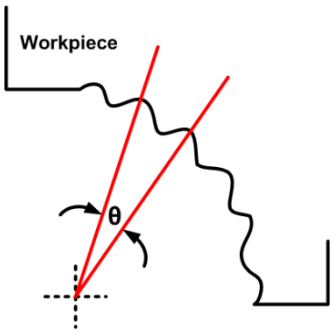

Figure 2.29. One full vibration wave on the cutting surface.

The analyses of the optimum points are concluded for different radial depth of cuts and spindle speeds. The results are listed in Table 2.3.

Table 2.3. Comparison of β and ε values for different radial immersions.

Radial Immersion	**Optimum Variations**			$\boldsymbol{\beta + \varepsilon}$
	Pitch Variation Measure [ΔP]	**Spindle Speed [rpm]**	**Chatter Frequency [Hz]**	
1 mm	8.8°	3000	4124	0.932
	7.8°	3500	4120	1.0308
	8.1°	3750	4143	0.9815
	9.4°	3800	4181	0.9148
3 mm	9.7°	3000	4062	1.005
	9.2°	3750	4064	0.87
	9.8°	4000	4066	0.894
6 mm	4.3°	3350	4024	0.988
	6.8°	3350	4024	1.057

	9.3°	3350	4024	1.127
	7.2°	3550	4030	0.9127
	9.9°	3550	4023	1.00

Table 2.3 shows the results of the pitch variation and phase difference analysis. $\beta + \varepsilon$ value is tested to check whether the optimum pitch variation measure cancels out the phase difference in the system or not. The values that are almost equal to 1, means that optimum pitch angle variation fully cancels out the phase difference. The other values which are almost 1, i.e. 0.932 and 1.127, minimize the delay in the system and increase the stability limits.

For the 1 mm of radial immersion value, optimum points which are 7.8° at 3500 rpm and 8.1° at 3750 rpm spindle speed show good agreement with our design criteria which based on the equality of β and ε values and the sum of these values are almost equals to 1. On the other hand, other optimum pitch variations minimize the delay in the system and increase the stability limits. The sum of the β and ε values for those points are nearly 1 and it helps us to understand that the delay is minimized at those pitch variations.

For the 3 and 6 mm radial immersion conditions, optimum points are exactly same as the phase difference in the system. This proves the fact that the optimum pitch variation cancel out the phase difference in the system, alters the delay and maximize the stability limits. Hence, it can be concluded that the optimum pitch variation is equal to the phase difference in the dynamic system and this enables us to develop the design methodology of optimum pitch geometry.

These previous analysis help us to understand the relation between the optimum tool geometry and phase difference in the system. Although the optimum pitch variation can be found by equating the phase difference to the corresponding wave length of optimum pitch variation, the chatter frequency is still required to find optimum geometries. Corresponding chatter frequency for the optimum pitch variation, on the other hand, can only be calculated in consequence of optimization simulations. As mentioned before, our aim is to develop a design methodology without making many simulations. Hence, a

new iterative method is developed to find the optimum pitch variation in a time efficient manner.

In the first step of the iterative method, first the target spindle speed must be specified. The cutting speeds in those applications are selected based on productivity and tool life requirements, so it is usually known by process planners. Then, the modal parameters are identified by modal tests conducted on a tool which has as close geometry as possible to the tool to be designed. This is a critical point since the optimal pitch variation depends on the cutting speed and the modal properties which define the delay in the system. However, since the modal test has to be done on a regular tool (as the variable pitch angles are not known yet) there may be slight variations in the modal frequencies between the regular tool tested and the optimal tool designed which will have different flute spacing. This slight difference in the frequencies will have a very small effect on the optimal pitch angles. However, if the difference is not so small, then the spindle speed can be tuned to adapt the tool to the new modal frequencies. In any case, these variations are not expected to be of significant amount. After the natural frequency is identified from the FRF of the tool, then the chatter frequency and the phase difference is calculated for the regular pitch milling tool. After that, the calculated chatter frequency and the phase difference are used in the single frequency averaging method to determine the optimal pitch variation (ΔP). This pitch variation is then used again in the single frequency method to determine a new chatter frequency and phase difference. This iterative solution procedure is necessary since chatter frequency is affected by the pitch angles whereas the optimal pitch variation depends on the chatter frequency. The iterations are continued until a convergence in the calculated optimal pitch variations is achieved with a reasonable tolerance. Once the convergence is achieved, the iteration is stopped and the ΔP obtained in the final step is taken as the optimal picth variation.

For better understanding of the iteration based design methodology, a flowchart of the method is illustrated in Figure 2.30.

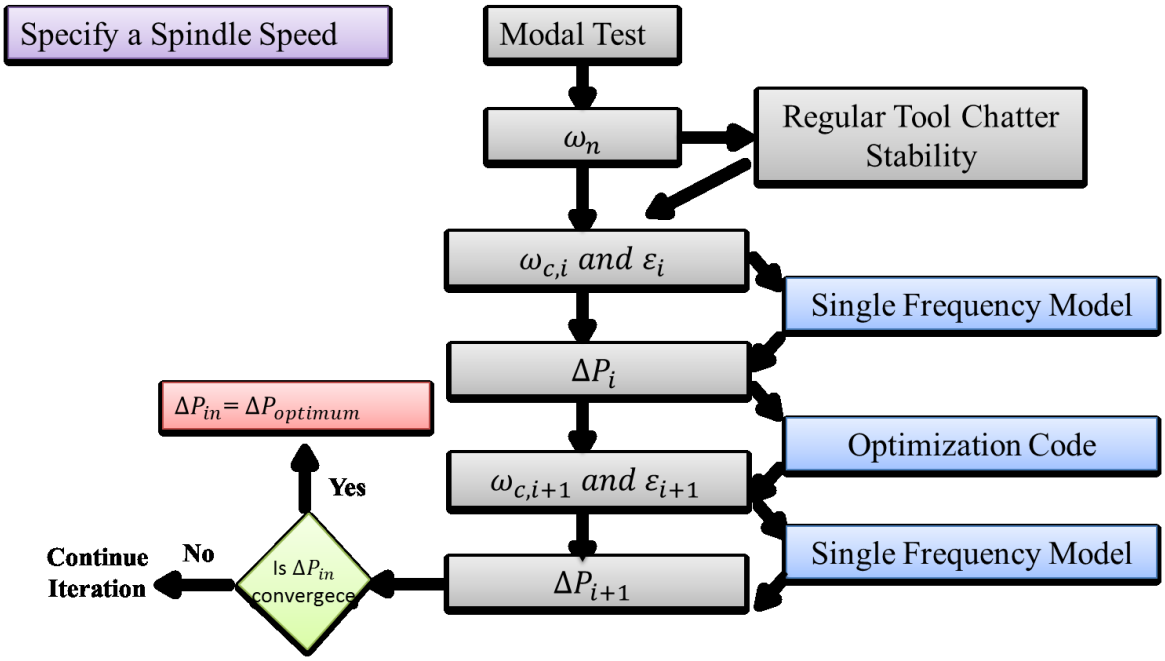

Figure 2.30. Flowchart of the iteration method for calculation of the optimal pitch variation.

Summary

In this chapter of the thesis, dynamics and stability of variable pitch and helix tools are modeled and solved in frequency domain and by using Semi-Discretization Method. Simulations were carried out to determine the optimum pitch and helix variations that provide higher stability limits. Both alternating and linear variations of variable helix and pitch milling tools are used in the optimization study. Results show that for the optimum pitch and helix angles, stable depth of cut limits are increased significantly. Then, simulations are verified by experimental chatter tests for two custom made variable helix tools. Sound data and surface photos are analyzed. Experiment results show good agreement with the simulations. After that, optimization studies are carried out and optimal design of variable pitch tools is investigated in detail. The relationship between the phase difference and the corresponding wave length of the optimum pitch variation is analyzed. The results show that optimum pitch variations determined by simulations are such that they cancel out the phase difference between the inner and outer modulations of the tool, thus maximize the stability limits. At the end of this chapter, a design methodology which is based on an iteration algorithm is developed.

This design method allows us to calculate the optimum pitch variation for a given condition without time consuming stability simulations.

CHAPTER 3

DYNAMICS AND CHATTER STABILITY OF SIMULTANEOUS MILLING OPERATIONS

Simultaneous machining operations have been continuing to spread in various sectors due to various advantages they offer particularly in aerospace and defense industries where the manufacturing of thin walled parts are limited by chatter vibrations. Parallel turning and parallel milling are two common examples of simultaneous machining operations which are usually performed on multi-purpose machine tools. Parallel milling involves more than one milling tool cutting the same or different surfaces at the same time. Cutters can be located at the same or different spindles or turrets. Parallel milling has the potential to increase productivity if correct machining conditions are used. As in standard machining operations, chatter vibrations may limit the full potential for productivity in parallel milling, too. On the other hand, if milling conditions are selected properly, chatter-free material removal rate can be increased. In such a case, dynamics cutting forces on both tools may cancel each other and increasing stability limits. Workpiece dynamics have great impact on the stability of parallel milling process due to its effects on dynamic coupling of two cutting tools.

Dynamics of the simultaneous milling operation is more complex compared to conventional single tool milling due to the existence of dynamic coupling between the tools and the workpiece. Workpiece dynamics have also great impact on the stability of parallel milling processes. If the workpiece is not flexible, dynamic coupling may exist only between the cutting tools through the machine tool structure. If there is no dynamic coupling between the tools they behave like two separate single-tool milling operations. Therefore, two sources of the dynamic coupling can be discussed in parallel milling

operations. First one is the dynamic workpiece compliance that the first cutting tool affects the dynamics of the other through a flexible workpiece (Figure 3.1 (a)). The second type of dynamic coupling is due to the dynamic machine compliance. This type of dynamic coupling is generally rare since the path between two tools is usually very long and rigid (Figure 3.1 (b)).

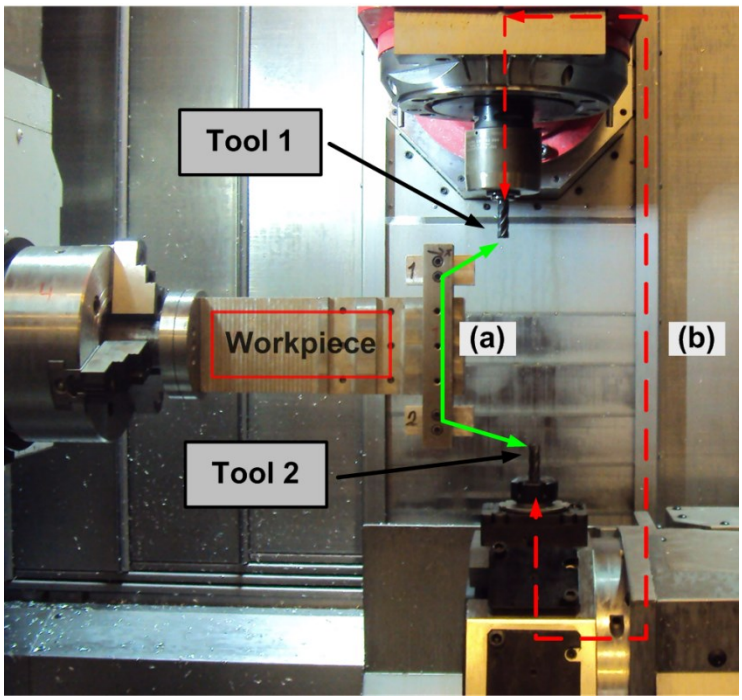

Figure 3.1. Illustration of dynamic couplings a) workpiece compliance b) machine tool compliance.

3.1. Dynamics of Parallel Milling Operations

Unlike the conventional single tool milling operations, cross transfer functions of both cutting tools and workpiece must be identified to be able to determine the stability lobes in simultaneous milling. In parallel milling, the machined part is excited by the cutting forces generated from both tools. Thus, each cutting tool is affected from the cutting forces originated from itself and the other cutting tool. At this point, identification of cross transfer functions is critical and significant for the dynamics and chatter analysis of the parallel cutting process. Dynamic cutting forces on two cutting tools are also dependent on each other and must be solved together.

3.1.1. Dynamic Responses and Chip Thickness Definition

In order to derive the dynamic cutting force expressions, dynamic responses at the tool-workpiece contact points should be identified. As shown in Figure 3.2, 1 and 2 refers to the contact points of the cutter 1 and the cutter 2 with the workpiece, respectively. The machined stock is flexible, so there is dynamic interaction between point 1 and 2. When both cutting tools perform the operation simultaneously, generated forces at point 1 affect also the dynamic response at point 2 and vice versa.

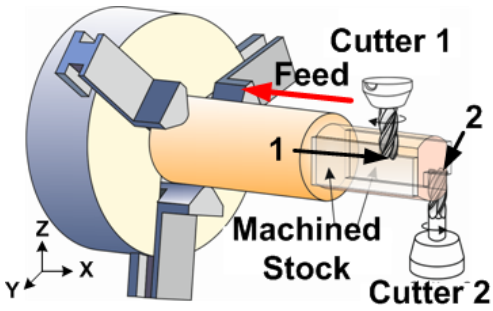

Figure 3.2. Geometry of simultaneous milling.

Dynamics responses at the first and the second points can be formulated as follows:

$$R_{ix} = F_{ix}G^{T}_{ixx} + F_{ix}G^{w}_{iixx} + F_{iy}G^{w}_{iiyx} + F_{iy}G^{T}_{iyx} + F_{jx}G^{w}_{jixx} + F_{jy}G^{w}_{jiyx} + F_{jx}G^{coup}_{jixx} + F_{jy}G^{coup}_{jiyx} \quad (3.1)$$

$$R_{iy} = F_{iy}G^{T}_{iyy} + F_{iy}G^{w}_{iiyy} + F_{ix}G^{w}_{iixy} + F_{ix}G^{T}_{ixy} + F_{jy}G^{w}_{jiyy} + F_{jx}G^{w}_{jixy} + F_{jy}G^{coup}_{jiyy} + F_{jx}G^{coup}_{jixy} \quad (3.2)$$

where $i\ and\ j = (1,2)$ indicates the first and second contact points, respectively. F_{ia} is the dynamic cutting force at i^{th} contact point in direction a $(a = x, y)$. Similarly, G^{w}_{ijab} is the workpiece transfer function measured at point "i" along the "a" direction and excited at point "j" along the "b" direction.

Response at point 1 is affected by the first and second cutting tool's dynamic forces, (F_1) and (F_2). Dynamic coupling between the points 1 and 2 is represented by the cross talk transfer functions G^{w}_{12} and G^{w}_{21}. G^{coup}_{12} is the cross transfer function due to the compliance through the machine structure.

Dynamic responses at points 1 and 2 include tool and workpiece vibrations which are caused by the dynamic forces from both tools are shown below.

$$\Delta x_1 = [x_1^T(t) - (x_1^w(t) + x_2^w(t))] - [x_1^T(t-\tau_1) - (x_1^w(t-\tau_1) + x_2^w(t-\tau_2))] \quad (3.3)$$

$$\Delta y_1 = [y_1^T(t) - (y_1^w(t) + y_2^w(t))] - [y_1^T(t-\tau_1) - (y_1^w(t-\tau_1) + y_2^w(t-\tau_2))] \quad (3.4)$$

where $x_1^T(t)$ and $x_1^w(t)$ are the displacements of the first tool and the workpiece (due to the first tool) in the x direction and $x_2^w(t)$ is the displacement in the x direction due to the second tool's contribution. The second part of the dynamic chip thickness represents the terms which belong to the previous pass which is one spindle revolution period $(\tau_1 - \tau_2)$ before on the same surface. Thus, the dynamic chip thickness for the first tool can be written as;

$$h_1 = \Delta x_1 sin\emptyset_{j1} + \Delta y_1 cos\emptyset_{j1} \quad (3.5)$$

where h_1 is the dynamic chip thickness at point 1 and $\emptyset_{j1}$is the immersion angle of the first tool. Dynamic chip thickness for the second cutting tool can be written in a similar way for $\emptyset_{j2}$.

3.1.2. General Force Formulation of Parallel Milling

Derivation of the force equations for parallel milling is similar to that of conventional milling [6]. Dynamic cutting forces in tangential, radial and axial directions for both cutting tools can be written as follows:

$$F_{ti} = K_{ti} a_i h_i \ , \ F_{ri} = K_{ri} a_i h_i \ , \ F_{ai} = K_{ai} a_i h_i \quad (3.6)$$

where K_{ti}, K_{ri} and K_{ai} are tangential, radial and axial cutting force coefficients, respectively, and a_i is the axial depth of cut. Then, the milling forces in x and y directions can be given as;

$$\begin{aligned} F_{xi} &= -F_{ti} cos\theta_{ji} - F_{r1} sin\theta_{ji} \\ F_{yi} &= \ F_{ti} sin\theta_{ji} - F_{ri} cos\theta_{ji} \end{aligned} \quad (3.7)$$

Force equations for both cutting tools can be written as,

$$\begin{Bmatrix} F_{xi} \\ F_{yi} \end{Bmatrix} = \frac{1}{2} K_{ti} a_i \begin{bmatrix} \alpha_{xxi} & \alpha_{xyi} \\ \alpha_{yxi} & \alpha_{yyi} \end{bmatrix} \begin{pmatrix} \Delta_{xi} \\ \Delta_{yi} \end{pmatrix} \tag{3.8}$$

α_{abi} is the directional dynamic force coefficient for the i^{th} tool in "a" and "b" directions, where $i = 1,2$. The directional dynamic cutting force coefficients are the same as in conventional milling process [32].

If Δx_i and Δy_i in Equation 3.8 substituted with Equations 3.3 and 3.4, the general form of the characteristic force equation is obtained as follows:

$$\begin{Bmatrix} \mathrm{F_{x1}} \\ \mathrm{F_{y1}} \\ \mathrm{F_{x2}} \\ \mathrm{F_{y2}} \end{Bmatrix} \mathrm{e}^{\mathrm{i}\omega_c \mathrm{t}} = \frac{1}{4\pi} [CPM] \bullet [DM] \bullet [APD] \bullet [OTF] \begin{Bmatrix} \mathrm{F_{x1}} \\ \mathrm{F_{y1}} \\ \mathrm{F_{x2}} \\ \mathrm{F_{y2}} \end{Bmatrix} \mathrm{e}^{\mathrm{i}\omega_c \mathrm{t}} \tag{3.9}$$

[CPM] is the cutting parameters matrix consisting of dynamic cutting force coefficient (K_{ti}), number of teeth (N_{ti}) and stable depth of cuts (a_i) for each tool. The explicit form of the [CPM] is shown in Equation 3.10.

$$[CPM] = \begin{pmatrix} K_{t1} N_{t1} a_1 \\ K_{t1} N_{t1} a_1 \\ K_{t2} N_{t2} a_2 \\ K_{t2} N_{t2} a_2 \end{pmatrix} \tag{3.10}$$

3.1.2.1. Delay Matrix and Transfer Functions Matrix

Unlike for the conventional milling processes, in parallel milling there are two delays, τ_1 and τ_2, since in general the rotational speeds are different for both tools. Both dynamic responses are affected by these two delay terms which make them dynamically coupled. As long as different delay terms affect dynamic response for each point, they can be grouped into a single matrix called as delay matrix or [DM] (Equation 3.11). Each delay term in the matrix corresponds to its equivalent force and transfer function pair in the general force equation.

$$[DM] = \begin{bmatrix} 1 - e^{-jwc\tau_1} & 1 - e^{-jwc\tau_1} & 1 - e^{-jwc\tau_2} & 1 - e^{-jwc\tau_2} \\ 1 - e^{-jwc\tau_1} & 1 - e^{-jwc\tau_1} & 1 - e^{-jwc\tau_2} & 1 - e^{-jwc\tau_2} \\ 1 - e^{-jwc\tau_1} & 1 - e^{-jwc\tau_1} & 1 - e^{-jwc\tau_2} & 1 - e^{-jwc\tau_2} \\ 1 - e^{-jwc\tau_1} & 1 - e^{-jwc\tau_1} & 1 - e^{-jwc\tau_2} & 1 - e^{-jwc\tau_2} \end{bmatrix}_{4\times4} \tag{3.11}$$

Due to the dynamic coupling, cross transfer functions play an important role on the dynamics of parallel milling processes. The transfer function matrix includes all direct

and cross transfer functions of cutting tools, workpiece and machine compliance as given below:

$$\begin{bmatrix} G^{T}_{1,xx} + G^{w}_{11,xx} & G^{T}_{1,xy} + G^{w}_{11,yx} & G^{w}_{21,xx} + G^{coup}_{21,xx} & G^{w}_{21,yx} + G^{coup}_{21,yx} \\ G^{T}_{1,yx} + G^{w}_{11,xy} & G^{T}_{1,yy} + G^{w}_{11,yy} & G^{w}_{21,xy} + G^{coup}_{21,xy} & G^{w}_{21,yy} + G^{coup}_{21,yy} \\ G^{w}_{12,xx} + G^{coup}_{12,xx} & G^{w}_{12,yx} + G^{coup}_{12,yx} & G^{T}_{2,xx} + G^{w}_{22,xx} & G^{T}_{2,xy} + G^{w}_{22,yx} \\ G^{w}_{12,xy} + G^{coup}_{12,xy} & G^{w}_{12,yy} + G^{coup}_{12,yy} & G^{T}_{2,yx} + G^{w}_{22,xy} & G^{T}_{2,yy} + G^{w}_{22,yy} \end{bmatrix}_{4\times4} \tag{3.12}$$

The first two columns of transfer function matrix are related with the dynamics first cutting tool whereas the last two columns are relevant with the dynamics of second tool. Hence delay terms in the equation (11) should correspond to the correct transfer function pair in the transfer function matrix given by equation (12).

On the other hand, the matrix that is denoted as [*OTF*], is the Oriented transfer function matrix which is a four by four matrix obtained by the multiplication of the transfer function matrix with the directional dynamic cutting force coefficients.

3.1.2.2. Relative Angular Position Offset

The angle between equivalent cutting tooth of the first and second tool is named as the relative angular position offset and shown in Figure 3.3. In parallel milling process, offset angle has the potential to change the whole dynamic behavior of the system creating an additional phase delay between the tool passing frequencies of each tool.

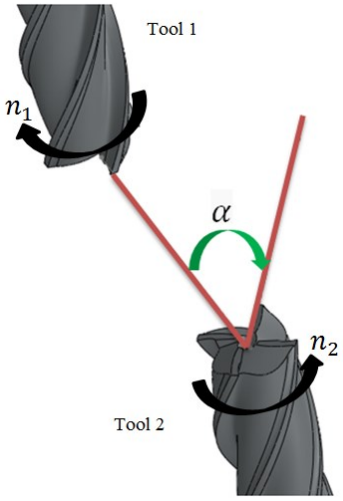

Figure 3.3. Angular offset between two milling tools.

Controlling of the angular offset during machining is almost impossible. Even if the spindle speeds are equal to each other, position of each equivalent tooth at the same time is hard to handle for both tools. However, since the offset angle causes another delay on the system, its effects on the stability needs to be investigated. The additional delay can be introduced to the milling equations as the $e^{\pm jw_c\vartheta}$ where,

$$\vartheta = \frac{\alpha}{60 * n_i} \tag{3.13}$$

α is the angular offset in radian and n_i is the spindle speed of one of the tool. If the second tool creates the phase shift, n_2 has to be considered in the equations. Angular delay offset needs to be inserted to the analytical equations beside the delay matrix by constituting as a four by four matrix, as following:

$$\text{Angular Position Delay Matrix} = \begin{bmatrix} 1 & 1 & e^{\pm jw_c\vartheta} & e^{\pm jw_c\vartheta} \\ 1 & 1 & e^{\pm jw_c\vartheta} & e^{\pm jw_c\vartheta} \\ 1 & 1 & e^{\pm jw_c\vartheta} & e^{\pm jw_c\vartheta} \\ 1 & 1 & e^{\pm jw_c\vartheta} & e^{\pm jw_c\vartheta} \end{bmatrix}_{4\times4} \tag{3.14}$$

Equation 3.9 represents an eigenvalue problem similar to the one obtained for conventional milling operations. On the other hand, in order to solve this eigenvalue problem, a new solution methodology has to be developed to find the stable depth of cut for each cutting tool for preset spindle speeds.

3.2. Chatter Stability of Parallel Milling Operations

The major difference in generating stability diagrams for parallel milling comes from the nature of the process which has two cutting tools with different spindle speeds. Another concern is that the relation between the chatter frequency and spindle speed cannot be established obviously. Due to the fact that there are two separate spindle speeds, chatter frequency cannot be linked directly to the spindle speeds. On the other hand, the chatter frequency is still unique; in other words there is a single chatter frequency that corresponds to two spindle speeds.

There are three cases considered for the solution of the stability problem. First one is that n_1 and n_2 are given beside the depth ratio and stable depth of cuts of both tools can be determined. In the second case, process parameters of one of the cutting tools are

fixed to obtain the stability diagram for other cutting tool. For example, the spindle speed and depth of cut of the second tool is preset. Then the stability diagram for the first cutting tool can be generated by solving the characteristic force equation of the parallel milling system. However, because the one of the spindle speed is not defined, the delay matrix cannot be generated completely and to be able to solve the characteristic equation, iteration method has to be applied. In the third case a_1 and a_2 are given, then the force equation is solved to determine the n_1 and n_2. However, selection of the axial depth of cuts at first may yield additional problems on the solution of the force equation. For instance, selection of an axial depth of cut that is already above from the stable depth of cut gives zero solution or empty set. On the other hand, if the axial depth of cut is selected below from the stable depth of cut, there are infinitely many solutions because at all the set of spindle speeds the solution becomes valid. Thus second and third cases are not suitable to implement whereas the first case is the most feasible and proper solution method. In this thesis first case is taken into consideration in all simulations.

In the beginning of the solution, the depth ratio (a_r) which is a_2/a_1 is defined, and then the matrices are re-arranged to simplify the eigenvalue solution. Equation (9) has a non-trivial solution only if its determinant is zero:

$$det(I - \lambda[A]) = 0 \tag{3.15}$$

where I is the 4×4 identity matrix. [A] is the multiplication of [OTF], [DM] and [CPM] matrices. λ in Equation 15 is defined as:

$$\lambda = \frac{1}{4\pi}[K_{t1} N_{t1} a_1] \tag{3.16}$$

Finally, the characteristic eigenvalue problem can be solved for predefined value of a_r, and then the stable depth for the first cutting tool a_1 can be calculated as follows:

$$a_1 = (4\pi\lambda / K_{t1} N_{t1}) \tag{3.17}$$

The eigenvalue solution provides four roots (eigenvalues) which, in general, are complex. However, considering Equation 15 and λ definition, the real part of the eigenvalues with zero imaginary part must be sought for the solution. The stability diagram for the first tool is constructed by calculating the stable depths for different

spindle speeds. The stable depths for the second cutting tool can easily be identified using the preset depth ratio, (a_r).

3.3. Simulations and Experimental Results

The presented analytical parallel milling chatter stability frequency method is simulated for different cases to analyze the effects of both cutting parameters on chatter stability and find out the optimum process parameters that offer high performance cutting conditions. In the first case, the effect of workpiece flexibility on the stable depth of cut is analyzed for zero angular position offset and stability diagram is constructed. Then, for different machining parameters like working modes of tools, number of tooth, radial depth of cuts and different spindle speeds of second tool, stability diagrams are generated and the effects are compared. In the second case, stability diagrams are generated for the case that have different modal parameters than the first case and the simulated case are verified my means of chatter tests on a multi-tasking machine tool (Mori Seiki NTX2000). At last case, a different workpiece is designed as thin walled part and effect of spindle speed of the cutting tools on the chatter stability is analyzed by constructing 3D graphs. Also, effect of in-process workpiece dynamics on the stability of process is investigated for the same case.

In the all three cases, in addition to the transfer functions of the tools, the workpiece transfer functions including the directional and point cross terms are also considered but the transfer functions for the machine tool (i.e. $G_{21,yx}^{coup}$) are taken as zero. The same cutting force coefficients are used for both tools since they are identical with 4 flutes and 12 mm diameter. Since the edge forces have no contribution on the regenerative mechanism, they are taken as zero.

3.3.1. First Case

The first case investigates the effect of flexibility of workpiece and cutting parameters on stability diagrams. Tangential cutting force coefficients (K_{tc}) are taken as 877 MPa for both tools. The spindle speeds for the first and the second tool are 12000 rpm and 4000 rpm, respectively. Radial depth of cut is 4 mm for both tools.

3.3.1.1. Workpiece Design and Modal Testing

The workpiece is designed to be more flexible than the cutting tools using FEA program. Modal analysis of the workpiece is performed in Abaqus© software and shown in Figure 3.4.

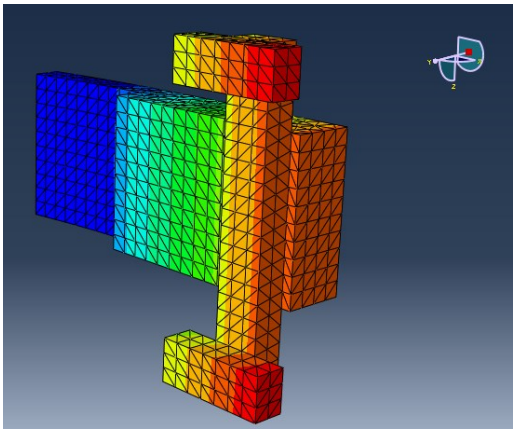

Figure 3.4. Modal analysis of the workpiece in Abaqus© software.

By investigating the modal analysis data from the software, the optimum design geometry of the workpiece is determined. Final geometry and technical drawing of the workpiece is sketched in Figure 3.5 and the parts of the workpiece are marked on the Figure 3.6.

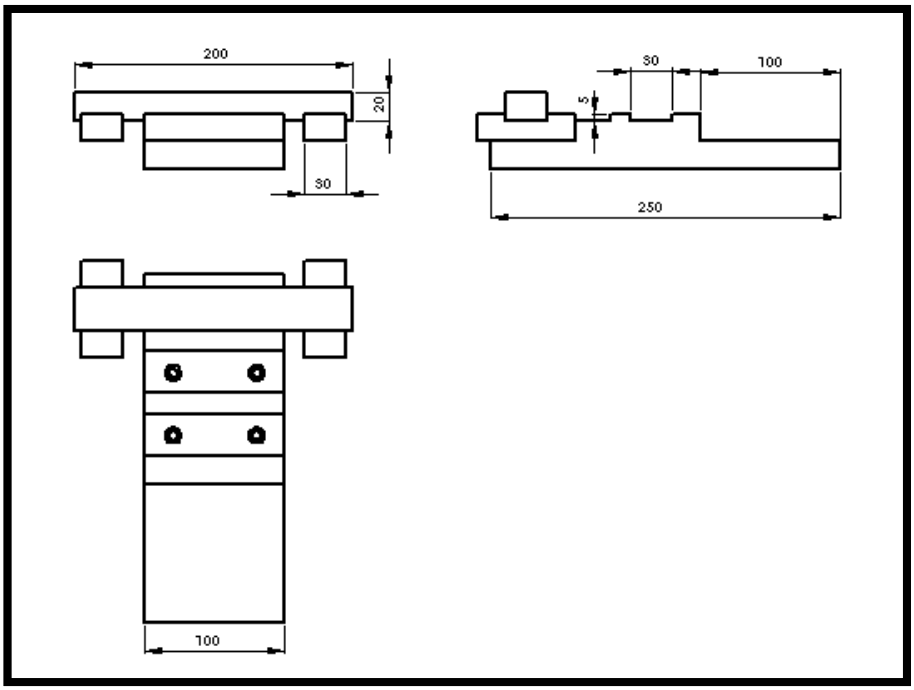

Figure 3.5. Technical drawing of the workpiece.

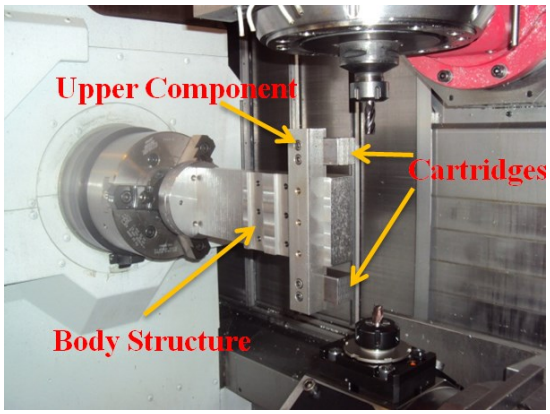

Figure 3.6. Designed workpiece.

The material of the workpiece body structure is cold drawing steel and the cartridges are selected aluminum. In order to be able to change the workpiece dynamics the cartridge holder can move on the body by changing the fixing position. The main objective here is to design a workpiece structure such that the variation of the workpiece dynamics due to cutting is minimized. Tools only cut the cartridges and the main structure of the workpiece is conserved so the workpiece dynamic does not change significantly during machining. Also different types of workpiece material can be used by easily changing the cartridges to change the whole workpiece.

In order to determine the tool and the workpiece dynamics, modal testing is performed for both workpiece and tools as shown in Figure 3.7.

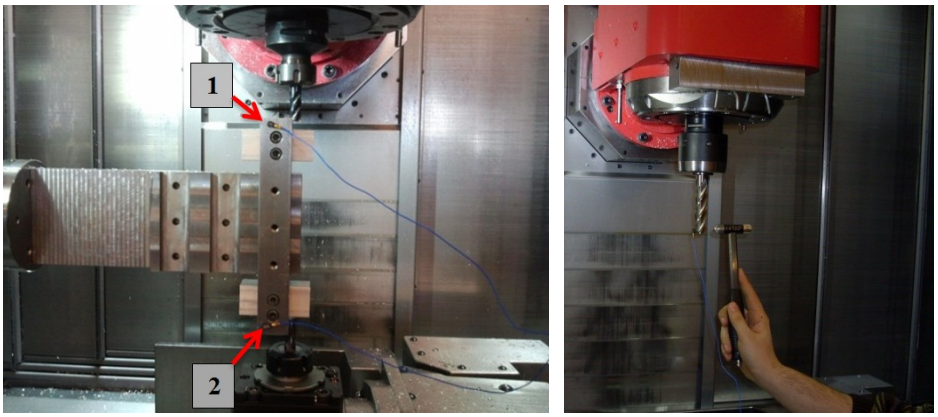

(a) (b)

Figure 3.7. Modal testing of (a) workpiece and (b) tools.

In the modal test, two accelerometers are attached at points 1 and 2 to determine the transfer functions at each point. The tools and the workpiece are excited by an instrumented hammer. Frequency responses of the workpiece and the tools are plotted together in Figure 3.8.

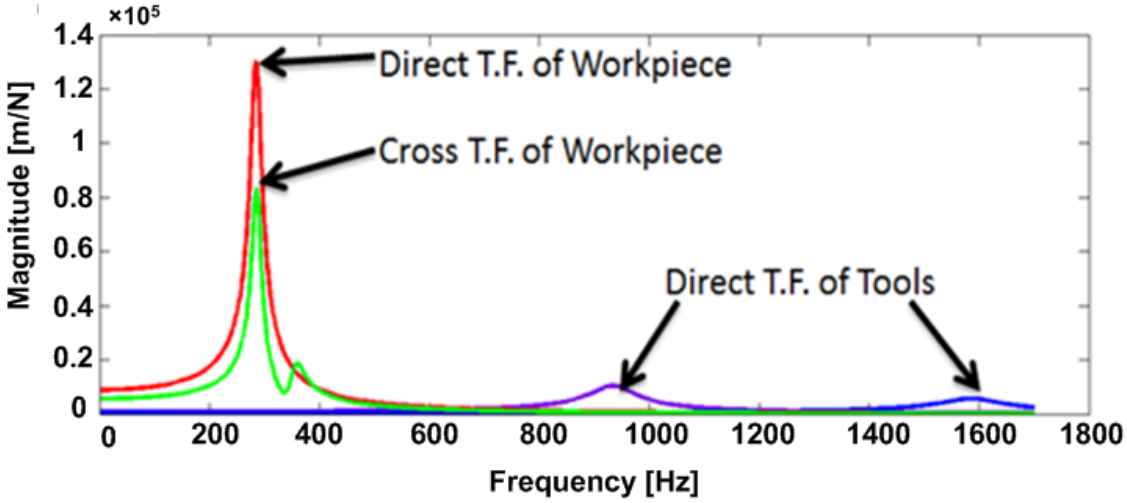

Figure 3.8. Frequency Response Function of workpiece and tools.

As expected the workpiece is an order of magnitude more flexible than the tools causing dynamic coupling between them. The measured modal data for the tools and the workpiece are given in Table 3.1 and Table 3.2, respectively. Only some important modal data for the workpiece is shown.

Table 3.1. Modal parameters of tools.

Modal Parameter of Tools	Tool 1		Tool 2	
	XX	*YY*	*XX*	*YY*
Natural Frequency *[Hz]*	935	940	1587	1594
Modal Stiffness *[m/N]*	1.09e7	1.18e7	2.43e7	2.41e7
Damping Ratio *[%]*	4.363	4.352	3.633	3.412

Table 3.2. Modal parameters of workpiece in different directions.

Modal Parameter of Workpiece	Gw11xx	Gw11yy	Gw12yy	Gw22yy
Natural Frequency *[Hz]*	593	284	285	278
Modal Stiffness *[m/N]*	1.73e07	1.12e06	2.19e06	1.14e+06
Damping Ratio *[%]*	2.487	3.43	2.766	4.052

3.3.1.2. Effect of Workpiece Flexibility on Process Stability

In the first example case, effect of workpiece flexibility on the chatter stability is investigated. The flexibility of the workpiece is varied for rigid, flexible and an intermediate states.

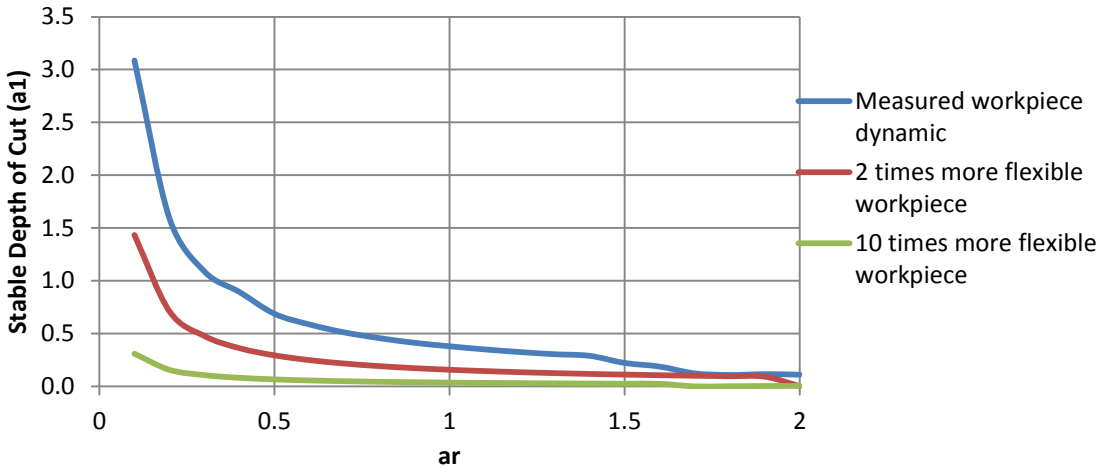

Figure 3.9. Effect of workpiece flexibility on stable depth of cuts.

The simulation result shows that workpiece dynamics have great impact on the stability of cutting process (Figure 3.9). If the tool is very rigid, the process becomes like two separate single milling operations due to lost coupling between the workpiece. In the first case, the measured workpiece modal data is used in the stability analysis which yielded stable depth of 3.08 mm. Then, flexibility of the workpiece is increased two times which resulted in the stable depth of cut to decrease down to 1.49 mm. In the last case, the workpiece becomes too flexible thus the stable depth of cut is decreased to 0.33 mm. While in the first case the workpiece is 12.5 times more flexible than the tools and in the last case it becomes 145 times more flexible. Other important point is that as the a_r ratio is increased, stable depth of cut of the first cutting tool is also decreased.

3.3.1.3. Effects of Cutting Parameters on Process Stability

Process parameters have significant effects on chatter stability of the parallel milling operation. In this section, effect of number of teeth, working modes of the tools, radial depth of cuts are investigated, respectively.

3.3.1.3.1. Effect of Different Number of Teeth on Stability

In this example case, number of tooth of the first cutting tool is changed as 2, 3 and 4 teeth and its effects on the stability of the parallel milling process is shown in Figure 3.10.

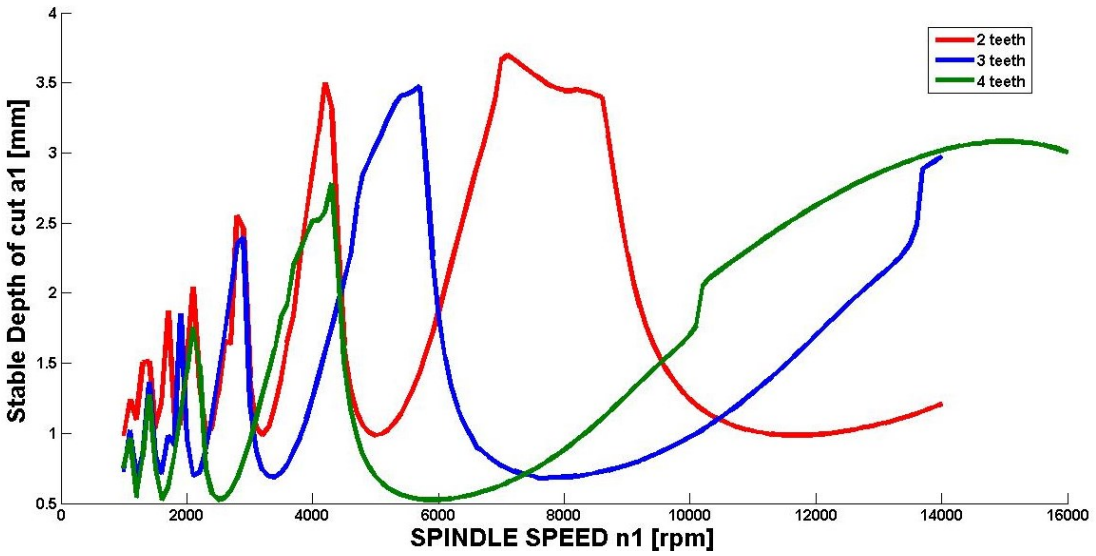

Figure 3.10. Effect of number of teeth on stability of the process.

As seen from the figure, different number of tooth changes the dynamics and stability of the operation. If the number of tooth on the cutting tool is decreased, absolute stability value is increased as seen from both Figure 3.10 and Figure 3.11. Another significant effect of the tooth number is the shifting of the diagram slightly to the right. Hence the maximum depth of cut at each stability lobe is changing according to the number of tooth.

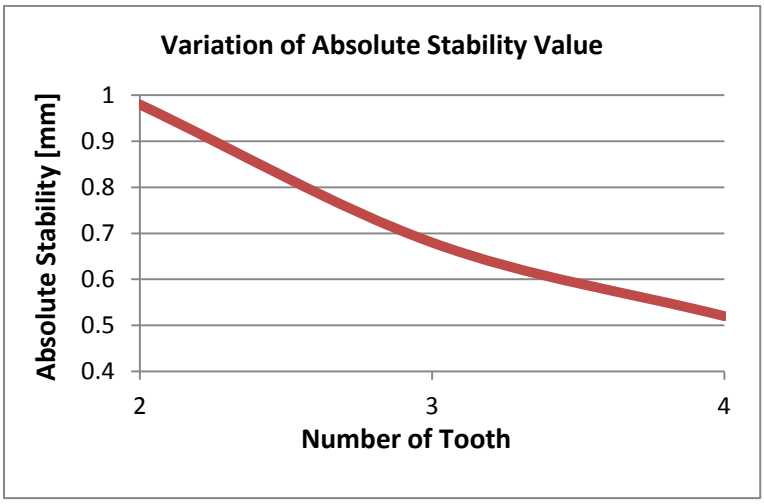

Figure 3.11. Variation of absolute stability value with number of tooth.

3.3.1.3.2. Effect of Working Mode of Cutting Tools

Working mode of the cutting tools has great impact on the stability of the process. If the modes are selected properly, the forces may cancel each other and stable depths of cuts

are increased (Figure 3.12). In this example case, effect of different working modes is demonstrated.

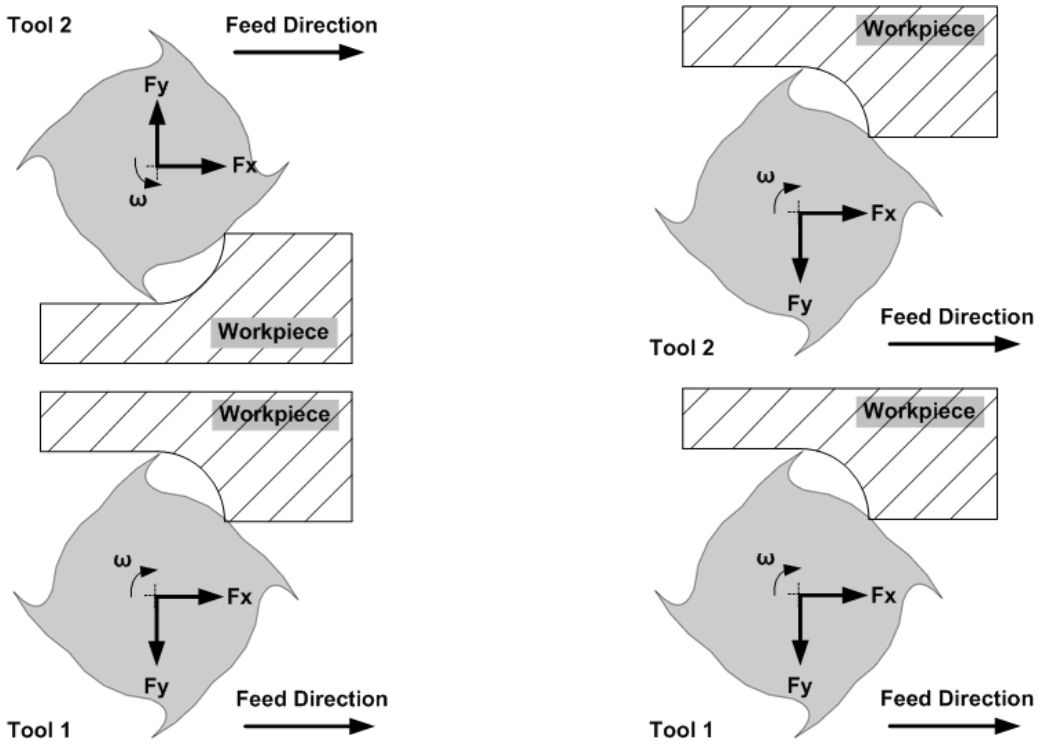

(a) (b)

Figure 3.12. Illustration of a) upmilling and b) downmilling operation in parallel milling.

First, the modes are selected as upmilling and downmilling for the first and second cutting tools, respectively. Then both cutting tools are performed upmilling operation. The difference between these two conditions is shown in Figure 3.13.

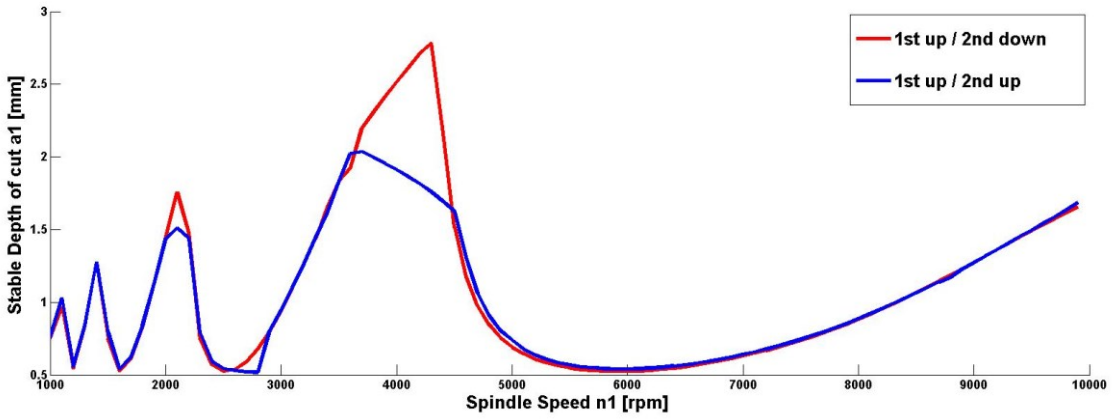

Figure 3.13. Effect of working modes to process stability.

The important point is that when the tools perform upmilling and downmilling together, the forces (or vibrations) along the y axis may cancel each other's, so the stability limit is increased in certain lobes. On the other hand, both upmilling operation of each tool cannot fulfill this condition and stability limit at some lobes is decreased.

3.3.1.3.3. Effect of Radial Immersion on Stability

In previous section, the effect of radial depth of cut on stability is shown indirectly. In single tool milling, the stable radial depth of cut is inversely correlated with the axial depth of cut. In this example case, the radial depth of cut of both cutting tools is changed as 4, 6 and 8 mm. The diameter of both tools is 12 mm and they have 4 flutes. Spindle speed of the first tool is fixed at 5000 rpm and the stability diagram of first cutting tool is generated as in Figure 3.14.

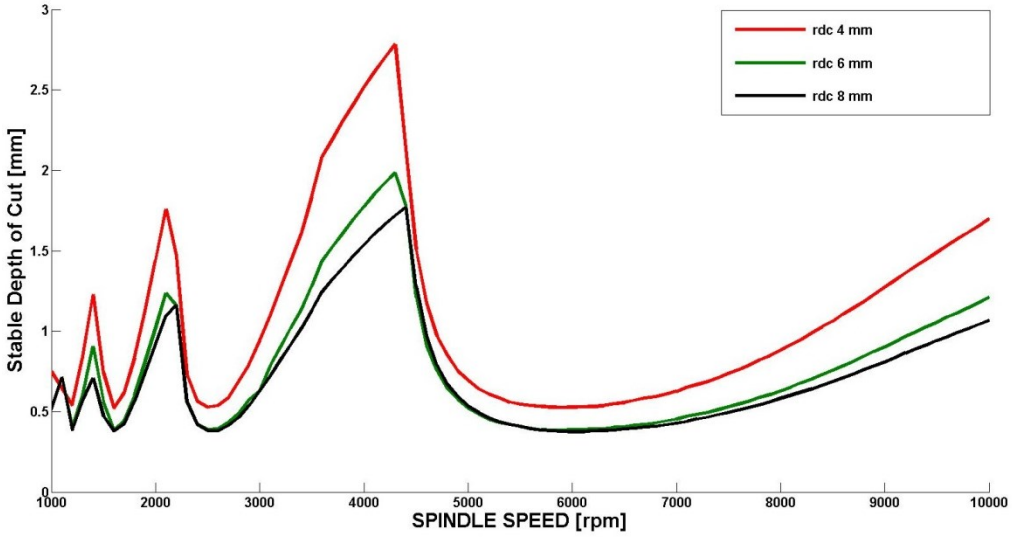

Figure 3.14. Effect of different radial depth of cut values on the stability diagram.

As seen from Figure 3.14, as the radial depth of cut is increased the stable depth of cut at any spindle speed is decreased, even the absolute stability value. As the tool diameter is 12 mm Figure 3.14 also shows diagrams for different the percentage of immersions as %33, %50 and %66 of the first and second tool.

3.3.2. Second Case

In this example case about the chatter stability of parallel milling operations, the workpiece with different modal parameters but the same body structure is investigated.

In order to be able to determine the frequency response functions and modal parameters of the workpiece and cutting tools, modal tests are performed by attaching two accelerometers at points 1 and 2 as shown in Figure 3.15

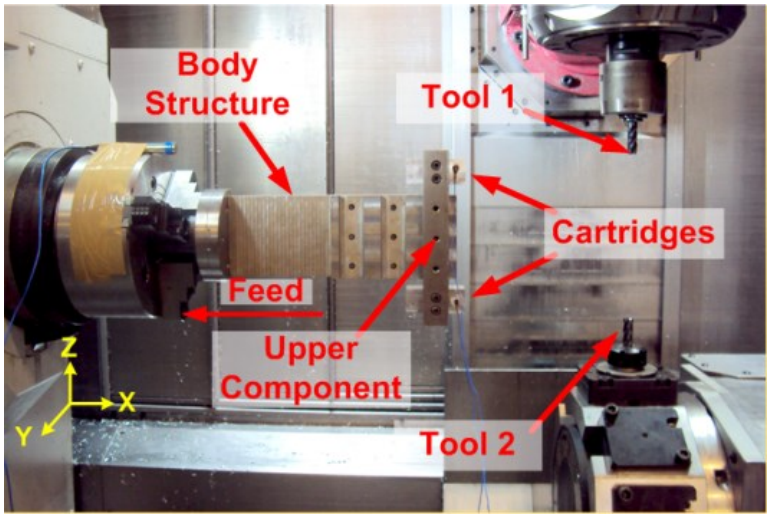

Figure 3.15. Workpiece and the test components for Case 2.

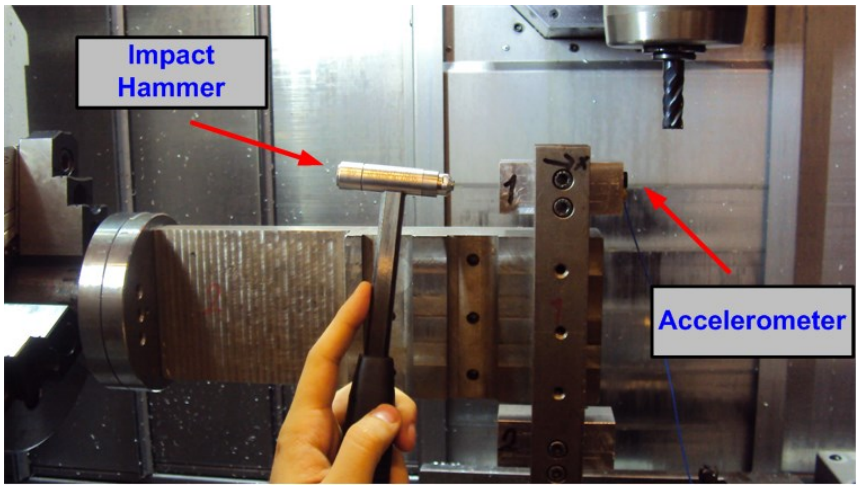

Figure 3.16. Test set up for modal (hammer) test.

The identified modal parameters of workpiece and cutting tools are listed in Table 3.3.

Table 3.3. Important modal parameters of workpiece and tools.

Transfer Functions	f_n[Hz]	k [N/m]	ζ [%]
Gw11yy	60	4.55+05	0.8
Gw12yy	60	5.33e+05	0.58
Gt1yy	3510	2.72e+07	1.288
Gt2yy	1680	1.13e+07	5.412

As expected the workpiece is an order of magnitude more flexible than the tools causing dynamic coupling between them like in Case 1. By solving the Equation 3.15, stable depths for the first tool are identified for corresponding spindle speeds in the frequency domain. The depth ratio is preset at 0.1 and the first tool performs up-milling whereas the second tool is in the down-milling mode. Both radial depth of cuts are 4 mm. The spindle speed of the second tool is fixed at 5000 rpm. Finally, the stability diagram shown in Figure 3.18 is obtained for the first tool.

Simulated cutting conditions are verified experimentally on a multi-tasking machine tool (Mori Seiki NTX2000) (Figure 3.17). Experimental cuts have been performed at different spindle speeds and depth of cuts to verify the stability diagram. Sound and accelerometer data are taken in each test. By analyzing the accelerometer data the tests are classified as chatter, marginally stable and stable. The acceleration spectrum for the sample points A and B are also shown in Figure 3.18. Results show relatively good agreement with the predictions.

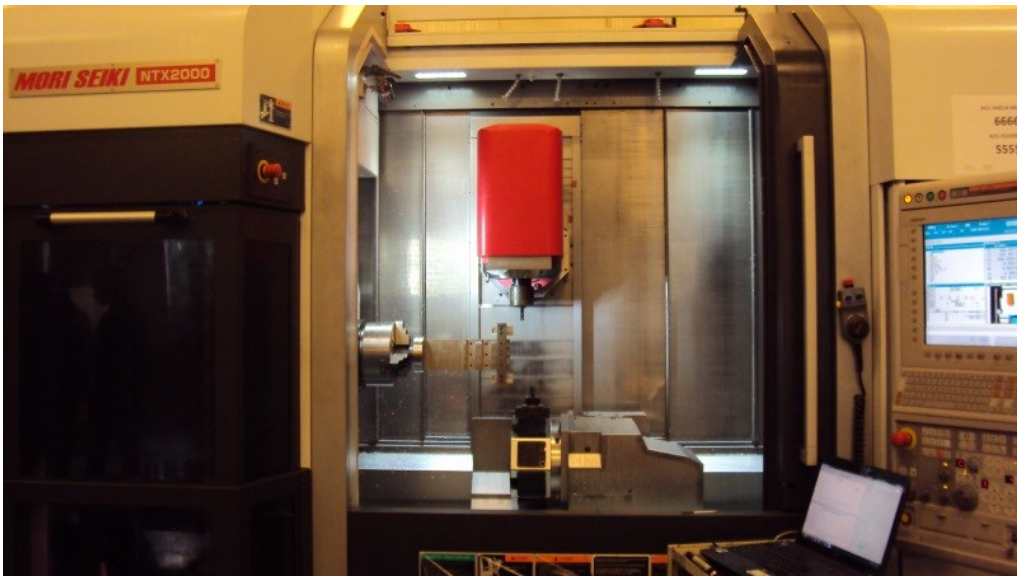

Figure 3.17. Mori Seiki NTX2000 multi-tasking machining centre.

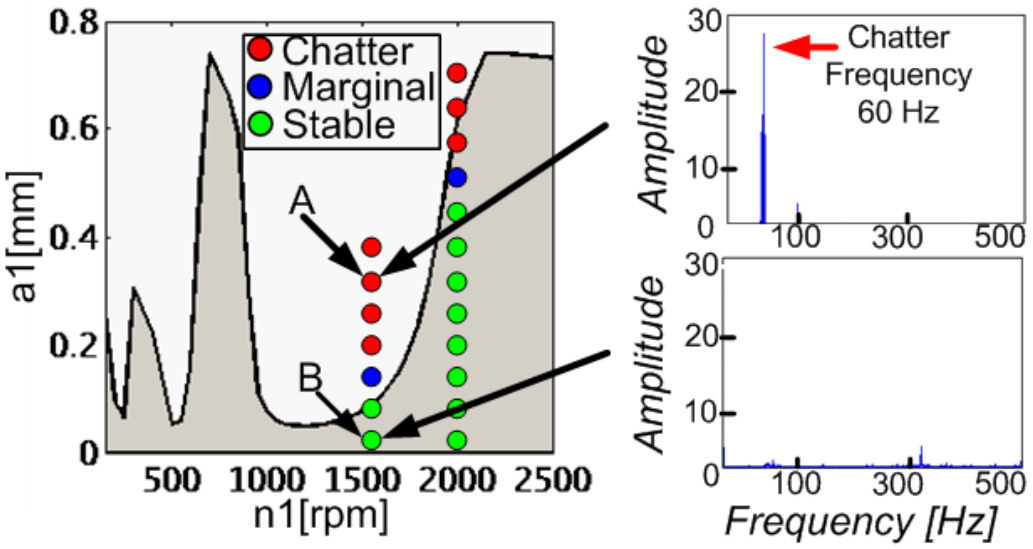

Figure 3.18. Predicted stability diagram and the experimental results.

3.3.3. Third Case

In this example case, stability diagram is generated by using the frequency domain model as in the first and second example cases. Then, the obtained stability diagram is verified by the time domain solution. Optimum spindle speed combinations of cutting tools for high performance machining conditions are found by constructing 3D stability diagrams. After that, effects of workpiece dynamics on the stability of the process are shown. Finally, predicted and simulated stability diagrams are verified through chatter experiments.

Unlike the first and second cases, thin-walled plate is designed as workpiece. The main objective of designing a thin-walled plate is to provide test conditions to analyze the effect of workpiece dynamics on the stability of process due to the mass removal during machining by two cutting tools. Another reason is to provide dynamic coupling between the tools.

In the computer environment, thin walled plate is designed in ANSYS© software. Three dimensions of the plate (length, width and thickness) are modified to create desired workpiece dynamics. The final designed part has 125 mm length, 70 mm width and 12 mm thickness (Figure 3.19). Aluminum (Al 6061) is selected as the workpiece material and the modal parameters both found from ANSYS and modal test are listed in Table 3.4. Cutting tools have the same dynamics as in the first and second case. It should be noted that the first mode of the system which is bending is taken into consideration in

the analysis as the most flexible and dominant mode of the system. The other modes of the system which are more rigid modes than the first mode have less influence on the dynamics of the system if the working frequency is far away these modes.

Table 3.4. Comparison of modal parameters of workpiece with modal test results and ANSYS© software.

Transfer Functions	f_n[Hz]		k [N/m]		ζ [%]	
	Modal Test	ANSYS	Modal Test	ANSYS	Modal Test	ANSYS
Gw11yy	427	421	1.16e+06	1.13e+06	2.002	2.004
Gw12yy	427	421	1.16e+06	1.13e+06	2.002	2.004

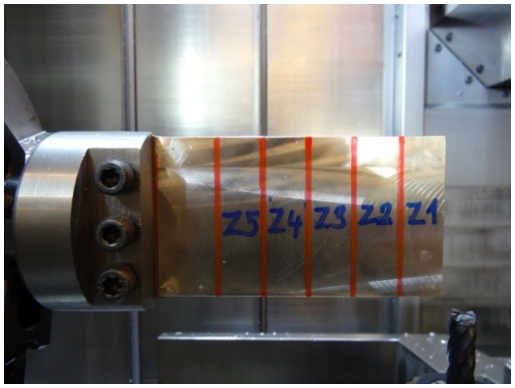

Figure 3.19. Designed workpiece.

First three modes of the thin walled plate are also shown in Figure 3.20. As stated before, the first mode of the workpiece is bending mode, the second mode is the torsional mode and the third mode is bending mode in z direction which is profoundly stiff.

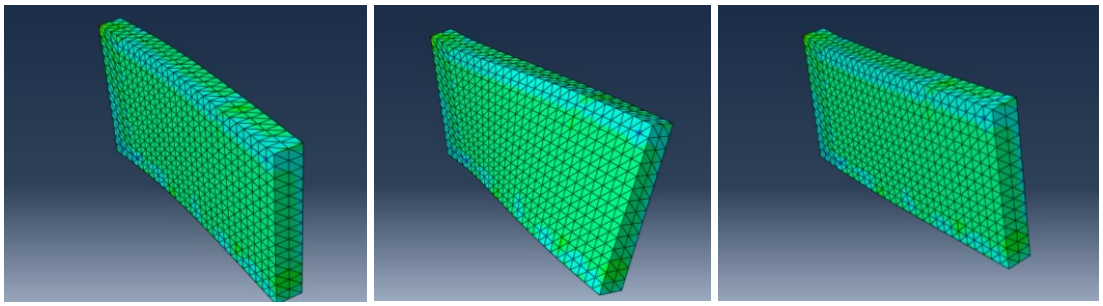

(a) (b) (c)

Figure 3.20. First three modes of the workpiece. (a) Bending mode (b) Torsional mode (c) Bending mode in z direction.

Since the plate is symmetrical, the direct and cross transfer functions at both points are equal to each other. The most flexible mode is the bending mode of the workpiece. In the simulations, the first tool is in up-milling mode with 4 mm radial depth of cut and the second tool is in down-milling mode removing 10 mm of radial depth. The depth ratio is fixed at 0.2.

Besides the workpiece dynamics, the spindle speed combination of the tools has a significant role on the stability limits offering a potential for maximization of the material removal rate. In this example, spindle speed of the second tool is varied between 1000 rpm and 6000 rpm and the resulting 3D stability diagram is shown in Figure 3.21.

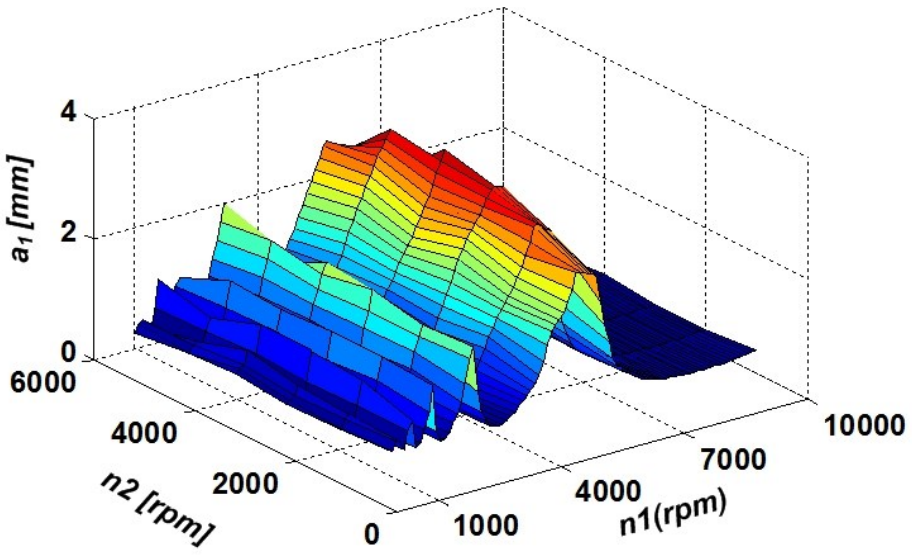

Figure 3.21. 3D stability diagram.

As shown in 3D stability diagram, variation of the spindle speed of the second tool has great impact on the stability limits of the tools. By adjusting the proper spindle speed of the first and second tools, high chatter free material removal rates can be obtained. It can be easily seen that the best spindle speed combinations of the first and second tools are 6000 rpm and 4000 rpm respectively. Considering the stable depth for the second tool, the total depth of cut for the operation is increased by 25% when proper spindle speed combination is selected.

In Figure 3.22, variation of the stability limit with the spindle speed of the second cutting tool is shown.

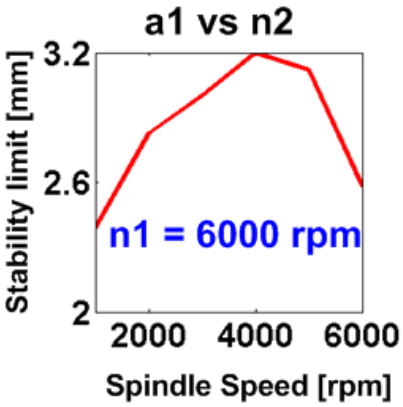

Figure 3.22. Variation of Stability limit with spindle speed of second tool.

Also, the cross section view of the 3D stability diagram at best condition that give highest stability limits is shown in Figure 3.23. Spindle speed of the second tool is 4000 rpm and the stability diagram is constructed for the first tool as seen below.

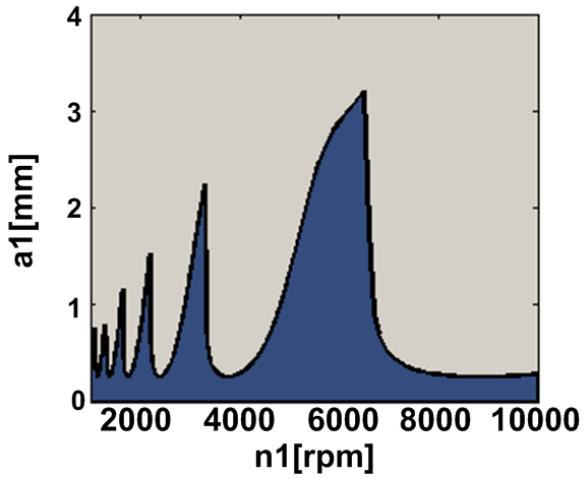

Figure 3.23. Stability diagram at spindle speed of 4000 rpm of the second tool.

3.3.3.1. Time Domain Verification of Analytical Frequency Method

The time domain model simulates the process at discrete time intervals once the process parameters, tool and workpiece modal data are given. Given the initial conditions, the dynamics displacements of the tools and the workpiece are calculated at each time step using the Runge-Kutta method from the equation of motion of the system. Then, dynamic cutting forces are determined using Equation 3.8 [24]. Finally, the responses of the system to the resulting forces, i.e. the tool and workpiece displacements, are calculated from the equation of motion with the updated initial conditions. These closed loop calculations are done consecutively for the specified time range. Moreover, there

can be an initial phase angle between the cutting tools' angular positions. Effect of the initial phase angle can also be included in the time domain simulations.

Time domain model results are used to verify the predictions of the frequency domain model for the optimum spindle speeds (E. Ozturk, personal communication, January 2013). For a representative case which is demonstrated in Figure 3.24, variations of the cutting forces at stable and unstable points are plotted. The time domain model predicts that there is a stability boundary at 3.1 mm which is close to the frequency domain model prediction. The force predictions on both tools are presented for a stable (a_I=2.5mm) and an unstable case (a_I=3.5mm), in Figure 3.24 (a) and (b), respectively.

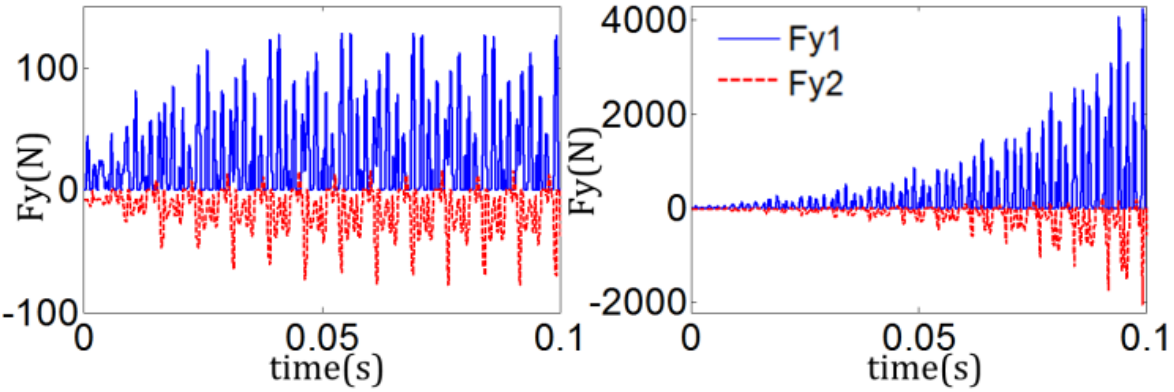

(a) (b)

Figure 3.24. Cutting forces in y direction (a) a1=2.5 mm (b) a1=3.5 mm

If the spindle speeds of the tools are different, the phase angle between the tools varies continuously. Hence, the initial phase angle does not affect the stability limits. However, the initial phase angle can have a considerable effect on the stability of the process when both cutting tools rotate at the same speed. In this case, the forces on the tools may counter each other provided that the forces have comparable magnitudes and act in opposite directions. Depth ratio, cutting type (up/down milling) and radial depths of cut are key parameters that affect the force profiles. For some example cases, the effect of initial phase angle on the stability limits of the first tool is presented in Figure 3.25. Spindle speeds and radial depths on both of the tools, and depth ratio are selected as 4000 rpm, 4 mm and 1, respectively. Limits for three different cutting type combinations were presented; namely, up/up, up/down and down/down for the first and the second tool. Effect of the cutting type selection on the limits is quite clear from the figure. In general, the effect of the phase angle is marginal except one point in up &

down configuration where phase angle is 45 deg. There is around 30% increase in the stability limit compared to the case with no phase angle difference for this set up.

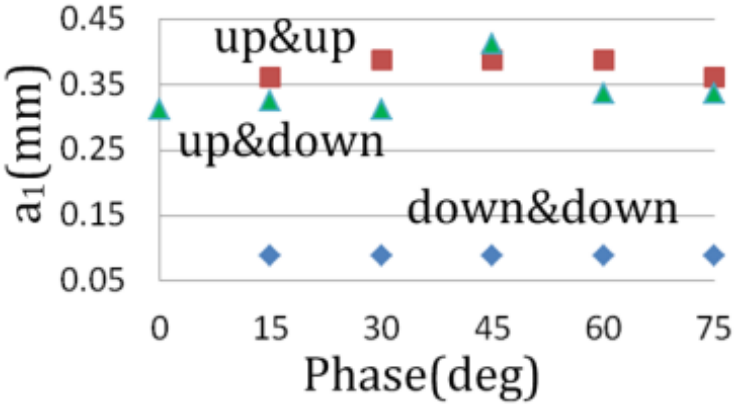

Figure 3.25. Effect of phase angle on stability limit, tool 1.

When the cutting tools work on different surfaces and the cutting types are the same on both tools, i.e., up/up (Figure 3.26) and down/down milling, the forces on the tools are exactly equal in magnitude and opposite in direction when the phase angle is zero. This results in zero displacement on the workpiece and thus increased stability limit. As rigid tool assumption was made, the stability limit reaches infinity for the cases where phase angle is zero.

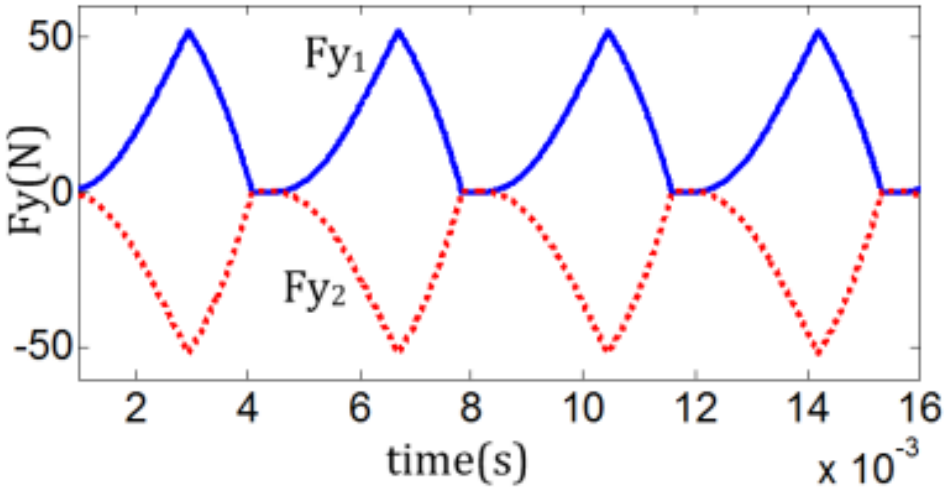

Figure 3.26. Cutting forces in y direction on the tools.

3.3.3.2. Effects of Workpiece Dynamics on Stability of the Process

In general, the total dynamic response at the cutting point including the cutting tool and workpiece frequency response function (FRF) needs to be known to generate stability

diagrams. The workpiece dynamics are usually ignored as their contribution is negligible compared to that of cutting tool, especially for long slender end-mills However, in some applications, the workpiece can be as flexible as, or much more flexible than, the cutting tool such as turbine blades which are representative examples of thin-walled parts.

Dynamic response of a workpiece varies continuously due to mass removal, so the stability limits vary during the process. Structural modification method can be used to model the in-process workpiece dynamics [33]. In this study, FRF of the workpiece at the most flexible point which is the tip of the plate is obtained, and it is modified in a FEA program (ANSYS©) by considering the removed volume at each step.

In the simulations and experiments, 90 mm length of the plate is divided into 5 equal pieces as shown is Figure 3.27. The axial depth of cut is selected as 6 mm for the first tool and 1.2 mm for the second tool. The optimum spindle speed combination (6000 rpm, 4000 rpm) is used for the tools. Other process parameters are same with the previous optimum spindle speed simulation. Each step has 20 mm length in the feed direction and FRFs are updated by considering the removed volume at each point.

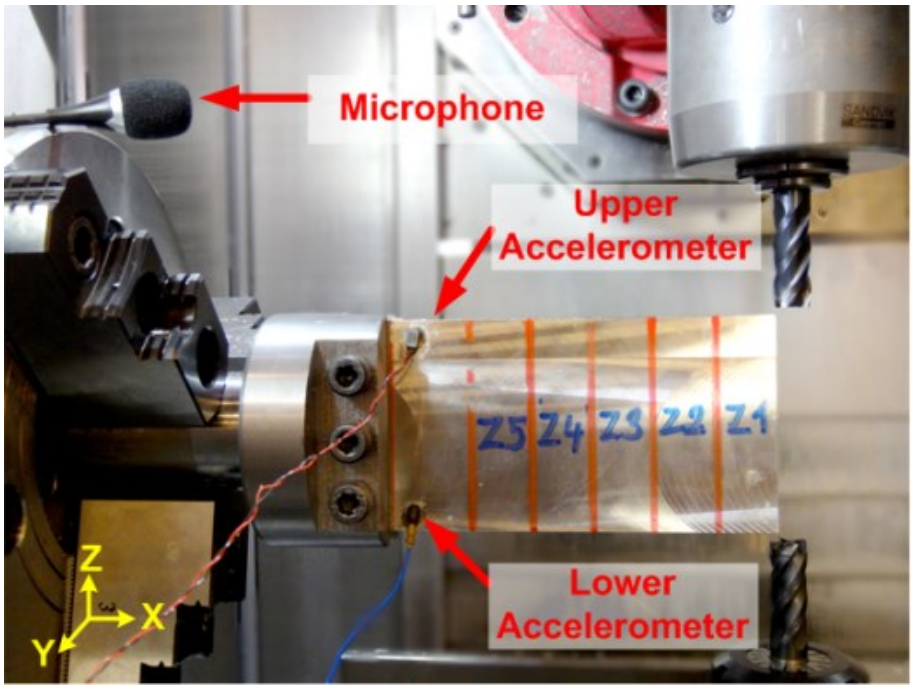

Figure 3.27. Workpiece and the experimental setup.

In ANSYS© software, each cutting zone is generated by removal of blocks from the main workpiece body block by modifying the corresponding *inp. file. Modified block

of workpiece is then meshed by quadratic elements (solid187). The most important point of the finite element analysis is selecting the proper nodes from the cutting zones. This operation is performed manually and three nodes from the cutting zone are taken and the node numbers are inserted into the inp file. After defining material properties, boundary conditions of the plate, the system is ready to solve. Block Lanczos Algorithm which is an eigenvalue extraction method and used for solving the large models with many constraints equations, is used to solve the problem. The resulting natural frequencies are written to the text file. For each cutting zone, this operation should be completed and the natural frequencies can be read from the text file. Sample workpiece block that is meshed and solved in ANSYS© is illustrated in Figure 3.28. The figure belongs to the fourth cutting zone.

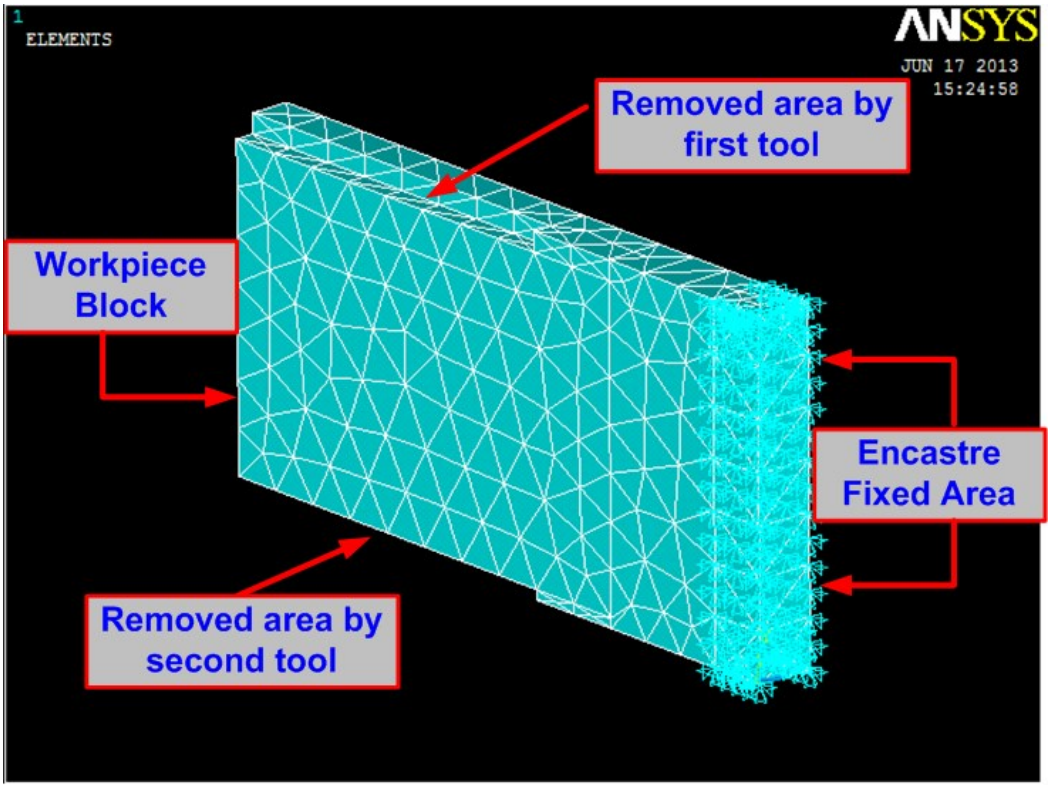

Figure 3.28. ANSYS example for the fourth zone.

Natural frequency of the workpiece increases from 427 Hz to 432.4 Hz whereas the modal stiffness varies from $1.16 \times 10^6\ N/m$ to $2.7 \times 10^7\ N/m$. Variations of modal parameters of the workpiece with the pre-determined zones are listed in Table 3.5. Damping ratio values are considered as constant during the machining, each of the zones.

Table 3.5. Variation of modal parameters in each cutting zone.

Cutting Zones	Natural Frequency [Hz]	Stiffness [N/m]
Z1	427	1,16e+06
Z2	430,4	1.44e+06
Z3	432	2.74e+06
Z4	432,4	6.51e+06
Z5	431,5	2.4 e+06

Then the stability diagram for each zone is generated considering the modal parameters in each zone. There are four different stability diagrams after the simulations were completed. These stability diagrams are plotted in the same graph and are shown in Figure 3.29.

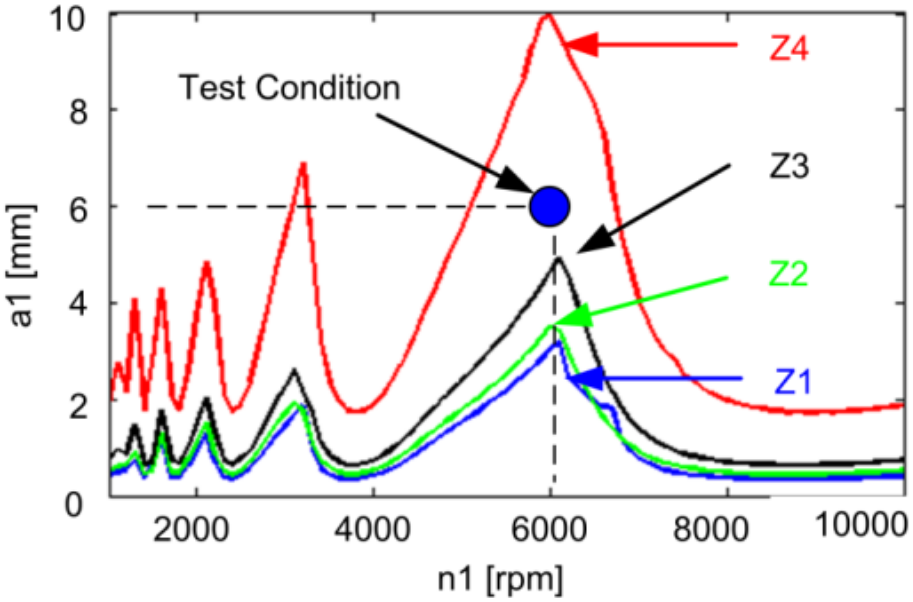

Figure 3.29. Stability diagrams for each zone.

The stability limit at 6000 rpm of the spindle speed of the first tool varies for each zone. In the first cutting zone which is 20 mm far away from the end of the plate, tool can machine 3.015 mm depth without chatter. At the second zone, stable depth of cut increases to 3.498 mm. At the third and fourth zones, stable depth of cuts are calculated as 4.919 and 9.962 mm, respectively.

Experimental verifications have been conducted for the simulated case in Figure 3.29, as shown in Figure 3.31 on the Mori Seiki NTX2000 multi-tasking machine tool where the setup is shown in Figure 3.30. As the test condition, 6 mm of axial depth of cut of

the first tool is selected. The depth ratio is preset as 0.2, so the second tool has 1.2 mm axial depth of cut. Two accelerometers and a microphone are used to analyze the data.

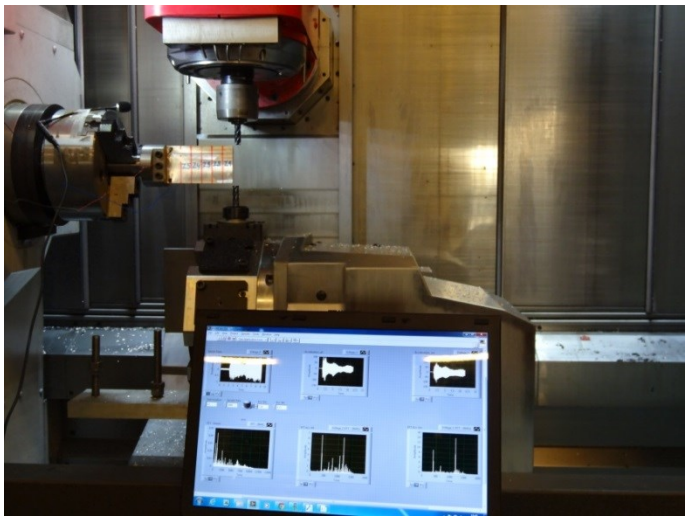

Figure 3.30. Experimental verifications.

As expected from the simulations, the process is unstable for the first 40 mm, then it goes into the stable zone and the chatter diminishes in rest of the cut. Surface photos are selected in three points which are in chatter, stable and marginal zones (Figure 3.31). Accelerometer spectrum also confirms the results.

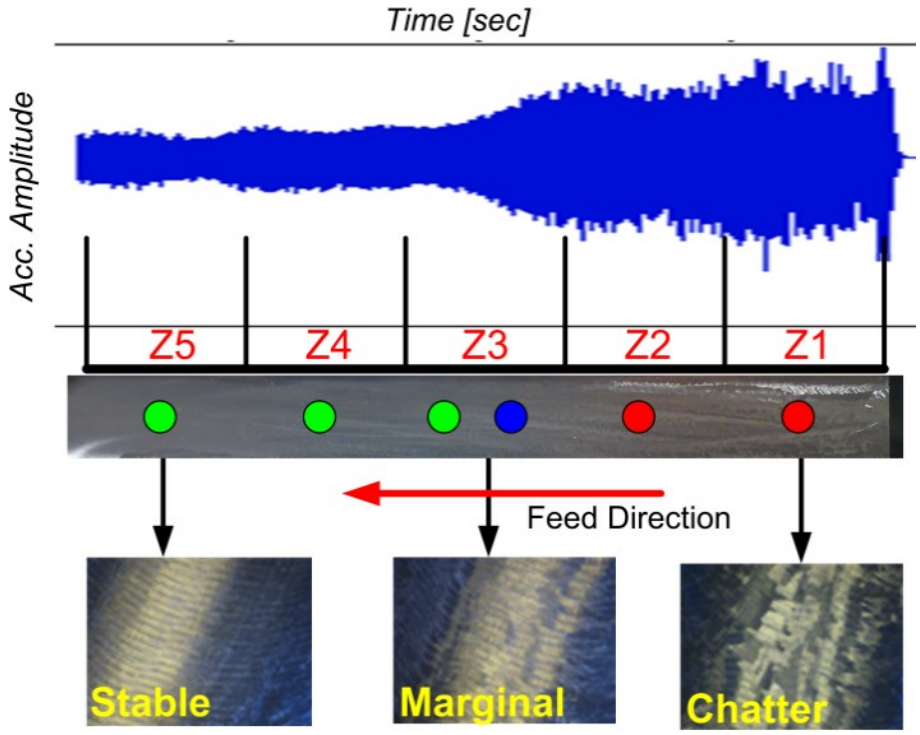

Figure 3.31. Accelerometer data and surfaces of stable and chatter zones.

Summary

In this chapter, dynamics and stability of simultaneous milling processes have been investigated through analytical, numerical and experimental studies. The modeling and the solution become complicated due to the dynamic coupling and the cross transfer functions between the tools and the workpiece. It is shown that the stability of the process can be improved compared to standard single tool milling if the process parameters such as spindle speeds for both tools are selected properly. In addition, the depth ratio, cutting type (up/down milling) and radial depth of cuts also have significant effects on the stable material removal rate. The initial phase angle between the tool positions may also have an effect on the stability limits when spindle speeds for both tools are the same. The application of the model is demonstrated by several cases where the predictions are verified by experimental results and time domain simulations.

CHAPTER 4

CHATTER STABILITY AND HIGH PERFORMANCE CUTTING CONDITIONS OF PARALLEL TURNING OPERATIONS

Parallel turning operations involve more than one cutting tool that removes material from a surface simultaneously. Due to existence of an additional cutting tool parallel turning operations provide higher productivity. On the other hand, dynamic interaction between the cutting tools may limit the full potential of parallel turning. If process parameters are not set properly additional stability problems may be presented. Hence, dynamics of the parallel turning operations should be modeled and investigated to establish the stability conditions.

In this chapter of the thesis, chatter stability of the parallel turning operations are explained briefly and mostly concentrated on the optimization of the parallel turning cutting conditions that provide higher stability limits. Stability models in frequency and time domain are used in optimization studies. The main objective of the optimization studies is to show the absorber effect the cutting tools. When two cutting tools perform cutting operation simultaneously, stability limits may be increased by changing the dynamic properties of the tools taking into consideration the absorber effect of one tool on the other cutting tool. Therefore, two different approaches to change the dynamics of the tools are investigated. First approach is by adding or subtracting mass from the cutter and the other one is by changing the length of one of the cutters. Both methods are used in the optimization studies by applying the frequency domain stability model. Then, optimized conditions are verified by time domain simulations. Results show that identification of optimum cutting conditions may increase the stability limits substantially.

4.1. Formulation of Dynamics and Chatter Stability of Parallel Turning

In this study, dynamics and chatter stability of two turning tools on different turrets are investigated, and optimization studies are carried out. A parallel turning process with two turning tools on different turrets is shown in Figure 4.1 [2]. In this case, the turning tools cut the same surface and they are dynamically coupled through the workpiece since the vibration waved left by each tooth on the surface alters the dynamic chip thickness of the other tool. In order to perform this parallel turning operation, depth of cuts of both tools should be different in general. According to the chatter stability model used in this thesis, the tool that has higher depth of cut is named as the second tool. Flexibility of the workpiece is neglected since it is relatively rigid with respect to the cutting tools in Z direction.

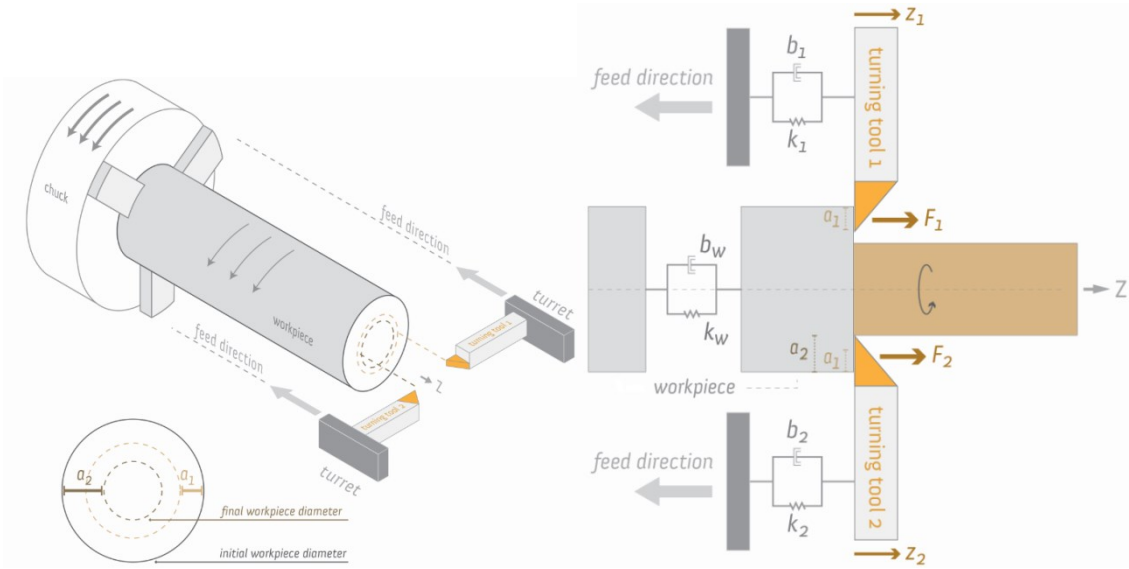

Figure 4.1. Parallel turning operation on the same surface.

Stability analysis of the parallel turning operations starts with the dynamic chip thickness formulation for each cutting tool. Dynamic cutting forces on each tool can be written as follows [2].

$$\begin{bmatrix} F_1(t) \\ F_2(t) \end{bmatrix} = K_f \begin{bmatrix} a_1\left(\frac{h_0}{2} - z_1(t) + z_2\left(t - \frac{\tau}{2}\right)\right) \\ a_1\left(\frac{h_0}{2} - z_2(t) + z_1\left(t - \frac{\tau}{2}\right)\right) + (a_2 - a_1)(h_0 - z_2(t) + z_2(t - \tau)) \end{bmatrix} \quad (4.1)$$

The region with depth of a_1 is removed by both tools. In this region, the dynamic chip thickness on a tool is affected by the displacement of the tool at the present pass and the displacement of the other tool at a half rotation period ($\tau/2$) before. The feed per revolution h_0 is shared between the tools in this region as the static chip thickness. On the other hand, the region with a depth of a_2-a_1 is only removed by the second tool. Hence, the dynamic chip thickness depends on the dynamic displacement of the second tool at the present time and at one rotational period (τ) before [2].

After some arrangements, the resulting eigenvalue problem takes the following form:

$$\begin{bmatrix} F_1 \\ F_2 \end{bmatrix} e^{i\omega_c t} = B \begin{bmatrix} F_1 \\ F_2 \end{bmatrix} e^{i\omega_c t} \tag{4.2}$$

where B is the matrix that depends on the a_1, a_2, ω_c, τ, K_f and transfer functions of the first and second tools.

This eigenvalue problem can be solved as follows. There are four unknowns which are a_1, a_2, ω_c and τ. For another parallel turning case (cutting tools on different turrets), the cutting depth on the second tool, a_2, should be selected before the stability analysis. Then, the stability diagram for a_1 can be obtained for a given a_2. But it should be remembered that that a_2 is selected as higher than a_1 in the related formulation. Hence, only the stability limit values for a_1 which are less than a_2 should be considered as real solution [2].

For parallel turning stability analysis, stability limit for the first tool, a_1, is calculated for given cutting depth for the second tool, a_2. It is observed that when a_2 is selected higher than the second tool's stability limit for the single tool operation (i.e. when a_2 is selected from the unstable region for the single tool process), two stability limits are observed for of a_1. This is presented in Figure 4.2 [2].

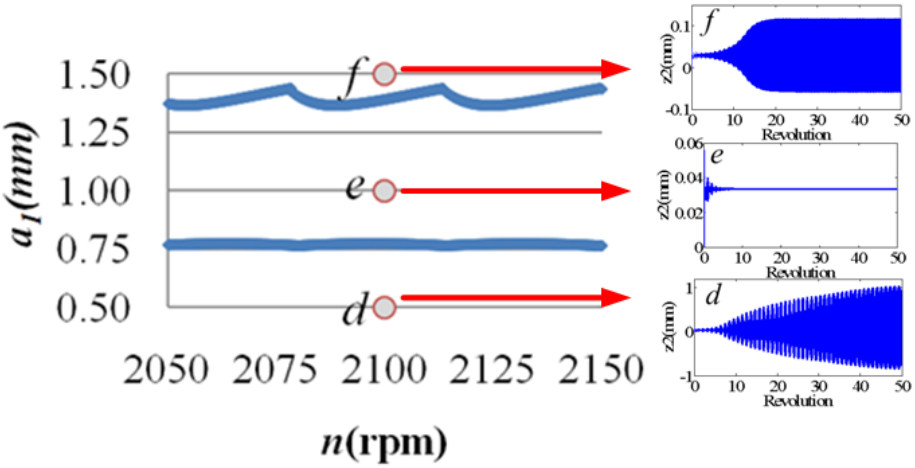

Figure 4.2. Stability diagram with two limits (a_2 = 1.5 mm).

Between these two limits, process in stable, otherwise it is unstable. Three sample points are selected on the stability diagram shown in Figure 4.2: f and d are at unstable region where point e is in the stable region.

Time-domain models simulate the dynamic forces and vibrations on the tools at each discrete time instance using the related cutting force and displacement equations (Equation 4.1) [2]. The calculation steps are continued with the next discrete time until the end of the simulation time. Depending on the variation of dynamic cutting forces and displacements processes can be classified as stable, marginal or unstable. Hence, by performing simulations at higher axial depths until instability is reached, the stability limit for a given spindle speed can be identified. Finally, repeating this step for different spindle speeds, the stability diagram can be determined for the given process.

Presented chatter stability of parallel turning model was also verified with experimental cuts [2].

4.2. Optimization of Parallel Turning Operations

In this section of the thesis, high performance stability conditions for parallel turning operations are investigated. The main objective in the optimization studies is to set the dynamic parameters of one of the cutting tools to increase the total stability of the process similar to the situation in tuned vibration absorbers. Dynamic parameters of the tools such as natural frequency, modal stiffness, damping ratio and modal mass are

varied to suppress chatter vibrations. This is achieved by two different proposed methods. In the first method, mass of the one of the cutters is changed by adding or subtracting mass to alter the dynamic properties of the cutter. In the second method, length of one of the cutters is changed within a certain range. Calculations are based on the "Euler-Bernoulli Beam Equations" formulation [34]. Both methods are simulated in frequency domain and the stability diagrams are constructed. Then, the obtained stability diagrams are verified by time domain simulations.

4.2.1. First Method: Mass Change at Cutters

In the first method, mass of one of the cutter is varied in a certain range while keeping the mass of other cutter fixed. There are two ways to change the mass of the cutter. First one is adding an additional mass for example fastening a screw or metal piece on the tool holder. Other way is by subtracting mass from the holder which can be done by drilling a hole.

Alteration of the effective mass changes the natural frequency and damping ratio of the beam. In the simulations, $20mm \times 20mm$ cross section for the holder is used and the cutters are selected as identical. Length of the cutters are 70 mm and the modulus of elasticity and density of the cutters are $2.1e^{11}\ N/m^2$ and 7800 kg/m^3, respectively. The moment of inertia of the beam is calculated as the following equation.

$$I = \frac{bh^3}{12} \tag{4.3}$$

where b and h are the width and thickness of the beam. By using this formulation, moment of inertia of the beam is calculated as $1.3e^{-8}\ m^4$. Considering Equation A.1 (See Appendix) first natural frequency of the beam is determined as 3420 Hz.

As stated before, dynamic parameters of only one of the cutters is changed. Modal parameters of the other cutter are fixed. In the simulations, dynamic parameters of the second tool are fixed and the values are listed in Table 4.1.

Table 4.1. Modal parameters of the second tool (fixed tool).

Modal Parameters	Natural Frequency [Hz]	Stiffness [m/N]	Damping Ratio [%]	Modal Mass [kg]
Tool 2	3420	2.45 e+07	0.907	0.05301

Effective mass of the first cutter is changed within a reasonable range. Initial effective mass the beam is the same as the second tool but up to 100 gr. mass is added to the initial mass. On the other hand, maximum 10 gr. mass is subtracted from the initial mass. All modal parameters for different mass modifications are calculated and shown in Table 4.2.

Table 4.2. Modal parameters of the first tool with respect to the adding mass.

Modal Parameters	Additional Mass [gr]	Total Mass [kg]	Natural Frequency [Hz]	Stiffness [m/N]	Damping Ratio [%]	Frequency Ratio [r]
First Tool	10	63	3137	2.45e+07	0.832	0.917
	20	73	2914	2.45e+07	0.773	0.852
	30	83	2733	2.45e+07	0.725	0.799
	40	93	2582	2.45e+07	0.685	0.755
	50	103	2453	2.45e+07	0.651	0.717
	60	113	2342	2.45e+07	0.621	0.685
	70	123	2245	2.45e+07	0.595	0.656
	80	133	2159	2.45e+07	0.573	0.631
	90	143	2082	2.45e+07	0.552	0.608
	100	153	2013	2.45e+07	0.534	0.588
	-5	48	3594	2.45e+07	0.953	1.051
	-6	47	3632	2.45e+07	0.963	1.062
	-7	46	3671	2.45e+07	0.974	1.073
	-8	45	3712	2.45e+07	0.984	1.085
	-9	44	3754	2.45e+07	0.996	1.097
	-10	43	3797	2.45e+07	1.007	1.110
	-15	38	4039	2.45e+07	1.071	1.181
	-20	33	4335	2.45e+07	1.149	1.267
	-25	28	4706	2.45e+07	1.248	1.375

“R” is the ratio of the natural frequencies of the cutters. For each of the “*r*” ratio from 0.588 to 1.375, stability diagram of the parallel turning operation is generated. Three

sample stability diagrams for the cases of $r < 1, r = 1$ and $r > 1$ are shown in Fig XXXX. Stability diagrams are constructed for the given depth of cut of the second tool, a_2. In the simulations, spindle speed range of 1600-1700 rpm is selected. The lobbing effect is negligible around the spindle speed of interest because of the low ratio of rotational frequency with respect to the chatter frequency. Hence, stability limits at the lobes are very close to the absolute stability limit for each tool, thus stable depth of cuts are taken as the absolute stability limit. Feed cutting force coefficient is taken as 1000 MPa.

Simulated stability diagrams in the frequency domain are verified by time domain simulations. Time-domain models simulate the dynamic cutting forces and vibrations on the tools at each discrete time step using the related cutting forces and displacement. The calculation steps are continued with the next discrete time until the end of the simulation time [2]. Depending on the variation of dynamic cutting forces and displacements processes can be classified as stable, marginal or unstable.

In time domain simulation depth of cut values of both cutters ($a_1$and a_2) are set, then the simulation is started. Dynamic cutting forces, chip thicknesses, displacements and frequency amplitude spectrum are obtained and by evaluating these results parallel turning process is classified as stable, marginally stable and (chatter) unstable.

A point related to the time domain simulations is that the depth of cut of the first cutter (a_1) must be smaller than the depth of cut of the second tool (a_2). Time domain method is applied to those points where $a_1 > a_2$ by reversing the modal parameters of the first and second tools.

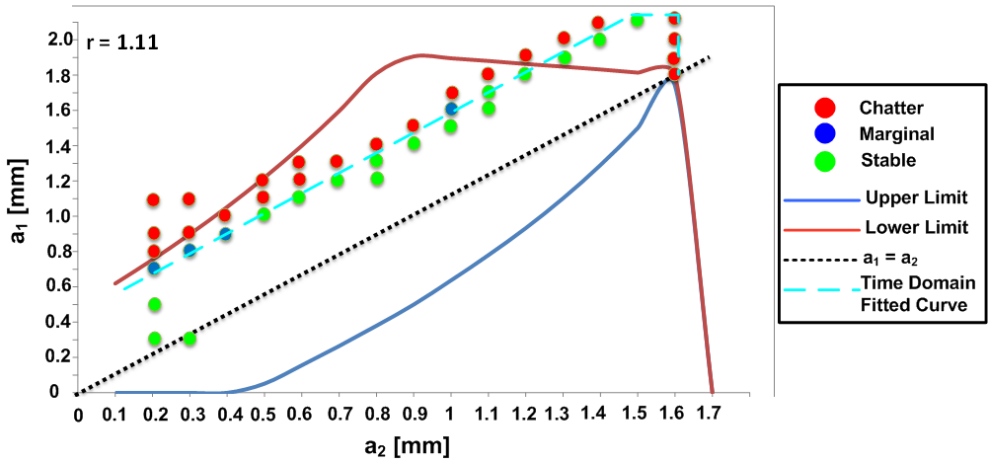

Figure 4.3. Stability diagram for the case of r = 1.11 and time domain verification.

As shown in Figure 4.3, using calculated rotational periods and given chatter frequency, frequency domain simulations provide two different stability limits which are which are upper and lower limits (red and blue lines). Between these two stability limits, operation is stable and for other a_1 and a_2 selections, process is unstable. In the stability diagram for $r > 1$ case, lower limit is zero until a certain depth of cut of the second tool. For this condition, this certain depth of cut is 0.4 mm which is the stability limit of the second tool when performing single tool turning operation. Then, limits converge to each other and after a certain limit, both limits becomes zero and process is unstable for every condition.

There are many points where $a_1 > a_2$. As stated before, these results from the frequency domain method are not real solutions according to the definition in the formulation. The dashed line represents the points where $a_1 = a_2$. The points below this line are real solution of the frequency domain method but above this line the points do not satisfy the assumption in the formulation. Time domain method is applied to those points by reversing the modal parameters of the first and second tools. The solutions are classified as unstable (chatter), marginally stable and stable. As seen from Figure 4.3, there is a slight inconsistency between the frequency and time domain solutions. However, time domain results are the real solutions where the frequency domain results are not. The stable region can be redefined between the "Fitted Time Domain Curve" and the lower limit of the first tool.

Similarly, for the $r = 1$ case, the stability diagram is generated as follows and verified by time domain method.

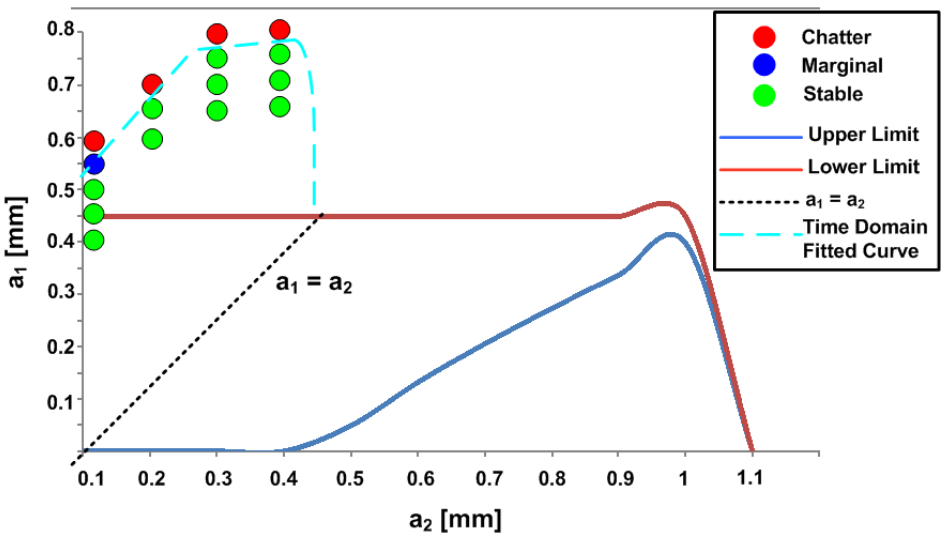

Figure 4.4. Stability diagram for the case r = 1.

As shown in Figure 4.4, upper stability limit of the second tool does not change with the increased depth of cut of the first tool according to the frequency domain model. After a specific depth of cut, both limits become zero and process in totally unstable. Similar to the r = 1.11 case, there are some points which do not satisfy the $a_1 < a_2$ condition. These points are verified by the time domain solution and the resultant stable region is between the "Fitted Time Domain Curve" and lower limit of the first tool. Frequency domain results are not real solution for the points where $a_1 > a_2$. Hence time domain results should be considered as the real solution of the system.

Similar to the case of above conditions, $r < 1$ case is also simulated. Stability diagram for this case is generated in Figure 4.5.

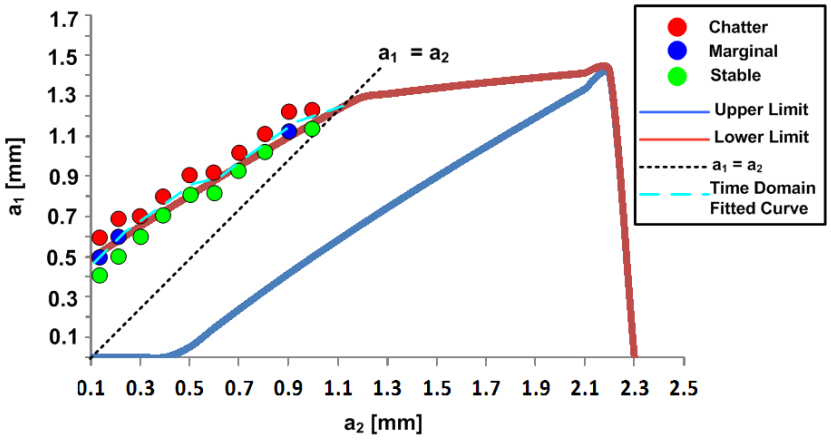

Figure 4.5. Stability diagram for the case of r = 0.91.

As seen from the Figure 4.5, time domain solution shows good agreement with the frequency domain results.

For different values of the "r" ratio, 3D stability diagrams are generated for lower, upper and both limits of a_1 and a_2. In Figure 4.6, 3D stability diagram of the condition which "r" ratio is smaller than 1, is shown.

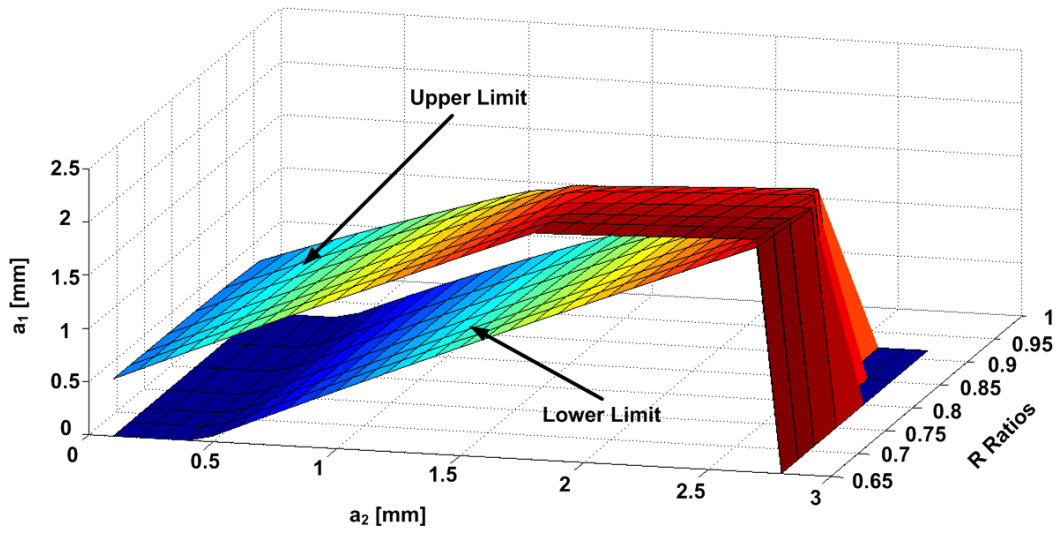

Figure 4.6. 3D stability diagram for the r < 1 case.

Similar to the r < 1 case, 3D stability diagram of the r > 1 case is generated (see Figure 4.7).

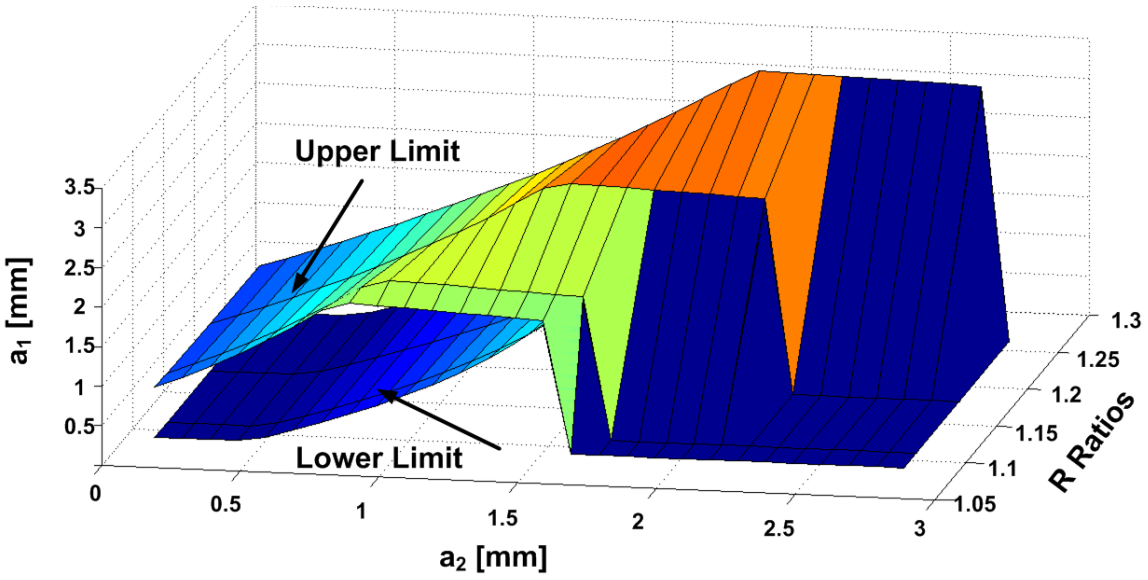

Figure 4.7. 3D stability diagram for the r >1 case.

Optimization studies have also been done for the constant value of a_2. Then, variation of the depth of cut for the first tool with the "r" is obtained. In the simulations, depth of cut of the second tool is fixed at 1.00 mm and the variations are shown in Figure 4.8.

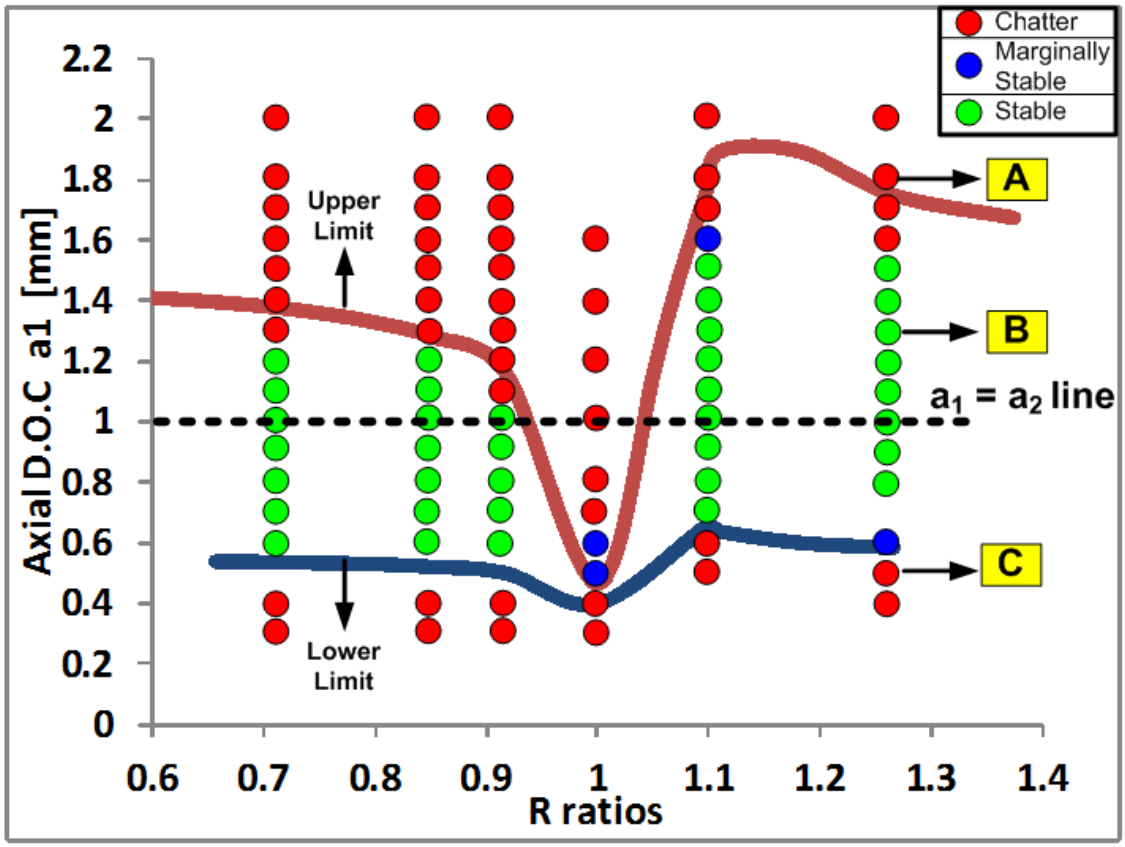

Figure 4.8. Variation of upper and lower limits of the first tool with different "r" ratios for a constant value of the a_2

Optimum cutting condition is determined as 1.9 mm for the ratio of 1.11. When the natural frequencies of the cutters are close to each other, stability limits decrease significantly. Moreover, time domain simulations accurately verified the frequency domain model at the points where $a_1 < a_2$. Frequency domain results are not valid for the points which are above the $a_1 = a_2$ line. For the points where $a_1 > a_2$ or above the $a_1 = a_2$ line, time domain model provides reasonable results. The slight inconsistency may be resulting from reversing the modal parameters of the tools.

In order to verify frequency domain solutions, three sample points (A, B and C) are selected and the variations of the cutting forces, dynamic displacements and chip thicknesses are illustrated in Figure 4.9.

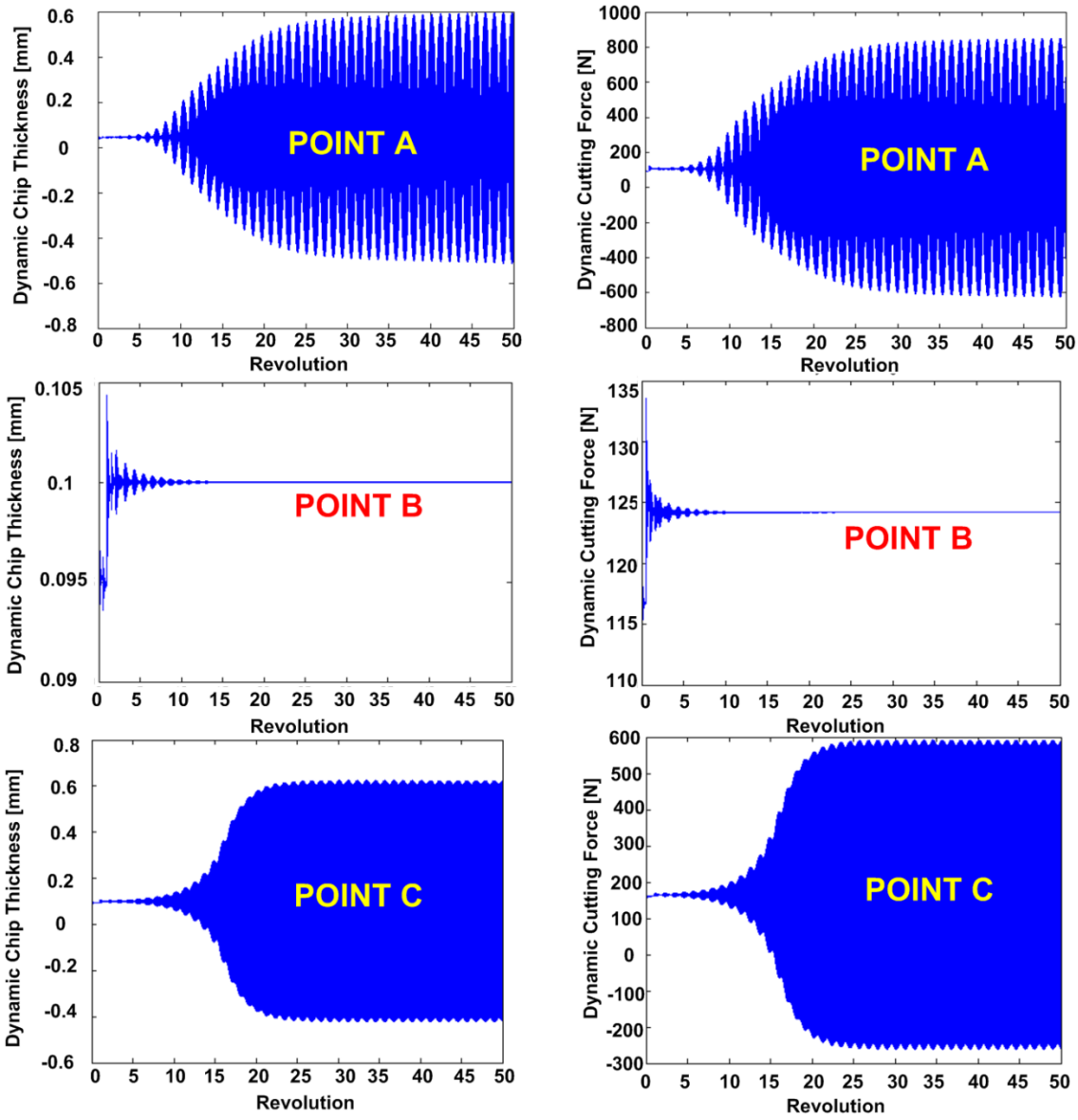

Figure 4.9. Variations of dynamic chip thickness and cutting forces at points A, B and C.

As shown from the Figure 4.8, "r=1" ratio is the worst case of the cutting process allowing almost zero stable cutting depth. This situation can be explained by examining the FRFs of the cutters. In Figure 9, for r=1, both the FRF amplitudes of the cutters overlap doubling the magnitude of the resultant FRF. FRF of each cutter at r=1 can be seen in Figure 4.10.

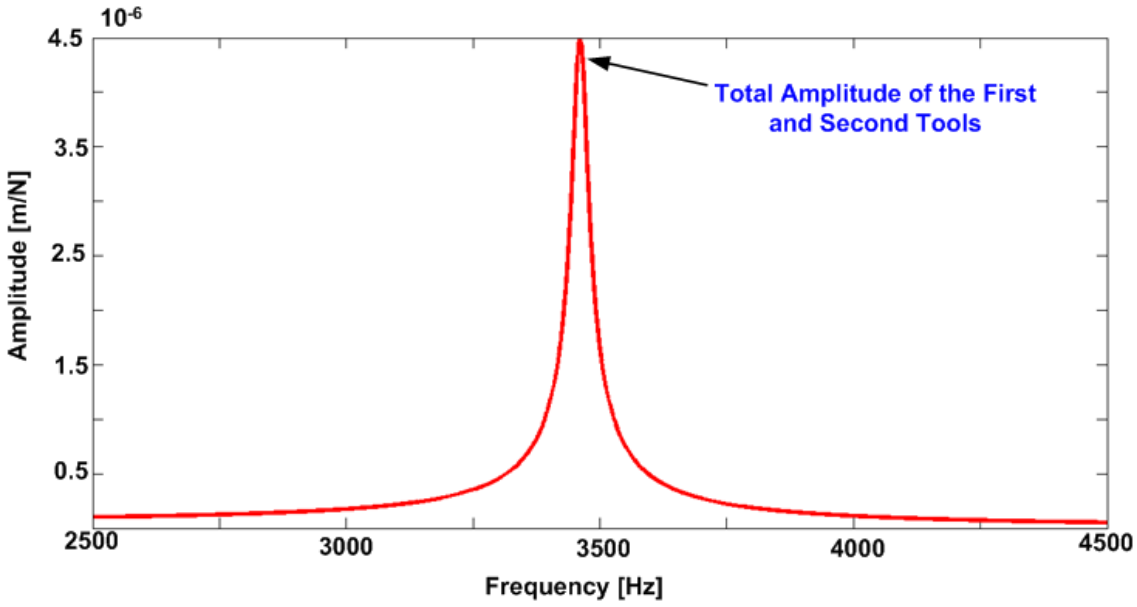

Figure 4.10. FRFs of the cutters when r=1.

As seen from Figure 4.10, total FRF amplitude at the most dominant mode is about 4.5×10^{-6} m/N which is two times of each FRF amplitudes of the cutters. Similarly, for the condition where $r = 0.8$, FRF of the each cutter is calculated in Figure 4.11.

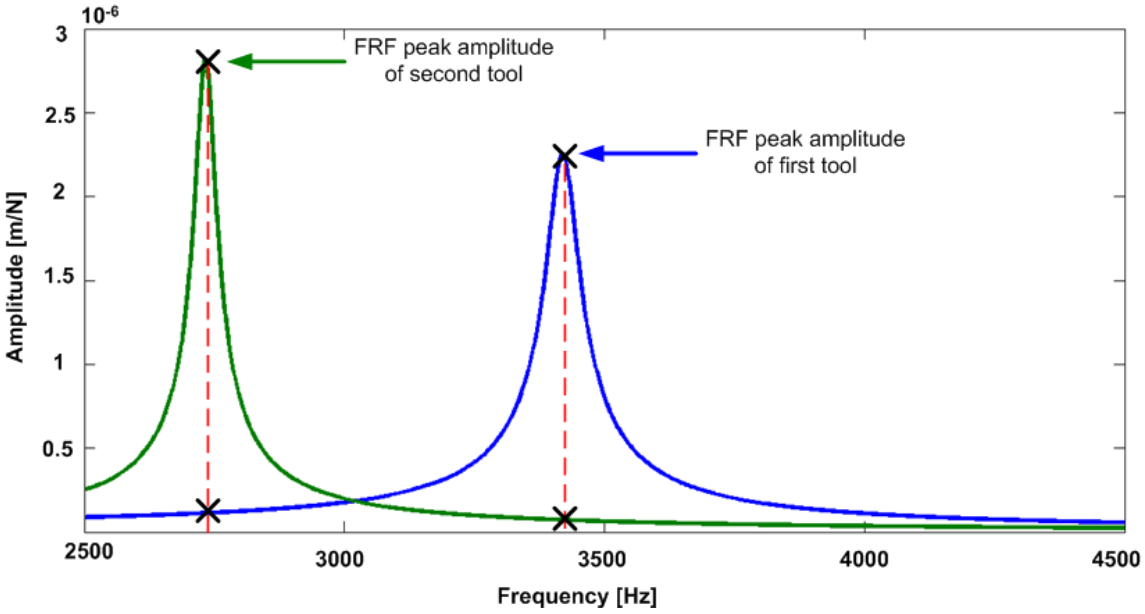

Figure 4.11. FRFs of the cutters where $r = 0.8$.

At this condition ($r = 0.8$), for the most flexible mode of the system which is at 2733 Hz, magnitude of peak FRF amplitude of the second the cutter is 2.81510^{-6} m/N and magnitude of peak FRF amplitude of the first cutter is 1.1310^{-7} m/N. Total maximum FRF amplitude at this most flexible mode of the system is about 2.92810^{-6} m/N.

Variation of total maximum FRF magnitude with the “r” ratio is demonstrated in Figure 4.12.

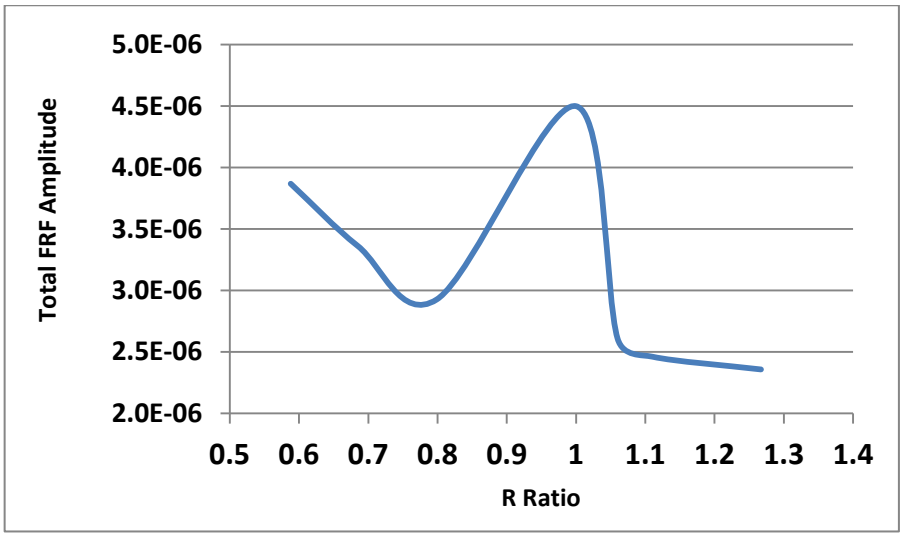

Figure 4.12. Variation of FRF amplitude with the r ratio.

Therefore, it can be concluded that the total maximum FRF amplitude of the system occurs for r = 1. Flexibility of the system is directly related to its FRF which increases when frequency ratio becomes close to 1. At the point where the natural frequencies are exactly equal to each other (r = 1), the system reach its maximum flexibility, and stability of the process is decreased. Thus, this explains the minimization of the stable depth of cut at the condition of r = 1.

4.2.2. Second Case: Length Change of Cutters

In the second method, length of one of the tool holders is changed within in a certain range while keeping the length of other tool holder fixed. Same cutter cross section geometry and material are used as in the first example case.

Any alteration in the length of the tool holders results a change on the natural frequency, modal stiffness and damping ratio of the cutter. Length of the cutter is changed from 60 mm to 100 mm where the length of the second cutter is fixed at 70 mm. Natural frequencies, modal stiffness and damping ratios for each of the condition is listed in Table 4.3.

Table 4.3. Modal parameters of the first tool with respect to length ratios.

First Cutter Length [mm]	Natural Frequency [Hz]	Stiffness [N/m]	Damping Ratio [%]	Length Ratio [L]
60	4658	3.89e+07	0.778	0.857
62	4362	3.52e+07	0.804	0.885
64	4094	3.20e+07	0.830	0.914
66	3849	2.92e+07	0.856	0.942
68	3626	2.67e+07	0.882	0.971
70	3422	2.45e+07	0.908	1
72	3235	2.25e+07	0.933	1.02
74	3062	2.07e+07	0.959	1.05
76	2903	1.91e+07	0.985	1.085
78	2756	1.77e+07	1.01	1.11
80	2620	1.64e+07	1.04	1.14
90	2070	1.15e+07	1.17	1.28
100	1677	8.40e+06	1.30	1.43

Variation of the length with the stiffness plays a decisive role in the optimization of the parallel turning operation and can be seen in Figure 4.13. There is an exponential relation between the length, natural frequency and the stiffness of the system.

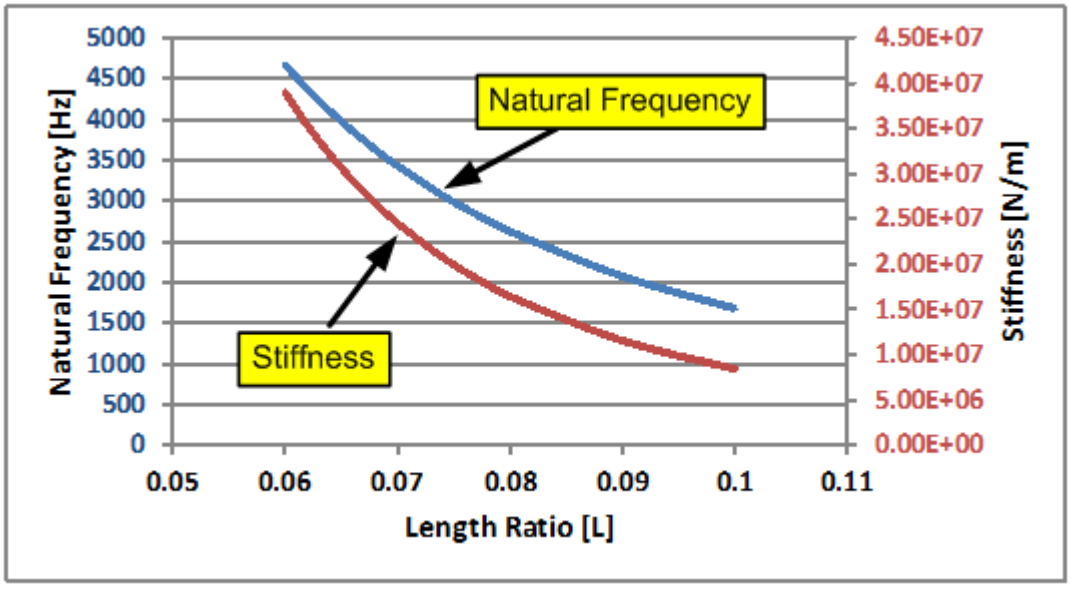

Figure 4.13. Variation of length of the cutter with its natural frequency.

"L" is the ratio of natural frequencies of the tool holders and calculated as "L_1/L_2". For each of the "L" ratio from 0.857 to 1.43, stability diagrams are generated. A sample stability diagram for the case of $L = 1.142$ is shown below. Stability diagram is constructed for the given depth of cut value of the second tool, a_2. In the simulations, spindle speed range of 1600-1700 rpm is selected. The lobbing effect is also neglected around the spindle speed of interest.

For the case of $L = 1.142$, stability diagram is generated and shown in Figure 4.14.

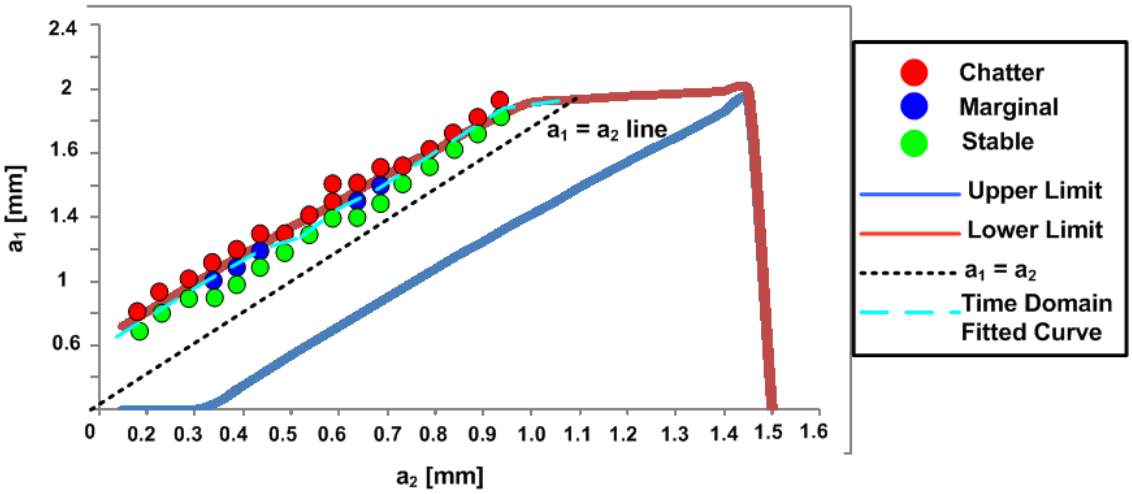

Figure 4.14. Variation of a_2 with the lower and upper limits of a_1 for L > 1.

As mentioned before, process is stable between the upper and lower limits of the a_1. After a certain depth of cut value, both the limits of a_1 and a_2 becomes zero and process becomes totally unstable. Frequency domain model results are not real solution of the system for the points where $a_1 > a_2$. For those points, time domain model is used and the results of the time domain model is valid. Also, time domain provide almost the same stability limits as the frequency domain solutions. For an accurate prediction, the stability limit values between the "Fitted Time Domain Curve" and the lower limit of the first tool should be considered.

For different values of the "L", 3D stability diagrams are generated for lower, upper and both limits of the a_1 and a_2. In Figure 4.15, 3D stability diagram of the condition which "L" is smaller than 1, is shown.

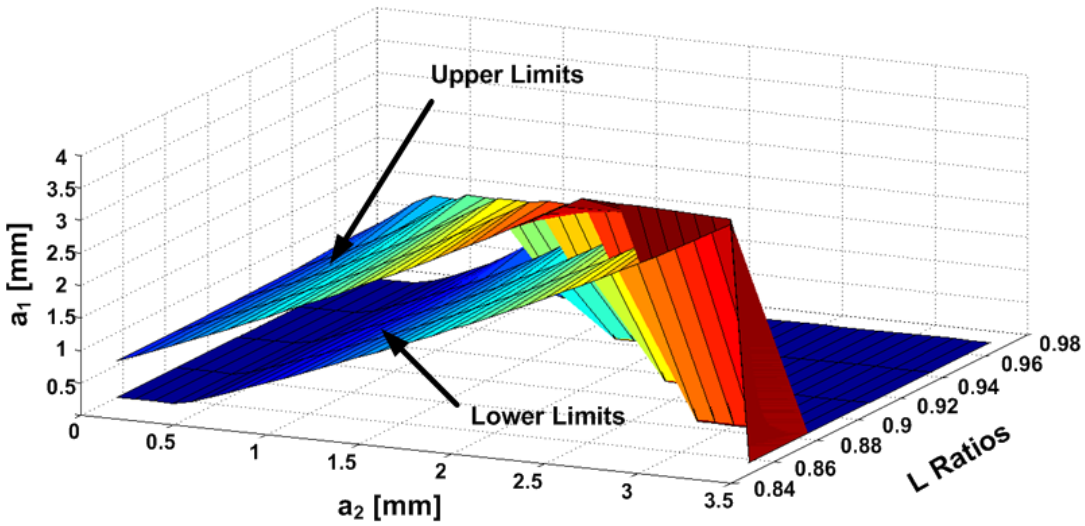

Figure 4.15. 3D stability diagram for the L < 1 case.

As seen from the Figure 4.15, ratios close to 1 provide smaller stable region and depth of cut compared to the ratios away from 1. Lower limits are zero at first and then both limits converge each other and maximize the stability. However, after a specific value of the a_2, both upper and lower limits become zero and process is totally unstable at every cutting conditions.

Similar to the above case, 3D stability diagram for the different values of L which are bigger than 1, are generated and shown in Figure 4.16.

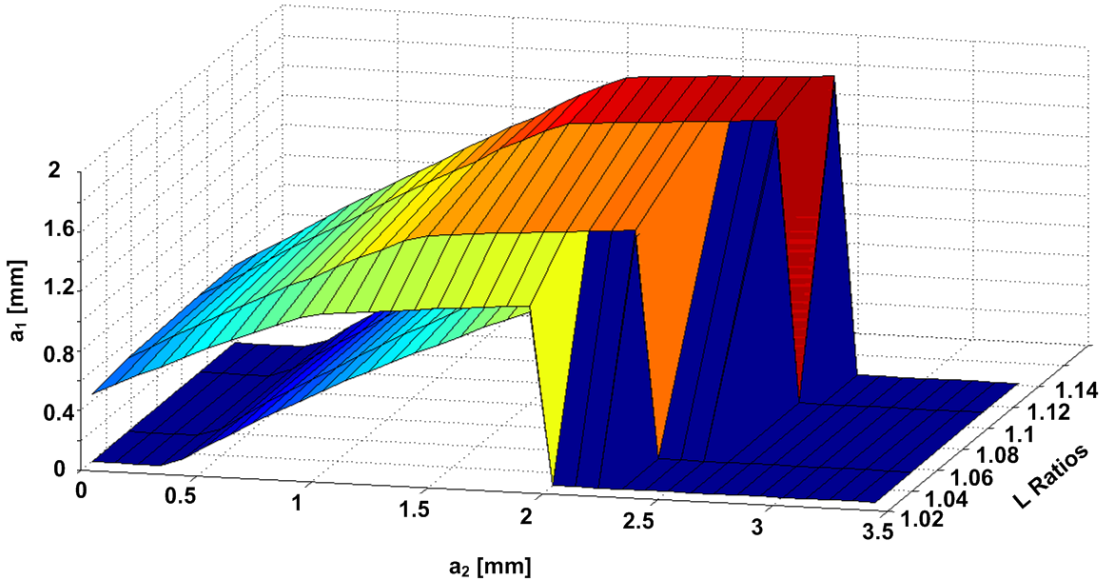

Figure 4.16. 3D stability diagram for the L > 1 case.

To understand the 3D plot better, cross-section view of the plot is demonstrated in Figure 4.17.

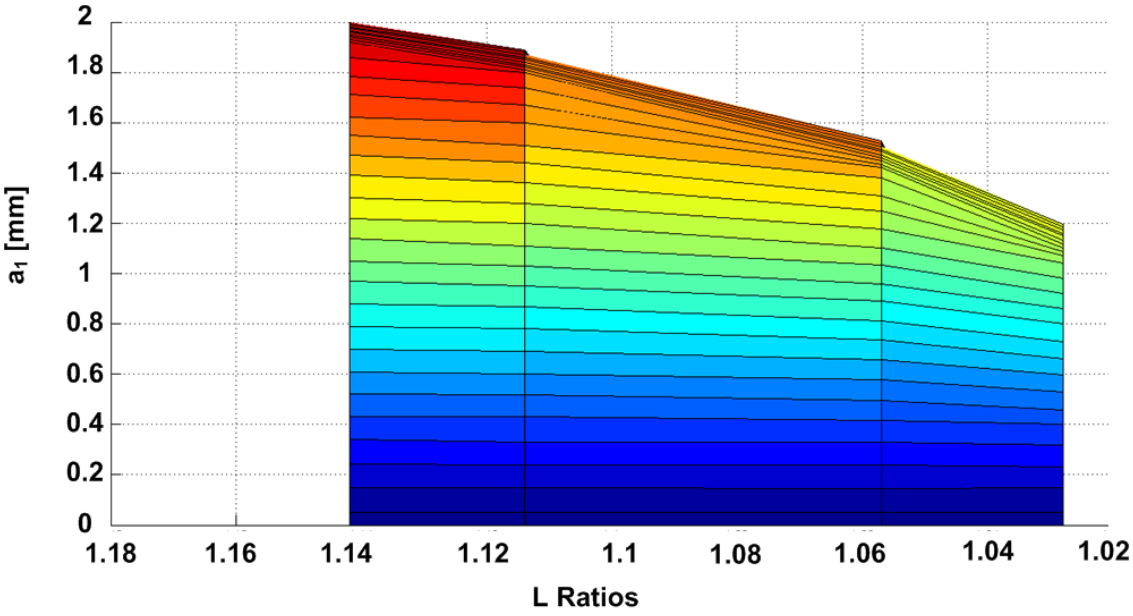

Figure 4.17. Cross-section view of 3D stability diagram for the case of L > 1.

For the constant values of depth of cut of the second tool, variation of the "L" with the upper and lower limits of depth of cut of the first tool is shown in Figure 4.18. Depth of cut of the second tool is fixed at 1.0 mm.

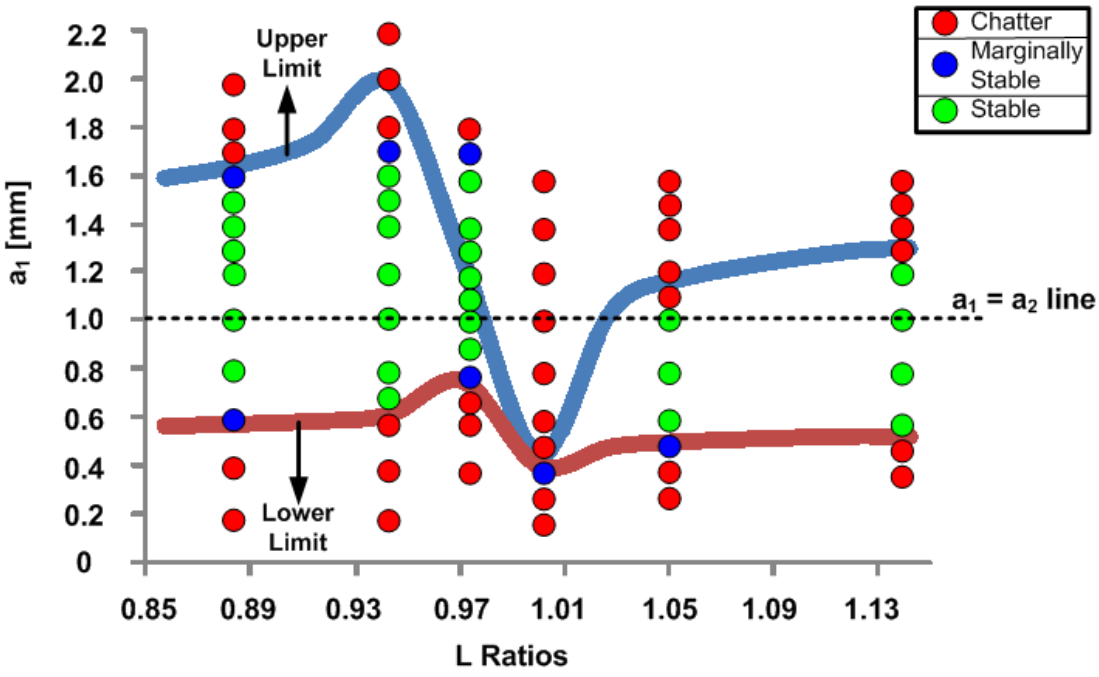

Figure 4.18. Variation of upper and lower limits of the first tool with different "L" ratios for a constant value of the a_2.

Similar to the first optimization case, optimization of the second case are also verified by time domain model. Dynamic cutting forces, chip thicknesses, displacements and frequency amplitude spectrum are obtained and by evaluating these results, parallel turning process is classified as stable, marginally stable and chatter (unstable). Points where $a_1 > a_2$ are evaluated based on the assumption given in previous time domain verification.

When the dynamic chip thickness and cutting forces are investigated at each point, similar to the mass change optimization case, points where $a_1 < a_2$ are verified exactly with the frequency domain results. Time domain simulations of points where $a_1 > a_2$ show relatively good agreement with the predictions and the differences between the time and frequency domain results are due to assumption previously explained.

As seen from the Figure 4.18, length ratio of 0.943 provides the highest stability limit which is 1.98 mm of the upper limit of the first tool. Similar to the first example case, when the length of the tool holders are equal which makes them identical, stability limit becomes almost zero and the stable region between the upper and lower limits of the stability diagram is very tight and impossible to perform any stable cutting operation. When the length ratio is moving away from the 1, stability limits are increasing. Also, this situation can be explained by the FRF magnitudes of the tool holders at different length ratios. When the length ratio equals to 1, both FRF amplitudes of the holders overlap doubling the magnitude of the resultant FRF of the system. Length ratios away from 1 provide smaller resultant FRF magnitude and the flexibility of the system is increased, so stability limits are increased substantially. Variations of the resultant FRF amplitudes with the length ratios are demonstrated in Figure 4.19.

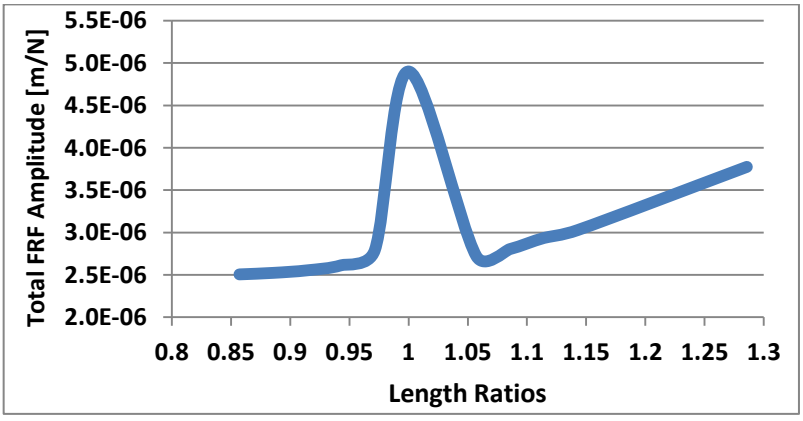

Figure 4.19. Variation of resultant FRF magnitude with length ratios.

Hence, it can be concluded that, when the total FRF of the system is increased at the length ratio of 1 which is the worst case and allowing almost zero stable cutting depth. When the length ratio moves away from the value of 1, stability limit is increased, so the stability limit in the parallel turning operations is directly related with the flexibility of the holders.

Summary

In this chapter of the thesis, chatter stability and the high performance cutting conditions of the parallel turning operations is investigated. First, theory of the chatter stability of parallel turning operations is explained briefly. Then, two optimization methods which are change of mass and length of the holders are discussed. Stability limits are obtained by using frequency domain model and verified by time domain results. As a consequence of optimization simulations, best conditions that provide higher stability limits are found. Also, the underlying reasons of the optimization results are explained by evaluating the resultant FRFs of the cutters.

CHAPTER 5

CONCLUSION

In this thesis, dynamics and chatter stability of multi delay systems are investigated. Variable tooth spacing tools such as variable pitch and helix tools and parallel milling operations are interested as the multi delay systems. Since containing single time delay term, chatter stability of parallel turning operations is shown briefly.

Chatter stability of variable tooth spacing tools is investigated briefly since there are few works about the analyzing and modeling of these special tools. Dynamics and stability of variable pitch and helix tools are modeled and solved in frequency domain and by using Semi-Discretization Method. Simulations were carried out to determine the optimum pitch and helix variations that provide higher stability limits. It was shown that chatter frequency is affected by the pitch or helix variations significantly. Thus, an iterative procedure has to be used for the optimization of pitch and helix variations. For the first time in literature, optimum variable tool geometry is determined for a given cutting condition without doing many optimization simulations. The iterative procedure based on the fact that optimum pitch angle cancels out the phase difference in the system and maximize the stability limit.

Dynamics and stability of simultaneous milling processes have been investigated through analytical, numerical and experimental studies. The modeling and the solution become complicated due to the dynamic coupling and the cross transfer functions between the tools and the workpiece. It is shown that the stability of the process can be improved compared to standard single tool milling if the process parameters such as spindle speeds for both tools are selected properly. In addition, the depth ratio, cutting type (up/down milling) and radial depth of cuts also have significant effects on the stable material removal rate. The initial phase angle between the tool positions may also

have an effect on the stability limits when spindle speeds for both tools are the same. For the first time in the literature, frequency domain solution of chatter stability of parallel milling operations is presented. Then optimum spindle speed combinations are demonstrated for high performance cutting condition.

Finally, chatter stability and the high performance cutting conditions of the parallel turning operations are investigated. First, theory of the chatter stability of parallel turning operations is explained briefly. Although the effect of depth ratio of cutting tools on the stability of parallel turning was analyzed in a previous study, the effect of frequency ratio of the tools on the chatter stability is shown for the first time in the literature. It is demonstrated that the stability can be increased substantially for certain frequency ratios which can be achieved by length or mass modifications on the tool holders. As a consequence of optimization simulations, best conditions that provide higher stability limits are found. Also, the underlying reasons of the optimization results are explained by evaluating the resultant FRFs of the cutters.

APPENDIX

Euler Bernoulli Beam Equations

Before explaining two methods used in the optimization studies, "Euler Bernoulli Beam Equations" which form the basis of the calculations is presented briefly. Euler Bernoulli equations simply describe the relationship between the deflection of the beam and applied load. Figure A.1, shows the demonstration of a fixed support beam. Beam is assumed to have uniform cross section.

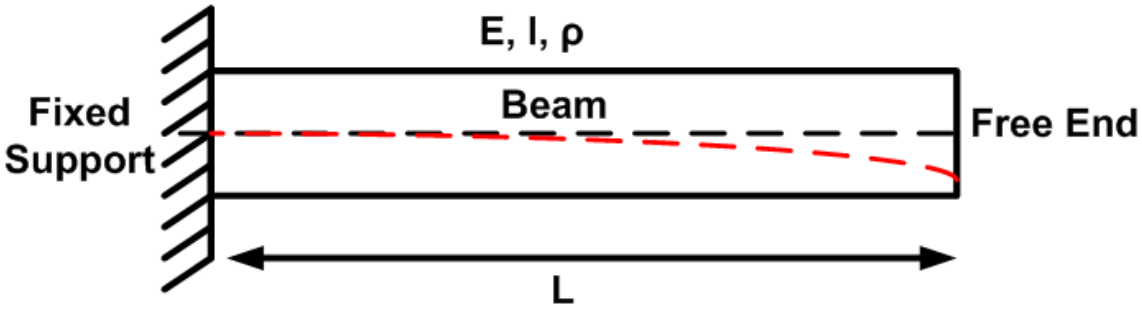

Figure A.1. "Euler Bernoulli" beam model.

Considering the cantilever beam is subjected to free vibration and the system is considered as the continuous system which the beam mass is distributed along the shaft of the beam, equations of motion for the beam can be written. After solving the governing equation, the first natural frequency of the beam can be calculated as follows:

$$f_1 = 1.875^2 \sqrt{\frac{EI}{\rho A L^4}} \tag{A.1}$$

where f_1 is the first natural frequency of the beam, E is the modulus of elasticity, I is area of moment of inertia, ρ is density of the beam material, A is the cross-section area of the beam and L is the length of the beam.

Effective mass of the beam can be calculated simply as:

$$m_{eff} = \frac{3EI}{L^3 \omega_n^2} \tag{A.2}$$

Practically, effective mass is about one fourth or fifth of the total mass of the beam. Total mass of the beam after mass modification is calculated as follows:

$$m_{total} = m_{eff} + m_{addititonal} \tag{A.3}$$

In the similar way, the stiffness of the beam is calculated as:

$$k = \omega_n^2 m_{eff} \tag{A.4}$$

Finally, damping ratio of the beam is found as follows:

$$\delta = \frac{c}{2\sqrt{k m_{eff}}} \tag{A.5}$$

where c is the damping coefficient, k is the stiffness of the beam and m_{eff} is the effective mass of the beam. C is related to the material of the beam. In the experiments and simulations, 4340 Steel is used as the cutter material and the damping coefficient of this material is found as 20.67 N s/m in modal tests.

In the optimization simulations, modal parameters can be calculated using the above equations.

BIBLIOGRAPHY

[1] Y. Altintas Manufacturing Automation Metal Cutting Mechanics, Machine Tool Vibrations, and CNC Design, Cambridge University Press, 2000.

[2] Ozturk, E., Budak, E., "Dynamics and Stability of Parallel Turning Operations", Annals of CIRP Vol. 60/1, 2011.

[3] Tobias, S.A., Fiswick, W., "Theory of Regenerative Machine Tool Chatter", The Engineer, London, 205: 1958.

[4] Tlusty, J., Polacek, M., "The Stability of Machine Tools Against Self Excited Vibrations in Machining", Int. Research in Production Engineering, ASME, 465-474, 1963.

[5] Tlusty, J. and Ismail, F., "Basic Non-linearity in Machining Chatter", Annals of the CIRP. 30/1: 21-25, 1981.

[6] Altintas, Y., Budak, E., "Analytical Prediction of Chatter Stability in Milling", Annals of the CIRP, 44/1: 357-362, 1995.

[7] Davies, M. A., Pratt, J. R., Dutterer, B., Burns, T., J., "Stability Prediction for Low Radial Immersion Milling", Journal of Manufacturing Science and Eng., 124: 217-225, 2010.

[8] Merdol, S., D., Altintas, Y., "Multi Frequency Solution of Chatter Stability for Low Immersion Milling", Journal of Manufacturing Science and Engineering, 126: 459-466, 2004.

[9] Slavicek, J., "The effect of irregular tooth pitch on stability in milling", Proc. 6th MTDR Conf., pp. 15–22, 1965.

[10] Opitz, H., "Investigation and calculation of the chatter behavior of lathes and milling machines" Annals of CIRP, vol. 18, pp: 335-342, 1970.

[11] Vanherck, P., "Increasing milling machine productivity by use of cutter with non- constant cutting-edge pitch", Proc. Adv. MTDR Conf., No. 8, pp. 947–960, 1967.

[12] Tlusty, J., Ismail, F., “Special Aspects of Chatter in Milling”, ASME, J. Eng. Ind, 105:24-32, 1983.

[13] Altintas, Y., Engin, S., Budak, E., “Analytical stability prediction and design of variable pitch cutters”, Journal of Manufacturing Science and Engineering, Vol.121, pp.173-178, 1999.

[14] Budak, E., “An analytical design method for milling cutter with nonconstant pitch to increase stability”, Journal of Manufacturing Science and Engineering, Vol.125, pp.35-38, 2003.

[15] Olgac, N., Sipahi, R., “Dynamics and stability of variable-pitch milling” Journal of Vibration and Control, Vol.13, pp.1031-1043, 2007.

[16] Ferry, W. B.S., “Virtual 5axis flank milling of jet engine impellers. Part I-II”, ASME Journal of Manufacturing Science and Engineering, Vol. 130, pp. 011005 – 011013, 2008.

[17] Turner, S., Merdol D., Altintas. Y., Ridgway, K., “Modelling of stability of variable helix end mills”, International Journal of Machine Tools and Manufacture, Vol.47, pp.1410, 2010.

[18] Zatarain, M., Muñoa, J., Peigné, G., Insperger, T. , “Analysis of the Influence of Mill Helix Angle on Chatter Stability”, Annals of the CIRP, Vol. 55/1:365–368, 2006.

[19] Sims, N. D., Mann, B., Huyanan, S., “Analytical prediction of chatter stability for variable pitch and variable helix milling tools”, Journal of Sound and Vibration, Vol.137, pp.664-686, 2008.

[20] Yusoff, A.R., Sims, N. D., “Optimization of variable helix end milling tools by minimizing self-excited vibration”, 7th International Conference on Modern Practice in Stress and Vibration Analysis, 2009.

[21] Insperger, T., Stephan, G., “Semi-discretization method for delayed systems”, International Journal for Numerical Methods in Engineering, Vol.55, pp.503-518, 2002.

[22] Insperger, T., Stephan, G., “Updated semi-discretization method for periodic delay-differential equations with discreet delay”, International Journal for Numerical Methods in Engineering, Vol.67, pp.117-141, 2004.

[23] Dombovari. Z., Stepan. G., “The effect of helix angle variation on milling stability”, Journal of Manufacturing Science and Technology, Vol. 134, pp. 0515, 2012.

[24] Ozturk, E., Budak, E., “Modeling Dynamics of Parallel Milling Processes in Time- Domain”, 2nd International CIRP Conference on Process Machine Interactions, Vancouver, Canada, 2010.

[25] Christian Brecher, “Yuri Trofimov, Stephan Baumler, Holistic Modelling of Process Machine Interactions in Parallel Milling”, CIRP Annals - Manufacturing Technology 60/1: 387–390, 2011.

[26] E. Shamoto, T. Mori, K. Nishimura, T. Hiramatsu, Y. Kurata, “Suppression of Regenerative Chatter Vibration in Simultaneous Double-Sided Milling of Flexible Plates by Speed Difference”, CIRP Annals - Manufacturing Technology, 59: 387–390, 2010.

[27] I. Lazoglu, M. Vogler, S.G. Kapoor, R.E DeVor, Dynamics of the Simultaneous Turning Process, Transactions of the North American Manufacturing Research Conference NAMRC XXVI (1998) 135-140.

[28] Ozdoganlar, O. B., Endres, W. J., “Parallel-Process (Simultaneous) Machining and Its Stability”, presented at ASME IMECE.99, Nashville, TN, and in Proc., Symp. on Mach. Sci. and Tech., MED-10, 361-368, 1999.

[29] L. Tang, R. G. Landers, S. N. Balakrishnan, Parallel Turning Process Parameter Optimization Based on a Novel Heuristic Approach, Journal of Manufacturing Science and Engineering 130 (2008)031002–31013.

[30] Koca, R., “Mechanics, Dynamics and Optimization of Special End Mills”, MSc Thesis, 2012, Sabanci University.

[31] Ozkirimli, Ö.M., “Mechanical and Dynamical Process Model for General Milling Tools in Multi Axis Machining”, MSc Thesis, 2011, Sabanci University.

[32] Kai Cheng, (ed), “Machining Dynamics, Fundamentals, Applications and Practices”, Springer, Londan, England, 2009.

[33] Budak, E., Tunc, L.T., Alan, S., Ozguven, H.N., “Prediction of Workpiece Dynamics and Its Effect on Chatter Stability in Milling”, CIRP Annals – Manufacturing Technology, 61/1: 339-342, 2012.

[34] Rao, S.N., (ed), “Mechanical Vibrations”, Prentice Hall, NJ, USA, 2011.